

DMB

INDIANA & MICHIGAN ELECTRIC COMPANY

P.O. BOX 16631
COLUMBUS, OHIO 43216

TE FILE COPY

February 6, 1984
AEP:NRC:0745K

Donald C. Cook Nuclear Plant Unit No. 1
Docket No. 50-315
License No. DPR-58
STARTUP REPORT FOR UNIT 1 CYCLE 8

PRINCIPAL STAFF		
✓ RA	<i>[Signature]</i>	DPRP
D/RA		DE
A/RA		DRMSP
RC		DRMA
PAO		SCS
SGA		VL
ENF		File

orig + 1

Mr. James G. Keppler, Regional Administrator
U.S. Nuclear Regulatory Commission
Office of Inspection and Enforcement
Region III
799 Roosevelt Road
Glen Ellyn, Illinois 60137

Dear Mr. Keppler:

This letter and its Attachment transmit a summary report of the Unit 1 Cycle 8 startup and power escalation testing.

This submittal is being made in compliance with Technical Specification No. 6.9.1.1, Items 2 and 3.

This document has been prepared following Corporate Procedures which incorporate a reasonable set of controls to ensure its accuracy and completeness prior to signature by the undersigned.

Very truly yours,

PBX 2/6/84

[Handwritten Signature]

M.P. Alexich
Vice President

MPA/bjs

cc: John E. Dolan
W.G. Smith, Jr. - Bridgman
R.C. Callen
G. Charnoff
E.R. Swanson, NRC Resident Inspector - Bridgman

app

FEB 11

8405040264 840206
PDR ADOCK 05000315
PDR

FEB 8 1984



[Faint, illegible text scattered across the page]

Mr. James G. Keppler

2

AEP:NRC:0745K

bc: J.G. Feinstein/J.M. Cleveland/W.L. Zimmermann
H.N. Scherer, Jr./S.H. Horowitz/R.C. Carruth
R.F. Hering/S.H. Steinhart/J.A. Kobyra
R.F. Kroeger
T.P. Beilman - Bridgman
J.A. DiBella
R.W. Jurgensen
B.H. Bennett/F.S. VanPelt, Jr.
J.F. Stietzel - Bridgman
J.B. Shinnock
D. Wigginton - NRC
AEP:NRC:0856A
AEP:NRC:0584A
DC-N-6500

10/10/1950

1

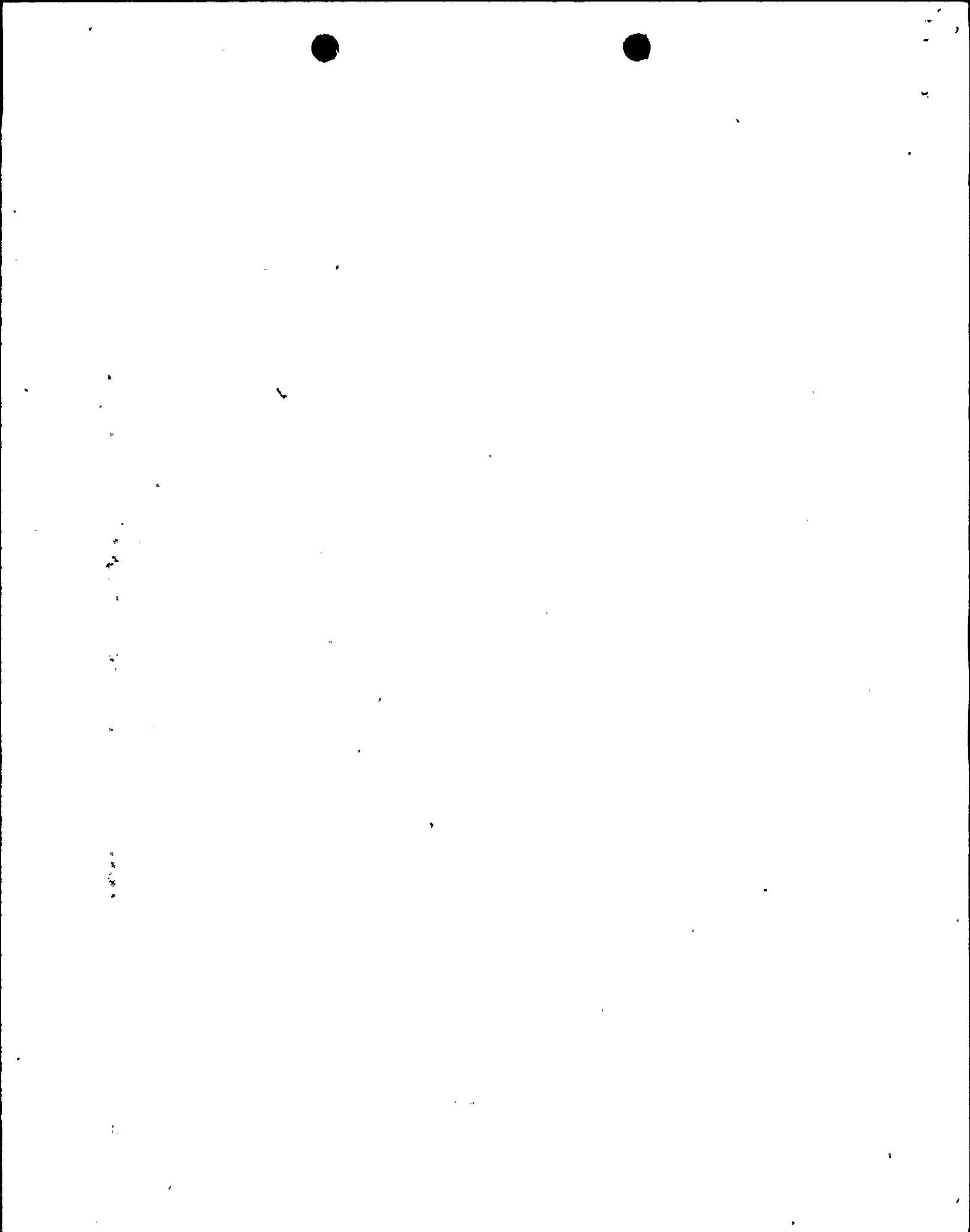
SECRET

MEMORANDUM FOR THE DIRECTOR, FBI
FROM: SAC, NEW YORK (100-100000)
SUBJECT: [Illegible]

[The following text is extremely faint and largely illegible due to the quality of the scan. It appears to be a memorandum or report detailing an investigation or administrative matter.]

TABLE OF CONTENTS

<u>SECTION</u>	<u>TITLE</u>
I	INTRODUCTION
II	CORE LOADING AND FUEL INSPECTION
III	INITIAL CRITICALITY
IVa	ZERO POWER PHYSICS TESTING
b	LOW LEAKAGE LOADING PATTERN (L^3P)
c	INVERSE COUNT RATE RATIO (ICRR) PLOT SHAPES FOR UNIT 1 CYCLE 8
d	PROBLEMS ASSOCIATED WITH FLUX MAPPING SYSTEM
Va	POWER ASCENSION TESTING
b	PLANT CHEMISTRY HISTORY
c	PLANT RADIATION SURVEYS
d	REACTOR COOLANT FLOW MEASUREMENT
e	PLANT THERMAL POWER CALIBRATION



I Introduction

The Unit 1 Cycle 7-8 outage began with reactor shutdown on July 16, 1983, after a twenty-eight (28) day power coastdown resulting in a total cycle 7 burnup of 10,446.8 MWD/MTU and final boron concentration at essentially zero ppm. One-hundred percent (100%) RTP was again reached on November 7, 1983. Startup testing was completed on November 8, 1983, with a full power flux map.

The fuel shuffle sequence for this outage was the typical shuffle. The fuel shuffle began on August 18, 1983, and was completed on August 23, 1983. Other than typical mechanical problems and one fuel shuffle sequence error, the shuffle was uneventful with no damaged fuel assemblies detected.

A total of eighty (80) Westinghouse Optimized Fuel Assemblies (OFA) were placed in the core with sixty-eight (68) of these fuel assemblies containing Wet Annular Burnable Absorbers (WABA). For the first time in Unit 1, the fresh assemblies were loaded into the core in a low neutron leakage pattern. Also for the first time, as a result of the WABA placement, the irradiated secondary sources were placed in fuel assemblies on the periphery of the core near the source range detectors. The placement of the secondary sources resulted in extensive analysis of their effect on the Inverse Count Rate Ratio (ICRR) during the approach to criticality.

The approach to criticality started with shutdown banks withdrawal at 0133 hours on October 19, 1983. Dilution toward criticality was halted at approximately 1700 ppm pending Plant Manager's approval prior to entering Mode 2. As a result of a problem with the Rod Position Indicators (RPI's), dilution to criticality from 1700 ppm was delayed approximately thirty (30) hours. Dilution resumed at 1812 hours October 20, 1983, and criticality was achieved at 2103 hours, October 20, 1983.

After stabilizing the reactor, data was obtained to determine the Zero Power Physics testing range and the point of nuclear heat.

Zero Power physics testing began at 0600 hours on October 21, 1983, and included the usual all rods out (ARO) Isothermal Temperature Coefficient (ITC), control rod worth, boron worth and boron endpoint tests along with ARO flux map. The measured ARO ITC was essentially the same as the design value, therefore, no rod withdrawal limits were required to ensure a negative MTC above 70% RTP. All rod worth and boron endpoint measurements compared favorably with design values.

Power ascension testing followed, starting on October 24, 1983, with a 30% RTP flux map, followed by a 48% RTP incore/excore cross calibration, Moderator Temperature Coefficient, Doppler Power Coefficient, $\Delta T/\Delta P$ ratio measurements and several flux maps. Power ascension went smoothly with the only unplanned hold being at 95% RTP, as the three-dimensional analytical factors were unavailable

for flux map processing. On November 4, 1983, the three-dimensional analytical factors were used in processing the 95% RTP flux map which resulted in an allowable power level (APL) greater than 100% RTP. The reactor power level was subsequently increased to 100% RTP.

In general, all startup tests were relatively routine. They were conducted in a timely and expedient manner and resulted in accurate startup information and data that compared favorably with design expectations and met acceptance criteria.

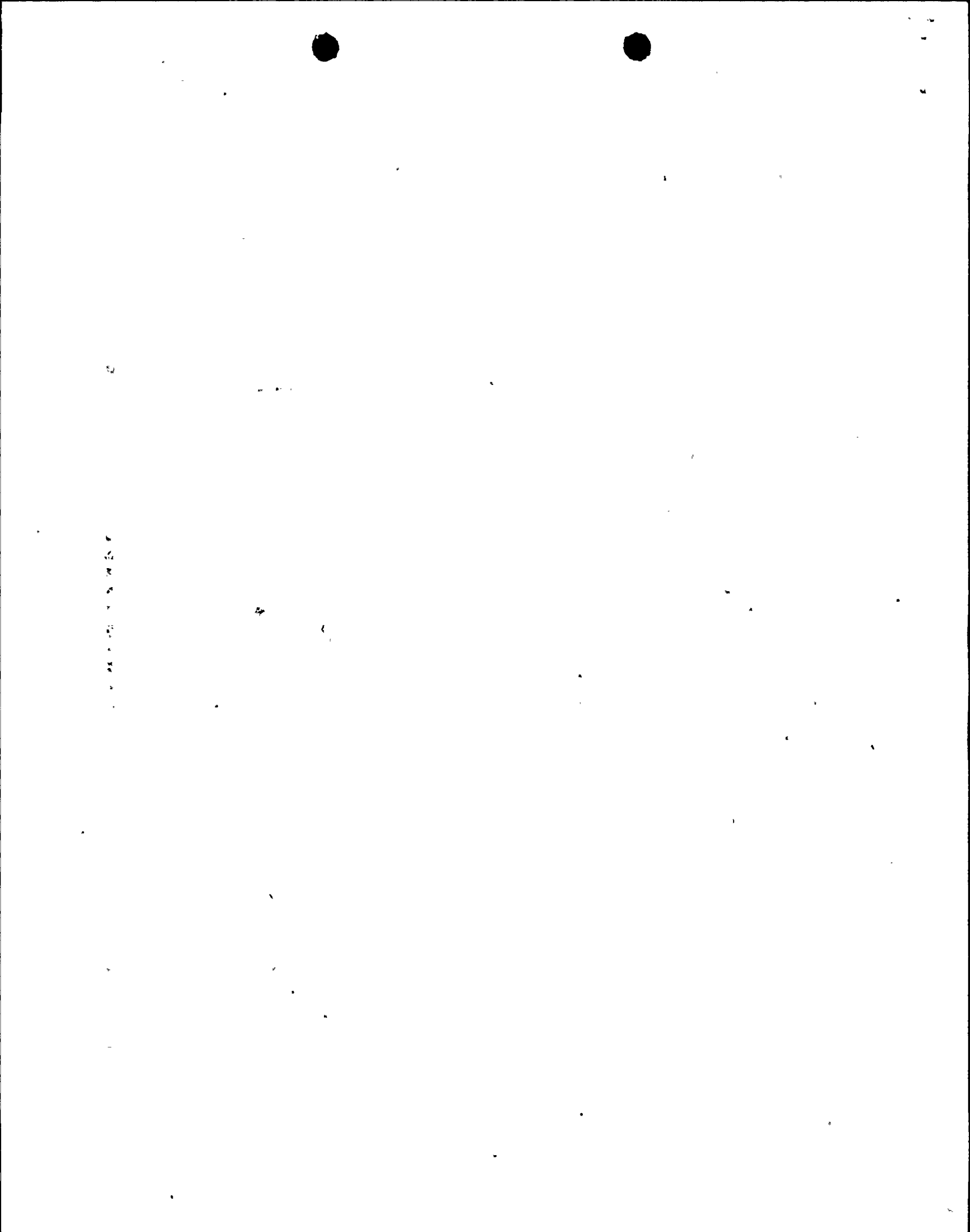
As stated in section 6.9.1.2 of Unit 1 Technical Specifications, the tests identified in the FSAR shall be addressed in the Startup Report. The tests in the FSAR are tests which were performed at the beginning of Unit 1 Cycle 1. Not all these tests need to be performed on a reload cycle. The FSAR tests that were required to be performed on this reload core are addressed in detail in this report. Those FSAR tests not required to be performed on this reload core are addressed in the Unit 1 Cycle 1 Startup Report.

II CORE LOADING AND FUEL INSPECTION

The Unit 1 Cycle 8 fuel assembly shuffle sequence commenced at 1250 hours on August 18, 1983, and was completed at 2245 hours on August 23, 1983. Eighty (80) depleted fuel assemblies (sixty-five [65] region G and fifteen [15] region H, all Exxon 15 x 15) were removed from the core. The depleted assemblies were replaced with eighty (80) Westinghouse 15 x 15 (region K) assemblies. The Westinghouse fuel assemblies are of the Optimized fuel assembly (OFA) design and many contain the recently designed part length Wet Annular Burnable Absorbers (WABA's). Both the OFA's and the WABA's are designed to increase the neutron economy and the cycle length of the core. Westinghouse's safety analysis of the reload fuel has shown the OFA's are mechanically and hydraulically compatible with the Exxon fuel assemblies, and with the control rods and reactor internals interfaces. A more detailed description of the new OFA's and WABA's is in the attached Appendix II A. The remaining one-hundred-thirteen (113) assemblies consisted of forty-nine (49) region H and sixty-four (64) region J fuel assemblies, all Exxon 15 x 15. Core loading diagrams for Unit 1 Cycle 7 and Cycle 8 are shown in Figures II.1 and II.2 respectively. (Core loading pattern diagrams, illustrating the difference between Cycle 7's core design and Cycle 8's new low-leakage core design, are shown in Figures II.3 and II.4 respectively.)

The first fuel shuffle problems occurred at approximately 1330 hours on August 18, 1983. The "frame down" light would not activate although the upender frame was down and the winch had shut off. After several seconds, the light activated, however, the winch cable then fell off the winch into the water. Apparently the cable had unwound to a point such that the "ball" that holds it was able to fall out. A diver was sent down to repair the winch while repairs were made to the limit and proximity switches. The system was declared operable at approximately 0100 hours on August 19, 1983.

At approximately 0630 hours on August 22, 1983, an error was discovered in the fuel shuffle procedure. An unusual pattern for the shuffle had been necessary because of the new WABA loading pattern and the addition of two (2) new secondary sources. This pattern, however, would not allow core subcritical behavior to be properly monitored on both source range channels while an activated secondary source, SS5, was absent from the core. Minor changes to the procedure corrected the error and the shuffle continued. This problem again occurred in the sequence involving SS6 and was handled in similar manner.



At approximately 0800 hours on August 23, 1983, a problem developed with the fuel transfer system. The pneumatic system air pressure dropped as the transfer cart traversed from containment to the spent fuel pit. Later, this same problem developed on the reverse path. After much discussion, it was decided to resume the shuffle to complete the remaining steps (approximately 10) without repairing the system. Problems later developed with the solenoid, which had to be repaired. The final steps consumed a great deal of time as the system further degraded. At this time, repairs have been made to the transfer system. The solenoid has been replaced with a new solenoid.

Westinghouse Fuel Assembly Handling Deviation Reports, FAHDR's, numbered approximately the same as the Cycle 7 fuel shuffle (27 versus 24). With the exception of the previously noted incidents, the majority of the reports involved problems associated with the insertion of assemblies into their specified core positions because of minor bowing or because of in-place assemblies leaning into open core locations. Some FAHDR's were the result of minor adjustments of the manipulator crane index.

Binocular inspection of new and irradiated assemblies took place both in the containment and in the spent fuel area, thus optimizing inspection conditions. All irradiated assemblies were observed from as many angles as possible as they were removed from the core. Additionally, those assemblies discharged to the spent fuel pit and all new assemblies underwent a more thorough inspection in the spent fuel pit. Each assembly was slowly rotated, thus allowing the observer a more careful inspection. All assemblies placed into the core were inspected as they were inserted as a final check for any damage. The binocular inspection of the assemblies revealed no structural damage or abnormalities.

FIGURE II.1,

D. C. COOK UNIT 1 CYCLE 7
 CORE LOADING DIAGRAM
 (INITIAL CONDITIONS)

R	P	N	M	L	K	J	H	G	F	E	D	C	B	A
				75 J59	105 J16	19 J23	91 J05	09 J07	15 J35	95 J38				
		52 J51	35 J02	126 J31	R35 640	67 J13	R37 630	90 J12	R25 616	94 J47	104 J61	57 J44		
	89 J43	R10 J20	26 642	R33 653	48 H49	R46 638	SS6 603	R18 618	72 H30	R26 648	41 614	R03 J25	130 J39	
	05 J09	115 609	R09 635	44 H40	129 H17	86 H14	R19 658	68 H59	84 H22	61 H21	R29 620	116 647	108 J06	
70 J50	03 J54	R12 611	46 H19	65 656	13 H24	36 H57	42 H18	R39 H37	77 H53	33 605	101 H48	R04 645	110 J28	32 J42
25 J15	R24 623	29 H15	69 H09	119 H28	R20 636	153 H45	R06 657	155 H41	R15 650	20 H62	87 H33	31 H34	R17 632	16 J01
07 J48	22 J10	R27 613	37 H12	R28 H03	74 H27	113 627	98 H55	99 628	158 H47	80 H04	43 H39	R16 643	78 J27	124 J52
128 J24	R53 625	160 602	R07 663	73 H26	R48 664	66 H11	R55 665	55 H10	R38 654	17 H16	R21 659	43 604	R08 631	106 J30
06 J26	56 J03	R02 637	103 H32	53 H23	97 H06	40 634	21 H60	127 621	157 H46	R40 H35	04 H08	R45 619	71 J55	92 J32
111 J33	R44 639	02 H43	122 H63	14 H50	R14 655	156 H44	R01 661	154 H25	R42 606	60 H31	96 H38	11 H20	R52 617	42 J04
50 J60	93 J45	R05 652	107 H29	109 607	01 H42	R36 H01	54 H64	49 H51	30 H05	12 651	82 H61	R22 660	121 J57	08 J37
	81 J29	120 641	R41 626	79 H52	23 H58	10 H07	R31 662	62 H54	76 H36	102 H13	R11 629	125 615	159 J63	
	123 J17	R34 J58	88 608	R30 610	27 H56	R50 612	SS5 601	R47 644	28 H02	R32 646	85 649	R23 J19	117 J22	
		45 J21	83 J18	51 J41	R49 622	59 J11	R13 624	47 J62	R51 633	118 J53	38 J56	39 J34		
				64 J36	100 J14	18 J40	58 J64	50 J46	24 J08	34 J49				

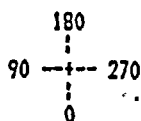
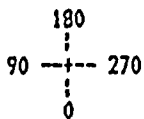


FIGURE II.2

D. C. COOK UNIT 1 CYCLE 8
CORE LOADING DIAGRAM
(FINAL CONDITIONS)

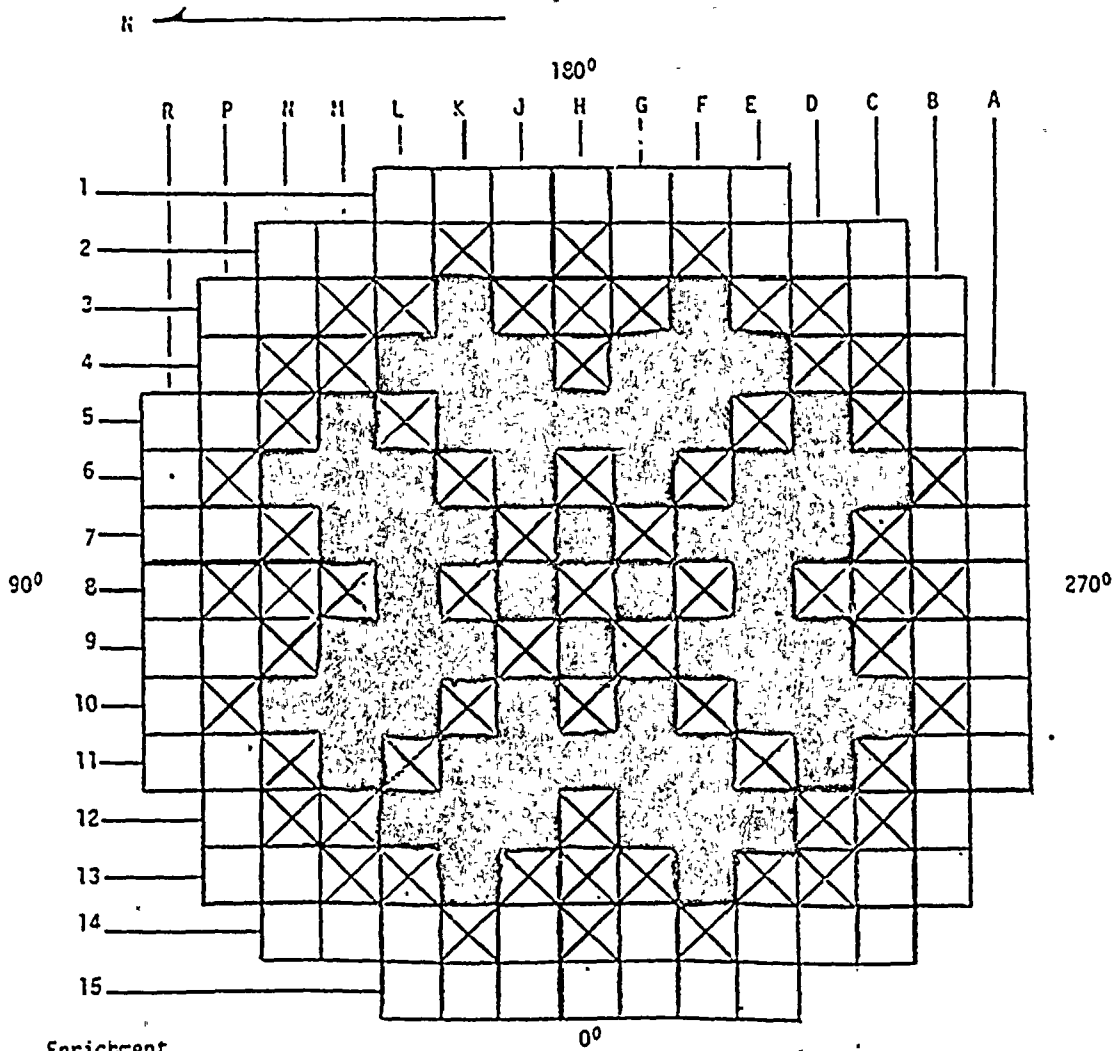
	R	P	N	M	L	K	J	H	G	F	E	D	C	B	A
1					76 H36	SS6 K46	4PK09Z K55	803Z K59	4PK04Z K72	802Z K77	23 H59				
2			28 H02	126 J31	12PK10 K79	R35 J51	12PK17 K11	R37 H13	12PK32 K01	R25 J44	12PK12 K75	94 J47	27 H56		
3		11 H20	R09 J15	12PK18 K48	R33 J06	16PK09 K44	R46 H32	16PK26 K15	R19 H08	16PK12 K40	R25 J09	12PK22 K66	R29 J35	02 H43	
4		03 J54	12PK13 K60	R10 J20	64 J36	47 J62	16PK05 K10	R19 J46	16PK19 K14	59 J11	34 J49	R03 J25	12PK20 K69	110 J28	
5	96 H38	12PK19 K56	R12 J18	32 J42	55 H10	16PK11 K02	153 H45	91 J05	R39 H41	16PK23 K32	21 H60	70 J50	R04 J56	12PK27 K54	122 H63
6	804Z K65	R24 J43	16PK13 K39	71 J55	16PK09 K33	R20 H52	12PK04 K21	R05 H18	12PK07 K18	R15 H19	16PK18 K22	56 J03	16PK14 K26	R17 J39	806Z K73
7	4PK02Z K67	12PK21 K16	R27 H59	16PK06 K43	R28 H27	12PK25 K13	07 J48	SS12 J16	09 J07	12PK15 K35	159 H47	16PK22 K05	R16 H14	12PK03 K36	4PK07Z K49
8	809Z K51	R53 H48	16PK04 K41	R07 J52	128 J24	R48 H26	111 J33	R55 H05	16 J01	R38 H16	106 J30	R21 J26	16PK03 K28	R08 H29	801Z K52
9	4PK05Z K76	12PK08 K42	R02 H54	16PK10 K17	97 H06	12PK11 K27	18 J40	24 J08	92 J32	12PK28 K09	R40 H46	16PK20 K31	R45 H07	12PK31 K37	4PK01Z K71
10	805Z K45	R44 J17	16PK01 K08	78 J27	16PK24 K23	R14 H61	12PK29 K04	R01 H64	12PK02 K07	R42 H21	16PK15 K25	22 J10	16PK25 K30	R52 J22	807Z K84
11	87 H33	12PK06 K74	R05 J02	08 J37	98 H55	16PK21 K12	R36 H44	SS11 J64	154 H25	16PK17 K03	66 H11	50 J60	R22 J61	12PK26 K63	69 H09
12		93 J45	12PK23 K80	R34 J58	75 J59	90 J12	16PK02 K24	R31 J23	16PK16 K29	67 J13	95 J38	R23 J19	12PK09 K59	121 J57	
13		31 H34	R41 J14	12PK14 K47	R30 J63	16PK28 K38	R50 H12	16PK07 K19	R47 H39	16PK27 K34	R32 J29	12PK05 K53	R11 J04	29 H15	
14			72 H30	51 J41	12PK03 K50	R49 J21	12PK24 K20	R13 H40	12PK01 K06	R51 J34	12PK16 K70	118 J53	48 H49		
15					84 H22	810Z K61	4PK03Z K68	808Z K62	4PK06Z K57	SS5 K78	129 H17				



*OFA THIMBLE PLUG

FIGURE II.3

UNIT 1 CYCLE 7
CORE LOADING DIAGRAM



Enrichment

Region 9 2.903

Region 8 2.905

Region 7 2.907

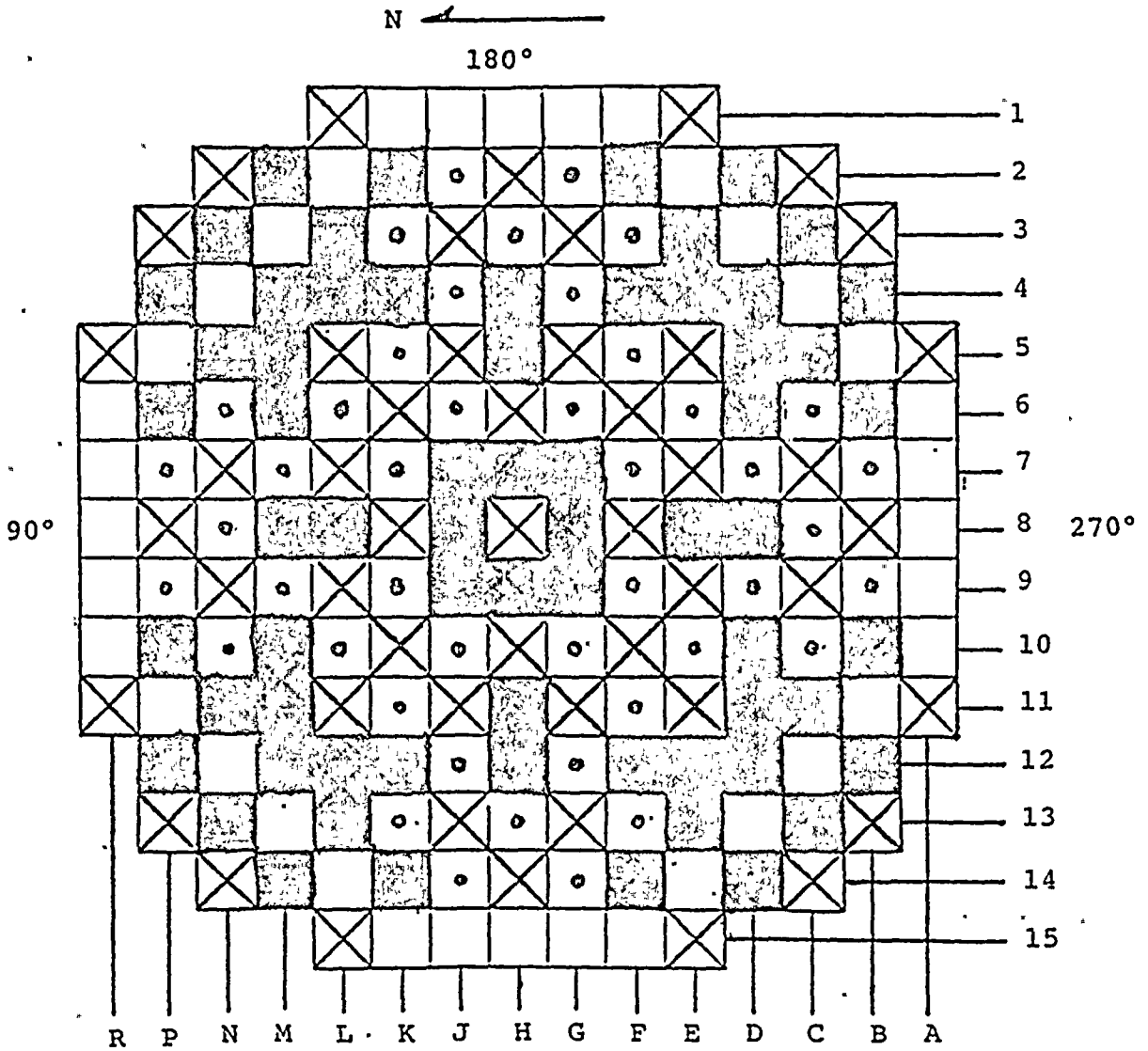


— Region 9 - J





— Region 6 - H

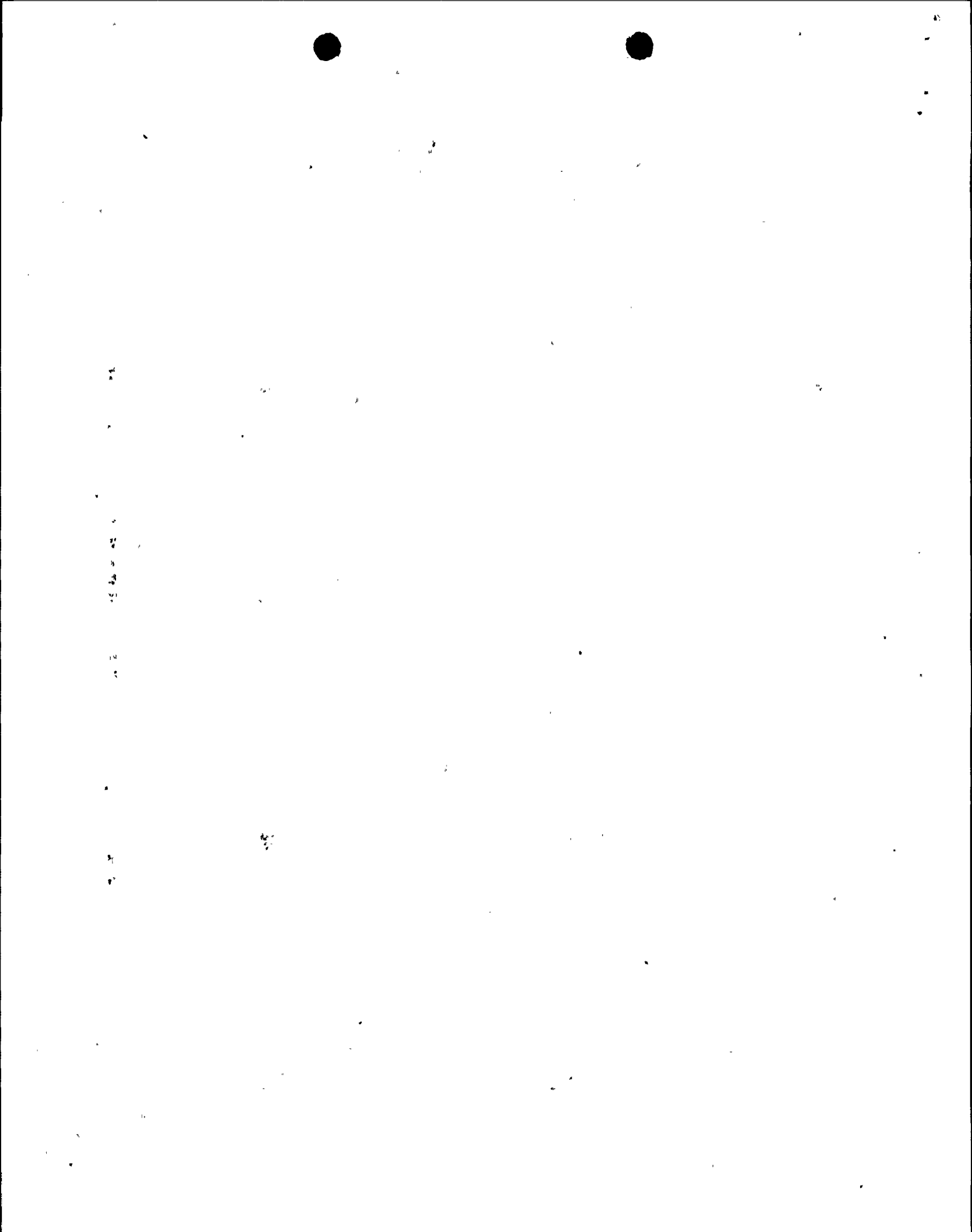
— Region 7 - G

FIGURE II.4
 D.C. COOK UNIT 1 CYCLE 8
 CORE LOADING DIAGRAM



0°

	- Region 8 - H	Enrichment: 2.905
	- Region 9 - J	2.903
	- Region 10A - K	3.3
	- Region 10B - K	3.6



Appendix II A

Westinghouse Optimized Fuel Assemblies (OFA's) and Wet Annular Burnable Poison Absorbers (WABA's)

Westinghouse, in order to demonstrate compatibility of the OFA with ENC fuel, chose the following approach. ENC, in establishing their fuel design, demonstrated compatibility with the Westinghouse LOPAR fuel used in Unit 1 Cycle 1. Westinghouse has shown compatibility of the 15 x 15 OFA design with the LOPAR design. Thus, compatibility between OFA and ENC fuel was shown.

The purpose of the new OFA design was to improve the utilization of Uranium while allowing operating margins to be maintained. The 15 x 15 OFA design is similar to the 15 x 15 LOPAR (low parasitic) design which was the initial Unit 1 fuel. The major difference in the two designs is that the five intermediate inconel grid straps of the LOPAR fuel were replaced with zircaloy grid straps. The very low thermal neutron cross-section of zircaloy makes it less parasitic and hence results in better neutron economy. The zircaloy straps are wider and thicker than the inconel grid straps in order to duplicate the inconel grid strength. The ENC grid straps are bi-metallic, consisting of zircaloy-4 straps with inconel springs. The grid heights of both OFA and ENC assemblies are equal. A comparison of Westinghouse 15 x 15 OFA and Exxon 15 x 15 assemblies appear in Figure II.5 and Table II.1. The OFA rods use the same design as the LOPAR rods.

As the zircaloy grid straps are thicker than the inconel, there has been a reduction in grid strap cell size. This reduction resulted in the OFA guide thimble tubes inner diameter above the dashpot being smaller than the ENC thimble tube inner diameter. Below the dashpot, the dimensions are the same. The reduced diameter provides sufficient space for all inserts; however, the Technical Specification rod drop time limit has been increased to allow for anticipated increases in rod drop times. All accident analyses used the lengthened rod drop time.

Minor differences between ENC assemblies and OFA's include 1) the overall height of top and bottom nozzles, 2) the adapter plate flow-slot configuration and holddown leaf springs. These differences have no adverse affect on the interaction of the two (2) types of assemblies. The OFA's use a 3-leaf holddown spring design (as previously used in LOPAR's) which provides additional holddown force margin compared to the 2-leaf ENC assembly spring. The OFA bottom nozzle, although similar in design to the ENC bottom nozzle, has a reconstitutable feature. This feature allows it to be easily removed. (See Figure II.5) The OFA design utilized a locking cup to lock the thimble screw of a guide tube in place, where as the LOPAR design utilized a lock-wire. This feature facilitates remote removal of the nozzle and relocking of the thimble screws as the nozzle is reattached.



The burnup dependent rod bow for the OFA design was conservatively assumed to be the same as for the LOPAR design. Significant rod bow is mainly caused by rod-grid and pellet clad interaction forces and wall thickness variation. OFA fuel rods and LOPAR rods are the same, thus eliminating the rod consideration. Grid forces are reduced because of the zircaloy springs in OFA, thus rod bow can be predicted to decrease. Fuel rod cladding wear is dependent on grid support and flow environment. Hydraulic tests between ENC and LOPAR assemblies and OFA and LOPAR assemblies showed similar crossflows between the two sets. The results showed small cross-flow between assemblies and no significant rod wear due to vibration. Extrapolation showed that clad wear would not impair fuel rod integrity.

The purpose of the new WABA design was to reduce residual poison penalty at the end of cycle. This in turn could 1) aid in reducing initial boron concentration and thus maintain a negative beginning of cycle moderator temperature coefficient and 2) aid in extending cycle length. Additionally, the WABA's aid in flattening the power distribution and in controlling power peaking. The improved WABA's are different from the older burnable poison rods in the following ways: 1) aluminum oxide-boron carbide is used instead of Borosilicate glass, 2) tubings are made of zircaloy instead of stainless steel, 3) the annular plenum contains helium instead of air and 4) the inner tube is open-ended allowing the reactor coolant flow through it instead of being filled with air. Additionally, the WABA rods are reduced in length to 123 inches and its centerline is positioned 1.5 inches above the fuel rod centerline. Thus the design benefits of the WABA are better neutron economy from the less parasitic zircaloy tubes, the increased water fraction in the cell which increases the thermal flux in the cell which increases the effect of the poison and the reduction on the end of cycle boron penalty.

Table II.1

Comparison of OFA and ENC Assembly Design

<u>Parameter</u>	<u>15x15 W Optimized Fuel Assembly Design</u>	<u>15x15 ENC Fuel Assembly Design</u>
Fuel Assembly Length, in.	159.765	159.71
Fuel Rod Length, in.	151.85	152.07
Assembly Envelope, in.	8.426	8.426
Compatible with Core Internals	Yes	Yes
Fuel Rod Pitch, in.	0.563	0.563
Number of Fuel Rods/Ass'y	204	204
Number of Guide Thimbles/Ass'y	20	20
Number of Instrumentation Tube/Ass'y	1	1
Compatible with Movable In-Core Detector System	Yes	Yes
Fuel Tube Material	Zircaloy-4	Zircaloy-4
Fuel Rod Clad OD, in.	0.422	0.424
Fuel Rod Clad Thickness, in.	0.0243	0.030
Fuel/Clad Gap, mil	7.5	7.5
Fuel Pellet Diameter, in.	0.3659	0.3565
Guide Thimble Material	Zircaloy-4	Zircaloy-4
Guide Thimble ID, in.*	0.499	0.511
Structural Material - Five Inner Grids	Zircaloy-4	Zircaloy-4 Straps Inconel Springs

*Above dashpot

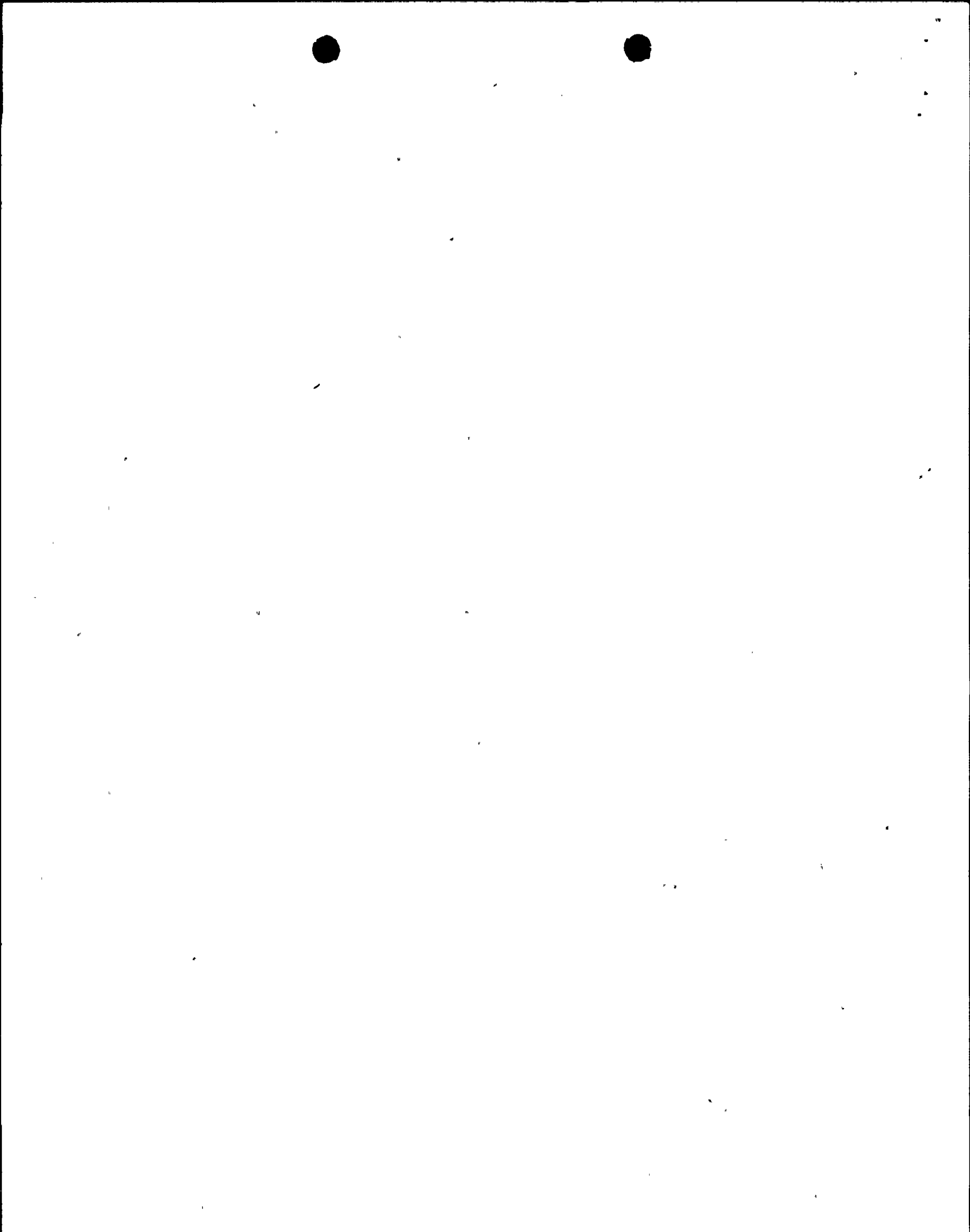
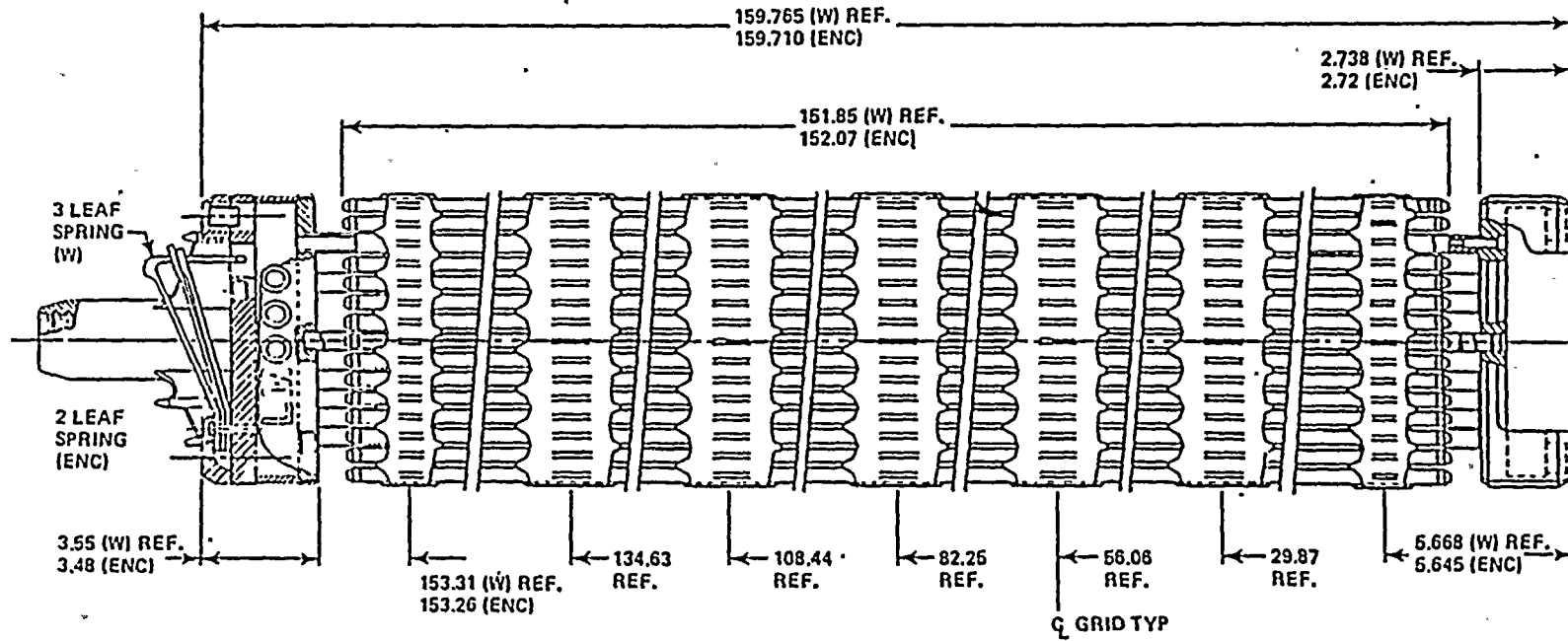


Table II.1
 ((continued))

<u>Parameter</u>	<u>15x15 W Optimized Fuel Assembly Design</u>	<u>15x15 ENC Fuel Assembly Design</u>
Structural Material - Two End Grids	Inconel	Zircaloy-4 Straps, Inconel Springs
Grid Height, in., Outer Straps, Valley-to Valley	2.25	2.25
Bottom Nozzle Top Nozzle Holddown Springs	Reconstitutable 3-leaf	2-leaf

FIGURE II.5

SCHEMATIC OF WESTINGHOUSE 15X15 OFA



W - WESTINGHOUSE 15X15 OPTIMIZED FUEL ASSEMBLY (OFA) DIMENSION
ENC - EXXON NUCLEAR COMPANY (ENC) 15X15 FUEL ASSEMBLY DIMENSION
NOTE: OFA AND ENC ASSEMBLY MID-GRIDS HAVE IDENTICAL AXIAL SPACINGS

ENC GRID HEIGHT - 2.25
WESTINGHOUSE TOP & BOTTOM GRID HEIGHTS - 1.5
WESTINGHOUSE MID GRID HEIGHT - 2.25

Comparison of ENC Fuel Assembly Dimensions With Westinghouse 15X15 OFA Schematic

III INITIAL CRITICALITY

Unit 1 Cycle 8 achieved initial criticality at 2103 hours on October 20, 1983. The All Rods Out (ARO) Boron was calculated to be 1572.4 ppm, as compared to a design value of 1534 ppm.

The approach to criticality began with the withdrawal of the Shutdown Banks. Shutdown Bank withdrawal began at 0133 hours and was completed at 0219 hours on October 19, 1983. The next step was to withdraw control banks in overlap, as shown in Figure III.1. The withdrawal of the control banks started at 0240 hours and was finished at 0400 hours on October 19, 1983, with Control Bank D (CBD) at 190 Steps (CBD at 190 Steps corresponded to approximately 100 pcm of negative reactivity still inserted in the core).

At 0420 hours, after the withdrawal of CBD to 190 Steps, RCS dilution began from approximately 2220 ppm to approximately 1700 ppm, at a dilution rate of 60 gpm. Because of the anticipated behavior in the Inverse Count Rate Ratio, ICRR, due to secondary source placement in the core, see Section IVc, the dilution rate was cut to 30 gpm at 0600 hours on October 19, 1983. Dilution was stopped, pending Plant Managers approval to enter Mode 2, at 1032 hours on October 19, 1983, at a boron concentration of 1729 ppm. While awaiting the Plant Managers approval to enter Mode 2, Control and Instrumentation (C&I) personnel performed THP 6030 IMP.038, A.R.P.I. Coil Stack Voltage Data. During the performance of this procedure, four (4) rod position indicators (RPI's) were determined to be out of specification. After a hold approximately 30 hours, during which Nuclear Section personnel performed a "glitch" test to verify the actual rod height of the RPI's in question and C&I personnel completed a recalibration of all of the RPI's, permission to dilute to critical was granted. Dilution to critical was reinitiated at a rate of 45 gpm at 1812 hours on October 20, 1983. Mode 2 was achieved at 1930 hours and the Unit was subsequently declared critical at 2103 hours on October 20, 1983. The Reactor's stable critical conditions were CBD at 169 steps, flux level at 10^{-8} amps, and a boron concentration of 1552 ppm. During the dilution to critical Inverse Count Rate Ratio, ICRR, data vs. Boron Concentration, Primary Water, and time were plotted, and is shown in Figures III.2, III.3, and III.4, respectively.

After the Reactor was stabilized at 10^{-8} amps, data was obtained to determine the Zero Power Physics Testing Range and Nuclear Heating Level. CBD was maneuvered between 169 and 176 Steps, at different flux levels, in order to obtain reactivity changes, (see Table III.1) From the data obtained, the Zero Power Physics Testing Range was determined to be from 3×10^{-8} amps to 3×10^{-7} amps. See Figure III.5. Nuclear Heating was determined to be at approximately 7×10^{-7} amps.

Nuclear Heating determination is made by observing a decay in the reactivity trace on the reactivity meter strip chart. At the same time, an increase in RCS temperature is noted, as the flux is slowly raised. The physics testing range is typically approximately two (2) decades above the γ background level, and approximately one (1) decade below Nuclear Heating. The γ background is measured prior to the introduction of positive reactivity for the approach to critical. At lower flux levels the reactivity changes is affected by small variations in flux. See Figure III.5. This is due to the fact that the background remains constant while the flux can be varied. At lower flux levels the background is more predominate. As the flux is increased, the background becomes less significant. A plateau is reached where the background does not have a significant effect on the observed reactivity.

Table III.1

Subcritical Data

Induced current with 1000. V applied = + 0.14×10^{-8} amp

90% value = 0.126×10^{-8} amp

50% value = 0.07×10^{-8} amp

Zero Power Physics Test Range Data

CBD initial position 169 steps, CBD final position 176 steps

($\Delta\rho$, pcm, for various compensating currents)

<u>Flux Level, amps</u>	<u>Disconnected</u>	<u>50% value</u>	<u>90% value</u>
$\approx 5 \times 10^{-9}$	21.6	24.5	27.7
$\approx 1 \times 10^{-8}$	24.3	25.5	26.2
$\approx 5 \times 10^{-8}$	26.1	27.0	26.0
$\approx 1 \times 10^{-7}$	26.5	26.0	26.0
$\approx 5 \times 10^{-7}$	26.5	25.7	25.2
$\approx 1 \times 10^{-6}$	25.7	25.4	24.7
$\approx 2 \times 10^{-7}$	25.6	26.0	25.0

CBD initial position 203 steps, final CBD position 211 steps

$\approx 0.3 \times 10^{-7}$ 26.1 27.0 27.4

$\approx 0.3 \times 10^{-6}$ 26.4 25.8 26.25

Nuclear Heating Level

Flux Level = 7×10^{-7} amps

Zero Power Physics Testing Range*

Flux Range = 0.03×10^{-6} amp to 0.3×10^{-6} amp

*Due to the quality of the data obtained, no compensating current was required during zero power physics testing.



1
2
3
4
5
6
7
8
9
10
11
12
13
14
15
16
17
18
19
20
21
22
23
24
25
26
27
28
29
30
31
32
33
34
35
36
37
38
39
40
41
42
43
44
45
46
47
48
49
50
51
52
53
54
55
56
57
58
59
60
61
62
63
64
65
66
67
68
69
70
71
72
73
74
75
76
77
78
79
80
81
82
83
84
85
86
87
88
89
90
91
92
93
94
95
96
97
98
99
100

1

2

3

4

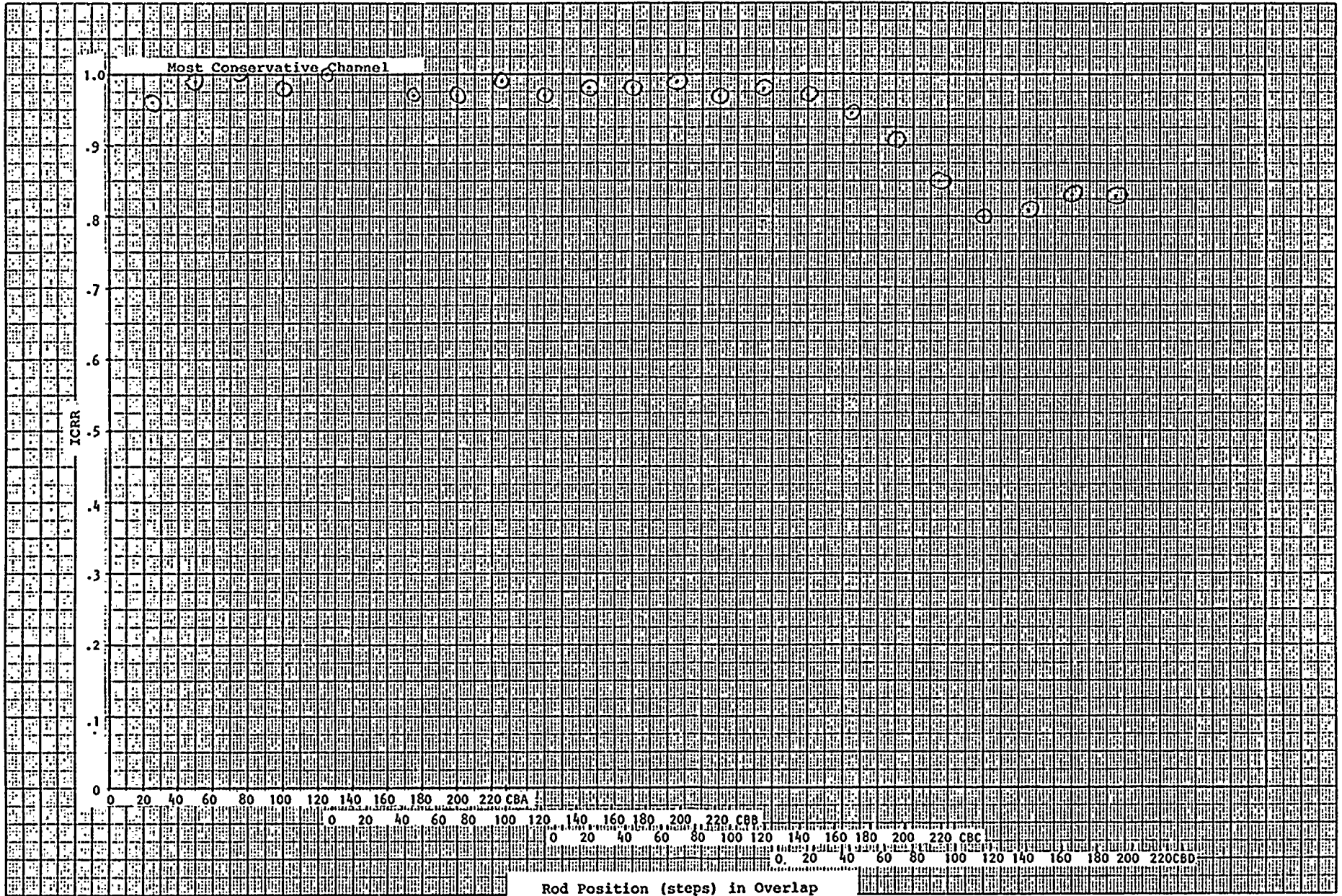
5

6

FIGURE III.1

ICRR vs. CONTROL BANK WITHDRAWAL IN OVERLAP

UNIT 1 CYCLE 8 STARTUP





Vertical text on the left side, possibly a page number or header.

Small text mark.

Small text mark.

Small text mark.

Small text mark.

Small text mark.

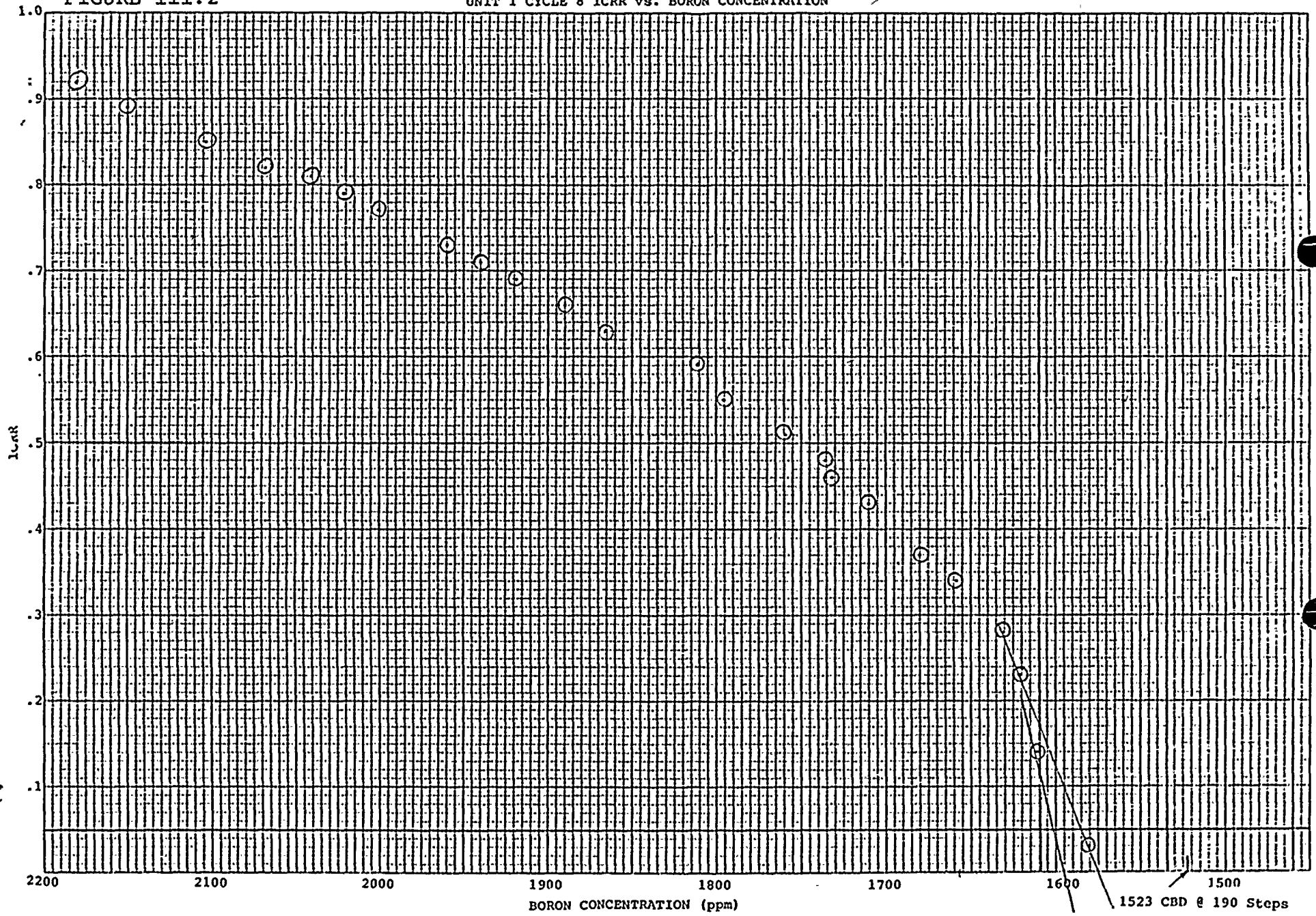
Small text mark.

Small text mark.

Small text mark at the top right.

FIGURE III.2

UNIT 1 CYCLE 8 ICRR vs. BORON CONCENTRATION



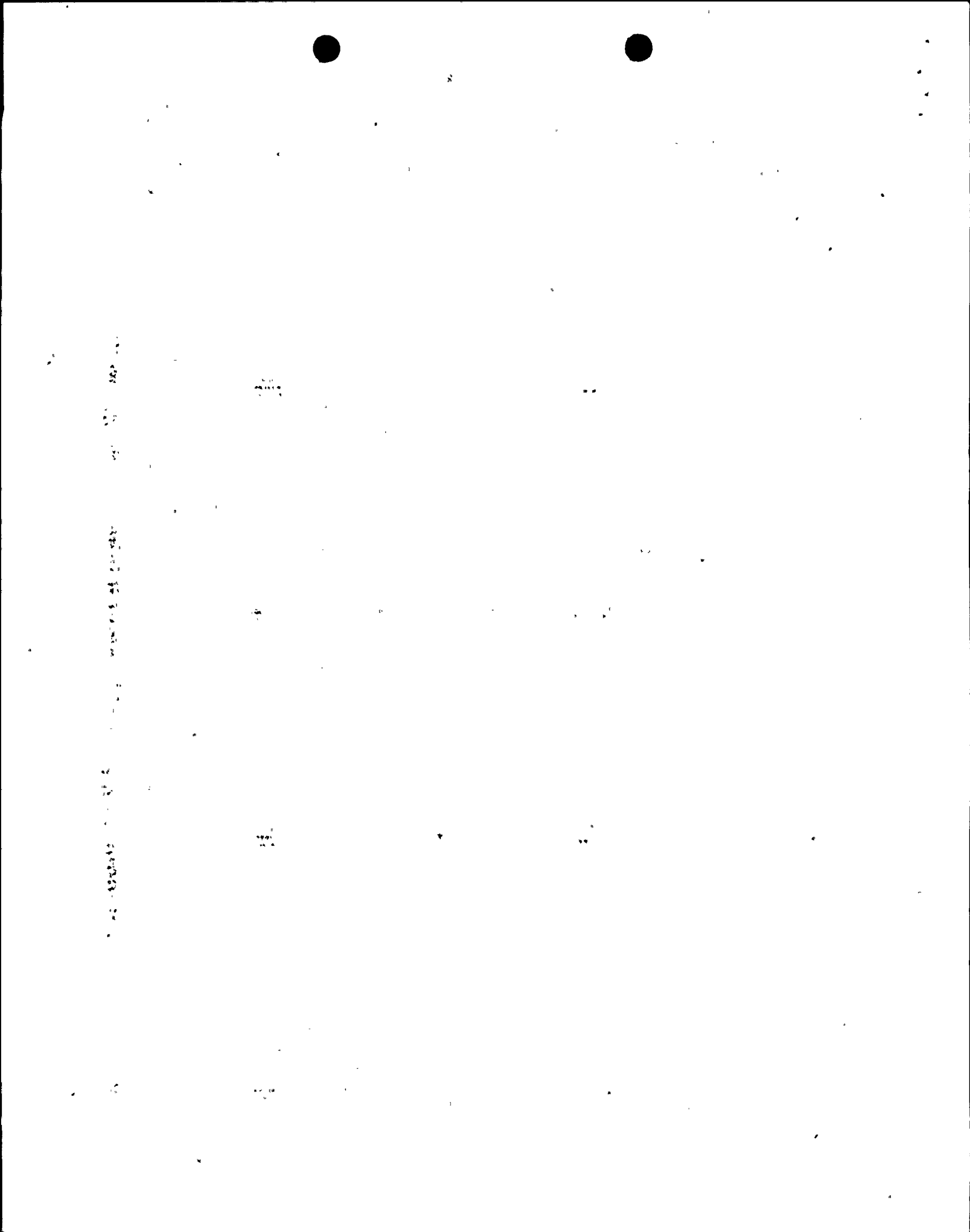
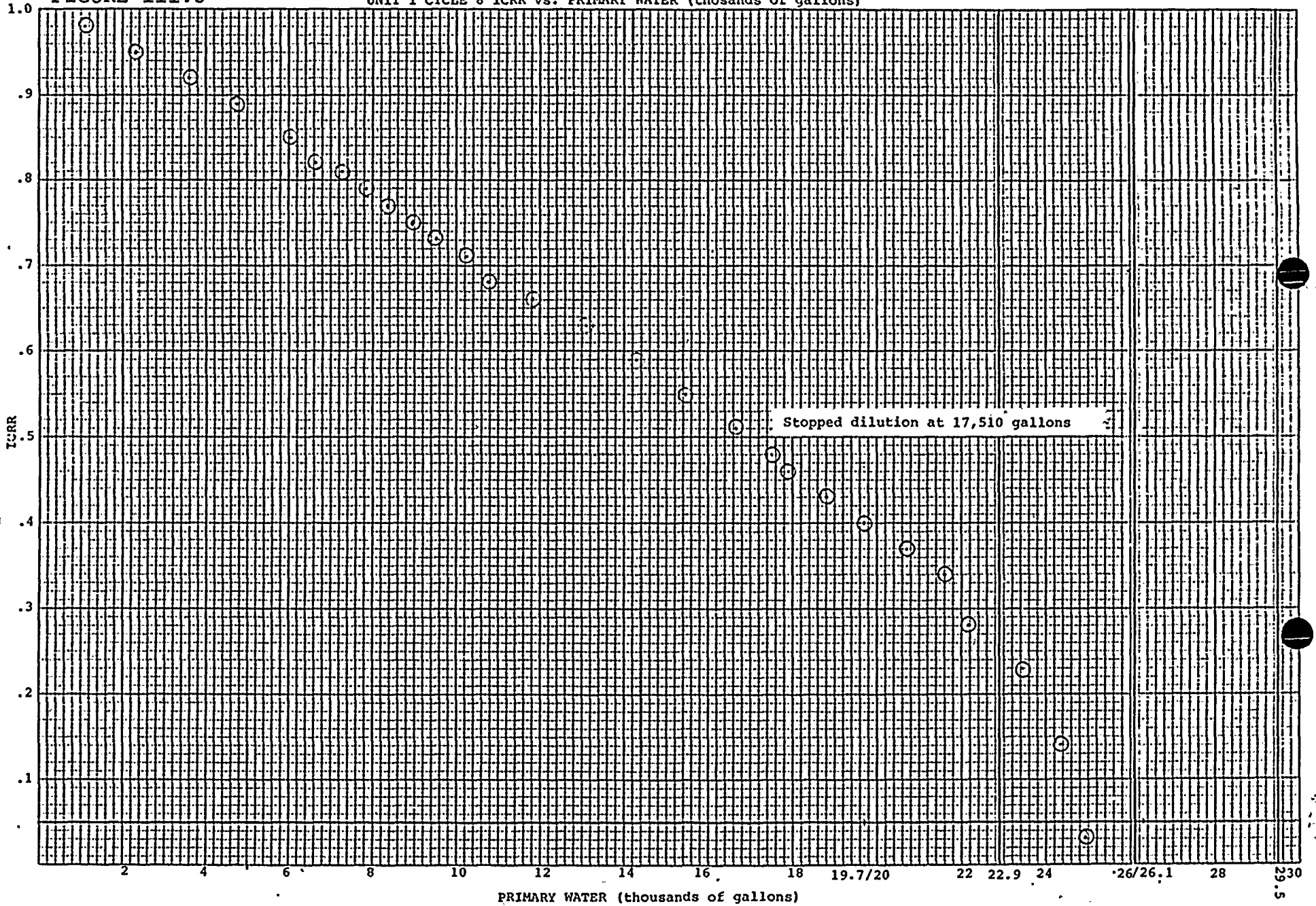


FIGURE III.3

UNIT 1 CYCLE 8 ICRR vs. PRIMARY WATER (thosands of gallons)





Vertical text on the right side of the page, possibly a page number or reference code.

Small vertical text mark.

Small vertical text mark.

Small vertical text mark.

Vertical text on the bottom left side of the page.

FIGURE III.4

UNIT 1 CYCLE 8 ICRR VS. TIME

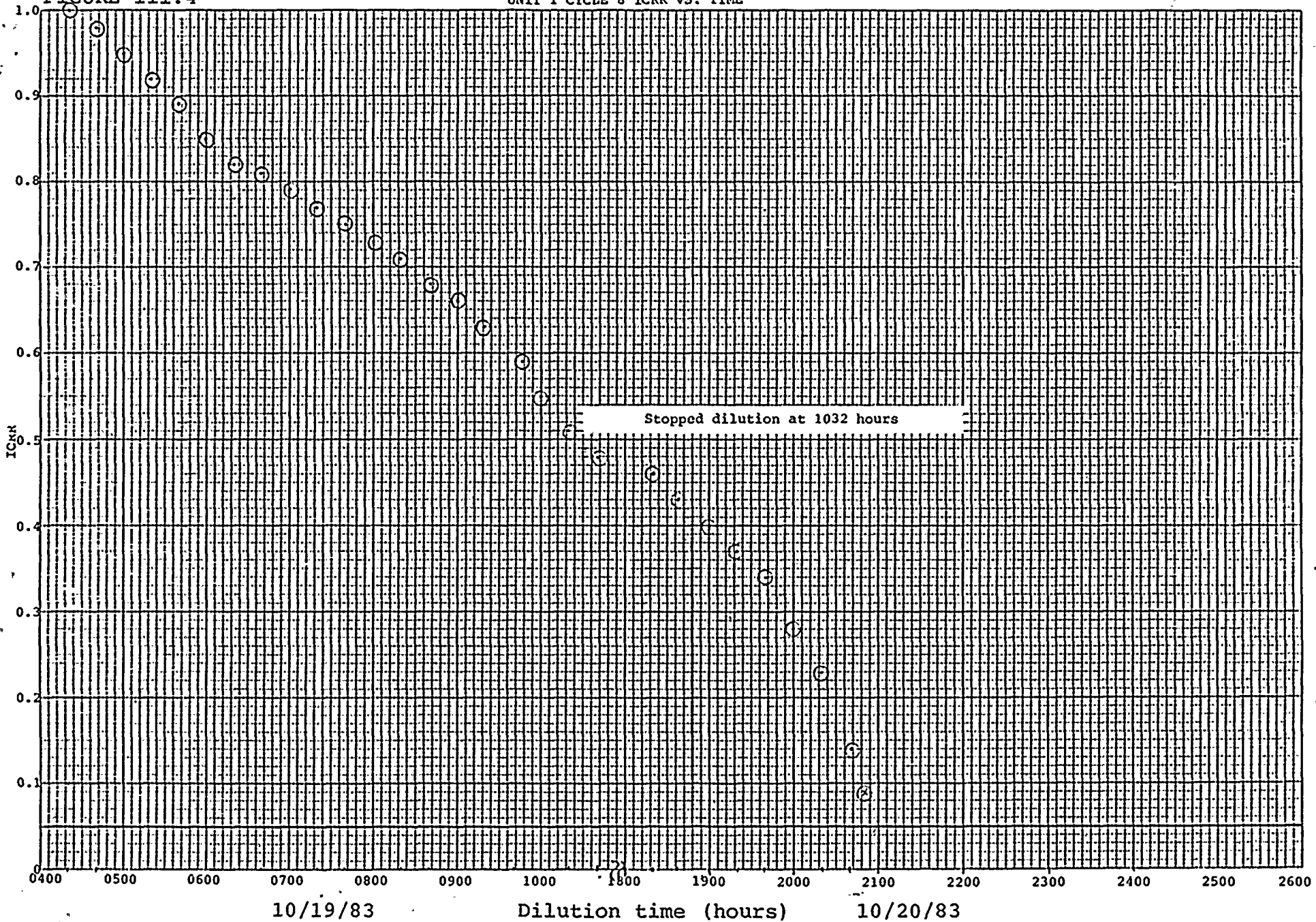


FIGURE III.5

Unit 1 Cycle 8

- No compensation current
- △ 50% comp. current
- 90% comp. current

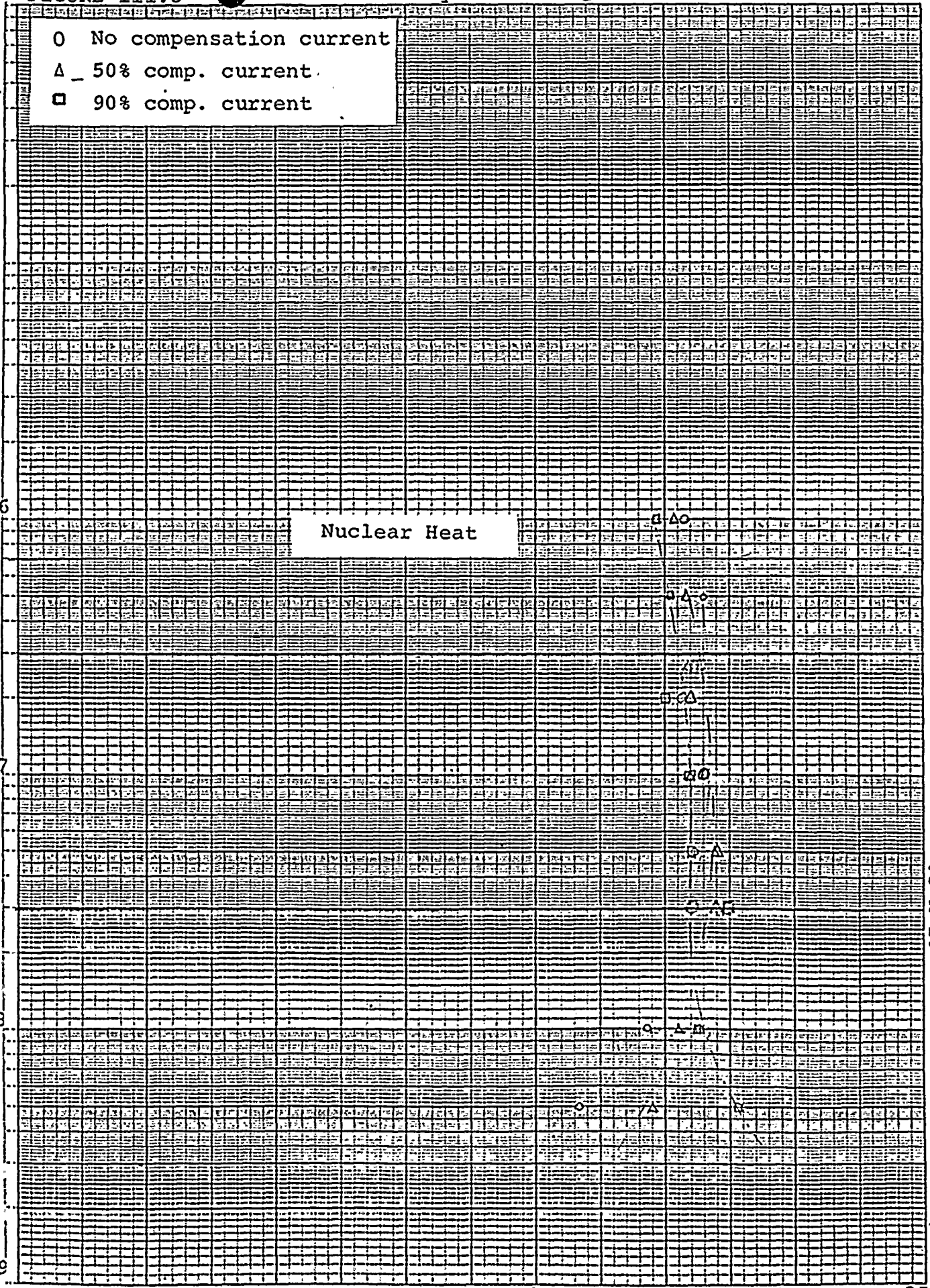
1×10^{-6}
 1×10^{-7}
 1×10^{-8}
 1×10^{-9}

Nuclear Heat

3×10^{-6}
 3×10^{-7}

Reactivity (pcm)

20 25 30 35



Iva ZERO POWER PHYSICS TESTING

Zero power physics testing commenced at 0600 hours on October 21, 1983, and was completed on October 22 at 1025 hours. The testing program consisted of

- 1) ARO Isothermal Temperature Coefficient
- 2) ARO Flux Map
- 3) Individual Control Bank Worths
- 4) Boron Endpoints and Boron Worths
- 5) Control Banks. Worth in Overlap

The testing program was routine and was completed with no problems. The data presented in the following tables and figures shows compliance with design values and acceptance criteria. The Moderator Temperature Coefficient calculated from the ARO ITC tests was 2.81 pcm/ $^{\circ}$ F, therefore, no rod withdrawal limits were required to ensure a negative MTC above 70% RTP. All control bank rod worth data presented here has been adjusted in accordance with Westinghouse's rod configuration β/λ correction factors. The design data utilized in this report has been taken from Westinghouse's Unit 1 Cycle 8 Core Physics Characteristics, WCAP-10376.

The Zero Power Physics testing is performed for the following reasons:

- 1) To determine the MTC and therefore, assure the MTC is less than the Technical Specification of 5 pcm/ $^{\circ}$ F below 70% RTP.
- 2) To measure control rod worths to assure an adequate shutdown margin.
- 3) To ensure power distribution is close enough to design values to permit power escalation.

A summary of the measured data and design predictions is given in Table IVa.1 with more detailed data presented in the following tables and figures:

<u>Parameter</u>	<u>Table</u>
Boron Endpoints	IVa.2
Rod Worths	IVa.3
Boron Worths	IVa.4
Isothermal Temperature Coefficient	IVa.5
Power Distribution, ARO, HZP	IVa.6
Relative Errors in Theoretical Factors, HZP, ARO	IVa.7
Nuclear Peaking Factors for Enthalpy Rise, HZP, ARO	IVa.8
Nuclear Peaking Factors for Heat Flux, HZP, ARO	IVa.9
Relative Errors in F_H from Theoretical Factors, HZP, ARO	IVa.10

The graphical results of the integral rod worths and reactivity vs. boron concentration are given as follows:

	<u>Figure</u>
Reactivity Inserted vs. Boron Concentration	IVa.1
Integral & Differential Overlap Rod Worth, HZP, BOC	IVa.2
Integral & Differential Worth of Control Bank D, HZP, BOC	IVa.3
Integral & Differential Worth of Control Bank C, HZP, BOC	IVa.4
Integral & Differential Worth of Control Bank B, HZP, BOC	IVa.5
Integral & Differential Worth of Control Bank A, HZP, BOC	IVa.6

Table IVa.1

D. C. Cook Unit 1 Cycle 8

Summary of Zero Power Physics Data

<u>BORON ENDPOINT</u>						
	<u>Design (ppm)</u>				<u>Measured (ppm)</u>	
ARO	1534				1578.7	
CBD in	1407				1450.5	
CBC in (D in)	1328				1374.2	
CBB in (C, D in)	1264				1293.0	
CBA in (B, C, D in)	1135				1168.2	

<u>ROD WORTH</u>			
	<u>Design (pcm)</u>	<u>Measured (pcm)</u>	<u>Corrected Measured (pcm)*</u>
CBD	1168	1191.3	1201.3
CBC (D in)	725	740.1	741.3
CBB (C, D in)	596	609.7	610.1
CBA (B, C, D in)	1190	1207.0	1179.6
Control Banks Total	3679	3748.1	3732.3
Control Banks Overlap	3679	3683.8	3668.2

<u>BORON WORTH</u>		
	<u>Design (pcm/ppm)</u>	<u>Measured (pcm/ppm)</u>
HZP BOL	-9.22	-9.13

<u>ITC</u>		
	<u>Design (pcm/°F)</u>	<u>Measured (pcm/°F)</u>
HZP BOL	0.71	0.70

<u>FLUX MAPS</u>						
	$F_{\Delta H}^{**}$		F_Q^{**}		F_Z (Core av)	
	<u>Design</u>	<u>Meas.</u>	<u>Design</u>	<u>Meas.</u>	<u>Design</u>	<u>Meas.</u>
HZP ARO	1.532	1.6296	2.027	2.2964	1.321	1.3546

* Adjusted for Westinghouse rod configuration β/λ correction factors.

** Measured, unpenalized.

Table IVa.2
 Unit 1 Cycle 8 Startup Tests
 Boron Endpoint Data ¹

ROD CONFIGURATION	C_B (ppm) INDIVIDUAL	C_B (ppm) DESIGN	ΔC_B (ppm) MEASURED-DESIGN
ARO	1572.4	1534	38.4
ARO	1585	1534	51
ARO avg	1578.7	1534	44.7
CBD IN	1450.5	1407	43.5
CBC IN	1374.2	1328	46.2
CBB IN	1293.0	1264	29.0
CBA IN	1168.2	1135	33.2

¹ The boron endpoint is the just critical boron concentration for the particular rod configuration.



Table IVa.3
 UNIT 1 CYCLE 8 STARTUP TESTS
 ROD WORTH DATA
 (in pcm)

Bank	Measured Worth	β/λ ¹ Corrected Worth	Design Worth	%Error ²
CBD	1191.3	1201.3	1168	+2.77
CBC	740.1	741.3	725	+2.20
CBB	609.7	610.1	596	+2.31
CBA	1207.0	1179.6	1190	-0.88
CONTROL BANKS TOTAL	3748.1	3732.3	3679	+1.43
CONTROL BANKS IN OVERLAP	3683.8	3668.2	3679	-0.29

1. Adjusted for Westinghouse β/λ Configuration Correction Factors. Tables A.1b and A.1c, Unit 1 Cycle 8 Design Manual (WCAP-10376).

2. %Error = $\frac{\text{Corrected Worth} - \text{Design Worth}}{\text{Corrected Worth}} \times 100\%$

Table IVa.4

UNIT 1 CYCLE 8 STARTUP TESTS

BORON WORTH DATA

BANK	BANK WORTH ¹ (pcm)	BORON ENDPOINT ² (ppm)	ΔC_B (ppm)	BORONWORTH (pcm/ppm)	DESIGN BORON WORTH (pcm/ppm)	%ERROR ³
ARO	/	1578.7	/	/	/	/
CBD	1201.3	1450.5	128.2	-9.37	-9.22	+1.60
CBC	741.3	1374.2	76.3	-9.72	-9.20	+5.35
CBB	610.1	1293.0	81.2	-7.51	-9.27	-23.44
CBA	1179.6	1168.2	124.8	-9.45	-9.24	+2.22
LEAST SQUARE FIT	--	--	--	-9.13	-9.22	-0.88

- Adjusted for Westinghouse β/λ Rod Configuration Factors. Tables A.1b and A.1c, Unit 1 Cycle 8 Design Manual (WCAP-10376).
- From Table IV.1
- $\%ERROR = \frac{\text{Calculated (measured) Worth} - \text{Design Worth}}{\text{Calculated (measured) Worth}} \times 100$

Table IVa.5
 Unit 1 Cycle 8 Startup Tests
 ARO Isothermal Temperature Coefficient

TEST NUMBER	ITC (pcm/°F)						
	DESIGN	HEATUP		COOLDOWN		AVERAGE	
		ITC	ERROR*	ITC	ERROR*	ITC	ERROR*
1	0.71 ± 3.0	0.67	0.04	0.75	-0.04	0.71	0.0
2	0.71 ± 3.0	0.58	0.13	0.78	-0.07	0.68	0.03

*Error = Design - Measured

Table IVa.6

Unit 1 Cycle 8 HZP Power Distribution

MAP	CBD (steps)	F_Q^N	F_Q^P	F_Q^T	$F_{\Delta H}^N$	$F_{\Delta H}^T$	Axial Offset (%)
108-01	226	2.2964	2.4835	3.8310	1.6296	1.9278	18.933

P Measured, penalized by 1.05 and 1.03

N Measured, upenalized

T Technical Specification Limit

Table IVa.7

10801 10/21/83 2% RTP BOL, HZP, ARO, 3D-ANALYTICAL FACTORS
AEP - THIMBLE DATA

RELATIVE ERRORS IN DETECTOR THEORETICAL FACTORS, (CALC.-MEAS.)/MEAS., FOR AXIAL CONFIGURATION 2

	R	P	N	M	L	K	J	H	G	F	E	D	C	B	A
1					*****	*****	*****	*****	*****	-0.045	*****				
2			0.031	*****	*****	-0.004	*****	-0.065	*****	*****	*****	*****	*****	*****	*****
3		*****	*****	*****	*****	*****	*****	-0.059	*****	*****	*****	0.010	*****	0.001	
4		0.008	0.033	*****	*****	*****	*****	-0.011	*****	*****	*****	*****	*****	*****	*****
5	*****	*****	*****	*****	0.060	*****	*****	*****	0.036	*****	*****	*****	*****	*****	*****
6	-0.009	*****	-0.017	*****	*****	0.073	*****	*****	*****	*****	*****	*****	*****	*****	-0.029
7	*****	*****	*****	0.009	*****	*****	0.077	*****	*****	0.068	*****	*****	0.006	*****	*****
8	*****	*****	-0.061	*****	*****	*****	0.069	*****	*****	0.071	*****	-0.026	-0.041	-0.035	*****
9	*****	-0.053	*****	*****	*****	*****	*****	*****	*****	*****	0.044	*****	*****	*****	-0.069
10	*****	*****	*****	*****	0.042	*****	0.036	*****	*****	*****	*****	0.041	*****	*****	*****
11	-0.025	*****	*****	*****	0.051	*****	*****	*****	*****	*****	0.073	*****	*****	*****	-0.026
12		*****	*****	*****	*****	*****	*****	*****	-0.002	*****	*****	0.026	*****	*****	*****
13		*****	0.005	*****	0.018	*****	*****	-0.061	*****	*****	*****	*****	*****	*****	*****
14			0.020	*****	*****	*****	*****	*****	*****	-0.017	*****	-0.005	*****		
15					-0.038	*****	*****	-0.074	*****	*****	*****				

THE MEAN VALUE = 0.0029 AND THE STANDARD DEVIATION = 0.0439 FOR THE ABOVE 46 VALUES

THE MEAN OF THE ABSOLUTE VALUES = 0.0365 . THE MAXIMUM MAGNITUDE = 0.0765 AT 7 - J . THE MAX NEG = -0.074 AT 15 - J

Table IVa.8

10801 10/21/83 2% RTP BOL, HZP, ARO, 3D-ANALYTICAL FACTORS
AEP - THIMBLE DATA

NUCLEAR PEAKING FACTORS FOR ENTHALPY RISE FOR ASSEMBLAGES IN THE POWER NORMALIZATION

	R	P	N	M	L	K	J	H	G	F	E	D	C	B	A
1					0.401	1.044	1.193	1.267	1.216	1.085	0.417				
2			0.248	0.560	1.094	1.251	1.430	1.120	1.447	1.319	1.124	0.561	0.254		
3		0.250	0.667	1.125	1.137	1.321	0.995	1.234	0.987	1.318	1.155	1.147	0.679	0.256	
4		0.565	1.121	1.112	1.146	1.038	1.170	1.077	1.142	1.056	1.184	1.134	1.155	0.576	
5	0.401	1.106	1.148	1.178	0.863	1.003	0.833	0.998	0.839	1.016	0.882	1.184	1.182	1.126	0.412
6	1.047	1.260	1.307	1.039	1.040	0.808	1.017	0.786	1.038	0.817	1.002	1.084	1.310	1.286	1.073
7	1.156	1.409	0.989	1.123	0.827	1.035	0.910	0.874	0.924	1.024	0.845	1.129	0.956	1.405	1.189
8	1.248	1.113	1.240	1.096	0.975	0.763	0.876	0.691	0.877	0.764	0.966	1.093	1.215	1.082	1.257
9	1.196	1.441	1.018	1.148	0.833	1.041	0.925	0.890	0.930	1.030	0.836	1.126	0.973	1.437	1.231
10	1.083	1.298	1.318	1.022	1.029	0.830	1.052	0.789	1.074	0.819	1.017	1.027	1.288	1.280	1.092
11	0.410	1.151	1.158	1.150	0.870	1.025	0.834	0.996	0.843	1.035	0.853	1.148	1.140	1.136	0.411
12		0.572	1.148	1.122	1.159	1.031	1.140	1.099	1.132	1.047	1.165	1.119	1.132	0.567	
13		0.252	0.679	1.146	1.150	1.313	0.924	1.238	0.989	1.319	1.149	1.149	0.675	0.255	
14			0.251	0.568	1.111	1.265	1.465	1.103	1.425	1.272	1.121	0.570	0.256		
15					0.416	1.102	1.217	1.284	1.205	1.090	0.406				

Table IVa.9

10801 10/21/83 2% RTP BOL, HZP, ARO, 3D-ANALYTICAL FACTORS

AEP - THIMBLE DATA

NUCLEAR PEAKING FACTORS FOR HEAT FLUX, F SUB Q, FOR ASSEMBLAGES IN THE POWER NORMALIZATION

	R	P	N	M	L	K	J	H	G	F	E	D	C	B	A
1					0.549	1.442	1.636	1.748	1.679	1.517	0.577				
2			0.340	0.765	1.494	1.713	1.935	1.511	1.968	1.809	1.550	0.774	0.347		
3		0.339	0.909	1.533	1.533	1.779	1.331	1.650	1.318	1.791	1.593	1.578	0.931	0.350	
4		0.764	1.520	1.502	1.546	1.388	1.553	1.437	1.517	1.412	1.636	1.566	1.578	0.782	
5	0.548	1.501	1.550	1.593	1.143	1.329	1.110	1.339	1.119	1.356	1.120	1.636	1.594	1.527	0.559
6	1.461	1.719	1.750	1.391	1.379	1.082	1.378	1.053	1.393	1.094	1.346	1.448	1.752	1.745	1.469
7	1.610	1.911	1.325	1.496	1.103	1.395	1.239	1.197	1.250	1.383	1.121	1.498	1.270	1.892	1.625
8	1.723	1.507	1.663	1.475	1.315	1.035	1.212	0.941	1.198	1.027	1.294	1.451	1.624	1.456	1.724
9	1.644	1.952	1.368	1.533	1.112	1.403	1.264	1.222	1.249	1.380	1.106	1.487	1.294	1.941	1.700
10	1.492	1.772	1.769	1.371	1.369	1.113	1.431	1.074	1.460	1.091	1.348	1.374	1.717	1.735	1.508
11	0.560	1.563	1.568	1.556	1.171	1.371	1.122	1.360	1.137	1.390	1.147	1.561	1.541	1.545	0.561
12		0.777	1.565	1.524	1.572	1.389	1.541	1.496	1.530	1.420	1.591	1.538	1.550	0.771	
13		0.344	0.923	1.560	1.569	1.776	1.330	1.673	1.341	1.791	1.569	1.567	0.924	0.348	
14			0.346	0.777	1.527	1.742	2.018	1.514	1.955	1.751	1.537	0.783	0.351		
15					0.577	1.545	1.703	1.806	1.679	1.524	0.558				

Table IVa.10

10801 10/21/83 2% RTP BOL, HZP, ARO, 3D-ANALYTICAL FACTORS
ACP - THIMBLE DATA

RELATIVE ERRORS IN F SUB DELTA H CALCULATED FROM WEIGHTED THEORETICAL FACTORS, (CALC.-MEAS.)/MEAS.

	R	P	N	M	L	K	J	H	G	F	E	D	C	B	A
1					0.001	-0.001	-0.034	-0.056	-0.052	-0.039	-0.036				
2			0.028	0.015	0.015	0.001	-0.042	-0.063	-0.053	-0.051	-0.012	0.012	0.005		
3		0.023	0.023	0.032	0.028	-0.029	-0.034	-0.059	-0.026	-0.027	0.012	0.012	0.005	-0.001	
4		0.006	0.036	0.032	0.045	0.027	-0.037	-0.015	-0.014	0.009	0.011	0.011	0.006	-0.014	
5	0.002	0.005	0.018	0.016	0.058	0.064	0.044	-0.016	0.036	0.051	0.035	0.011	-0.011	-0.013	-0.026
6	-0.004	-0.006	-0.019	0.025	0.027	0.069	0.070	0.039	0.049	0.057	0.065	-0.017	-0.021	-0.026	-0.028
7	-0.003	-0.027	-0.028	0.004	0.051	0.053	0.075	0.067	0.060	0.064	0.029	-0.002	0.006	-0.025	-0.031
8	-0.042	-0.057	-0.063	-0.032	0.007	0.070	0.065	0.069	0.065	0.069	0.016	-0.030	-0.044	-0.031	-0.019
9	-0.037	-0.049	-0.056	-0.019	0.043	0.046	0.058	0.049	0.052	0.057	0.040	0.001	-0.012	-0.046	-0.064
10	-0.037	-0.035	-0.027	0.042	0.038	0.041	0.035	0.035	0.014	0.054	0.050	0.038	-0.005	-0.022	-0.045
11	-0.020	-0.035	0.010	0.041	0.049	0.041	0.042	-0.014	0.031	0.032	0.069	0.043	0.026	-0.022	-0.023
12		-0.008	0.012	0.022	0.033	0.033	-0.012	-0.035	-0.005	0.018	0.027	0.025	0.026	0.001	
13		0.011	0.004	0.013	0.017	-0.024	-0.023	-0.062	-0.028	-0.028	0.018	0.011	0.010	-0.000	
14			0.018	0.001	-0.000	-0.010	-0.065	-0.048	-0.038	-0.016	-0.009	-0.004	-0.004		
15					-0.035	-0.053	-0.053	-0.069	-0.043	-0.044	-0.010				

THE MEAN VALUE = 0.0033 AND THE STANDARD DEVIATION = 0.0365 FOR THE ABOVE 193 VALUES

THE MEAN OF THE ABSOLUTE VALUES = 0.0307 . THE MAXIMUM MAGNITUDE = 0.0751 AT 7 -J . THE MAX. NEG. = -0.0686 AT 15-H .



1
2
3

1
2
3
4
5
6
7
8
9
10
11
12
13
14
15
16
17
18
19
20
21
22
23
24
25
26
27
28
29
30
31
32
33
34
35
36
37
38
39
40
41
42
43
44
45
46
47
48
49
50
51
52
53
54
55
56
57
58
59
60
61
62
63
64
65
66
67
68
69
70
71
72
73
74
75
76
77
78
79
80
81
82
83
84
85
86
87
88
89
90
91
92
93
94
95
96
97
98
99
100

22

22

1

FIGURE IVa.2

Unit 1 Cycle 8 Differential and Integral Rod Worth in Overlap

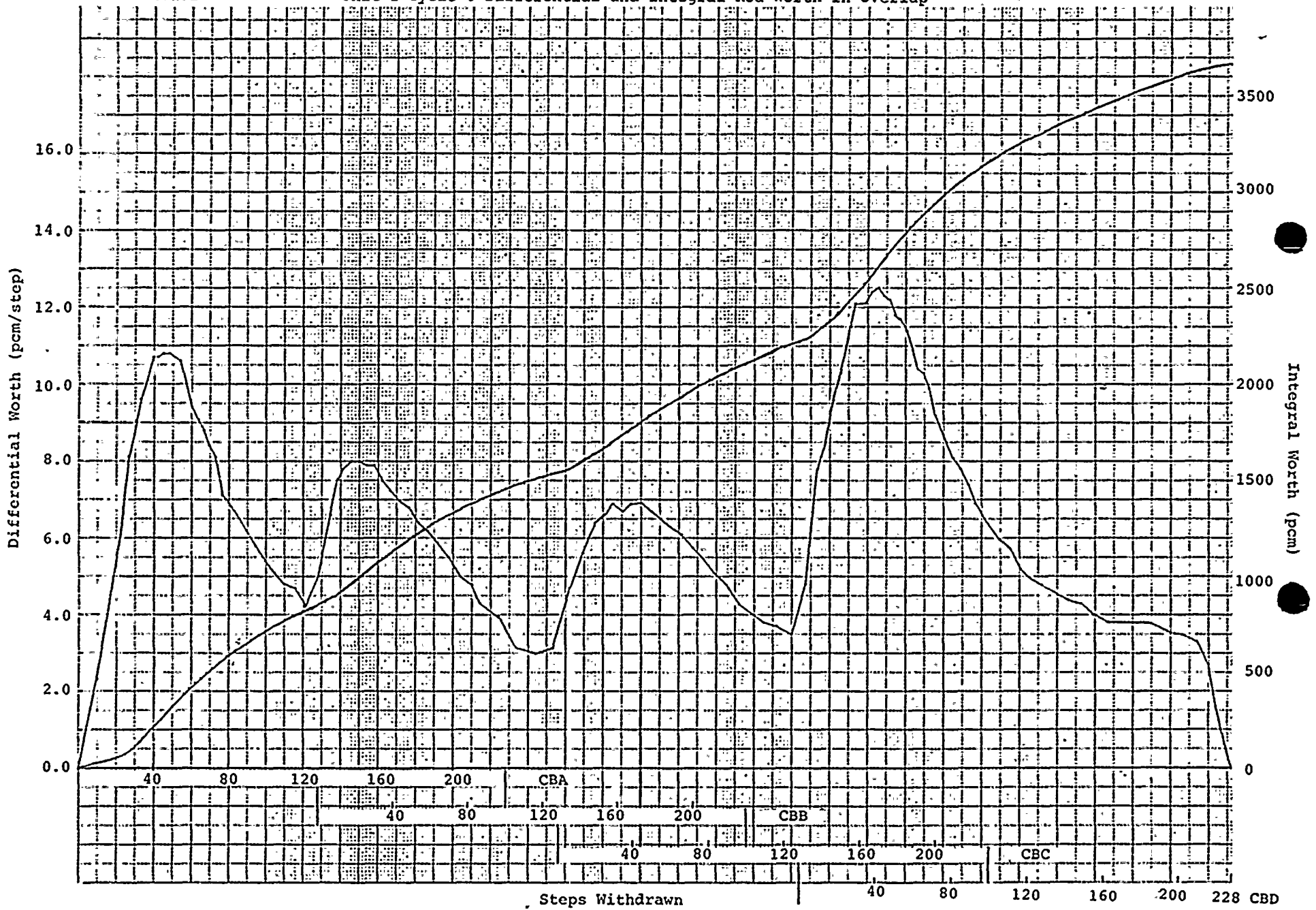


FIGURE IVa:1

Unit 1 Cycle 8

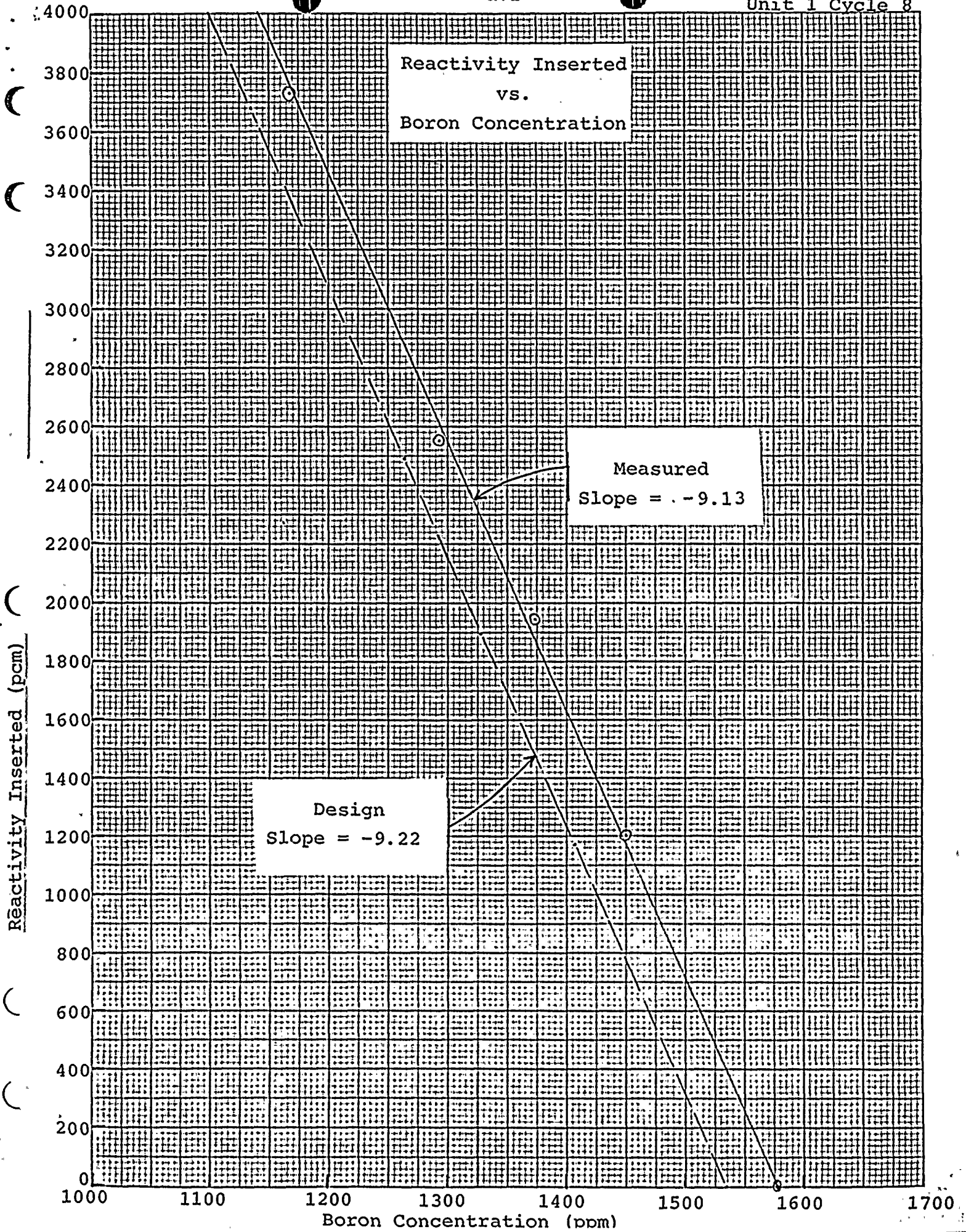
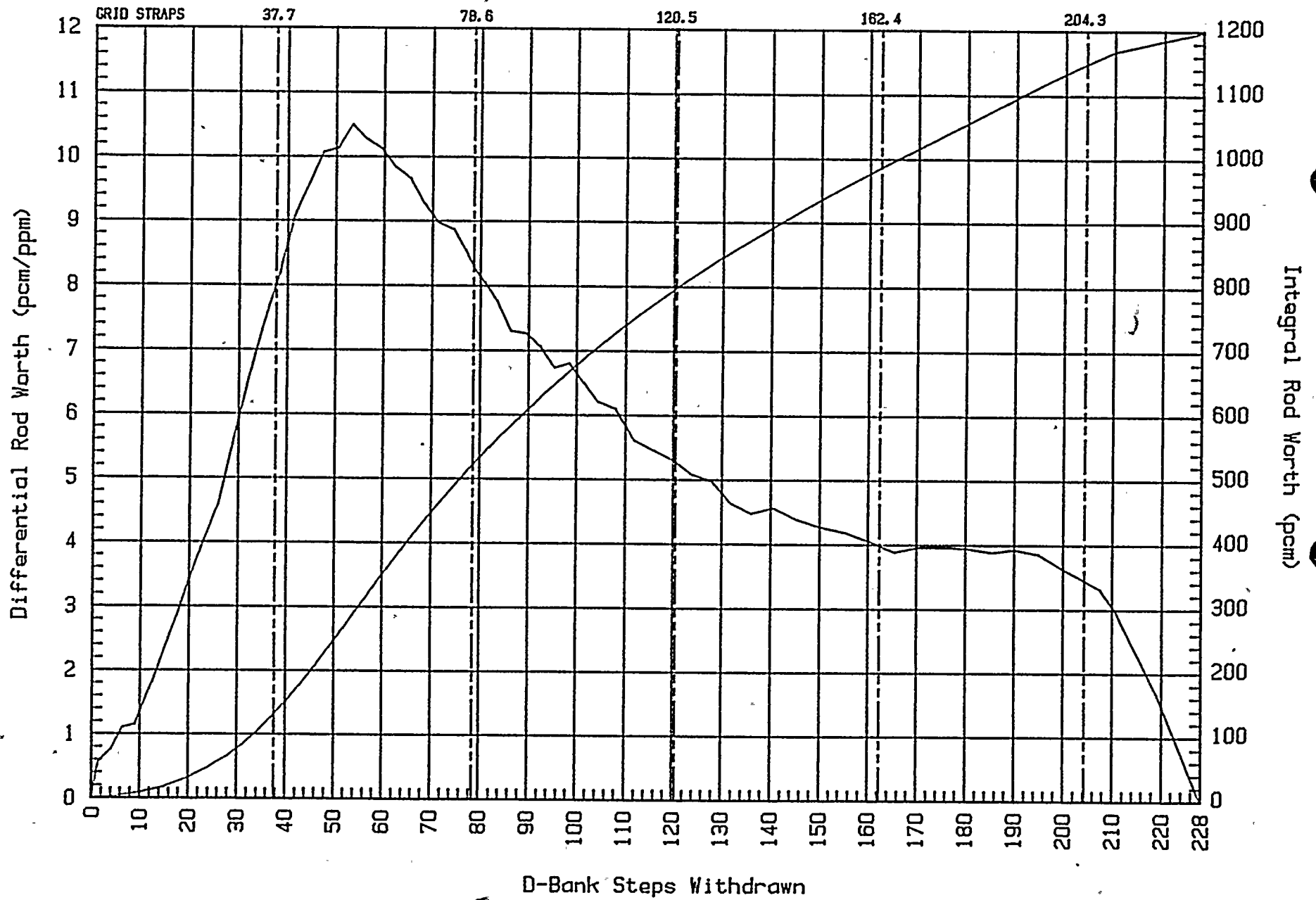


FIGURE IVa.3

D.C. Cook Unit 1 Cycle 8
Differential and Integral Rod Worth of D-Bank, HZP, BOC





•
•
•
•

2

1

1

1

1

1

1

1

1

1

1

1

1

1

2

1

1

1

1

1

1

1

1

1

1

1

1

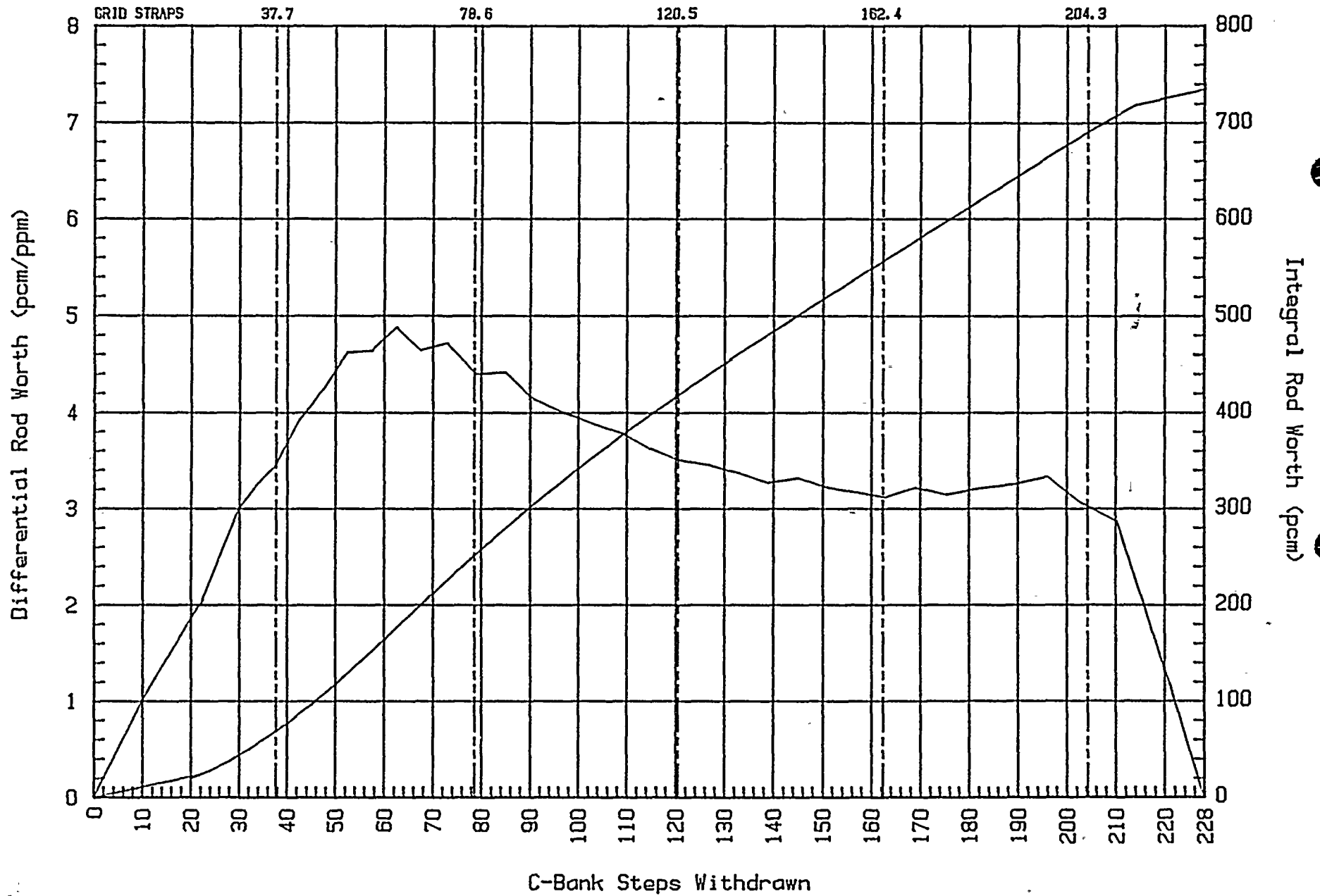
1

1

1

FIGURE IVa.4

D.C. Cook Unit 1 Cycle 8
Differential and Integral Rod Worth of C-Bank, HZP, 80C





..
..
..
..
..
..
..
..
..
..

..

..

..

..

..

..
..
..

FIGURE IVa.5

D.C. Cook Unit 1 Cycle 8
Differential and Integral Rod Worth of B-Bank, HZP, BOC

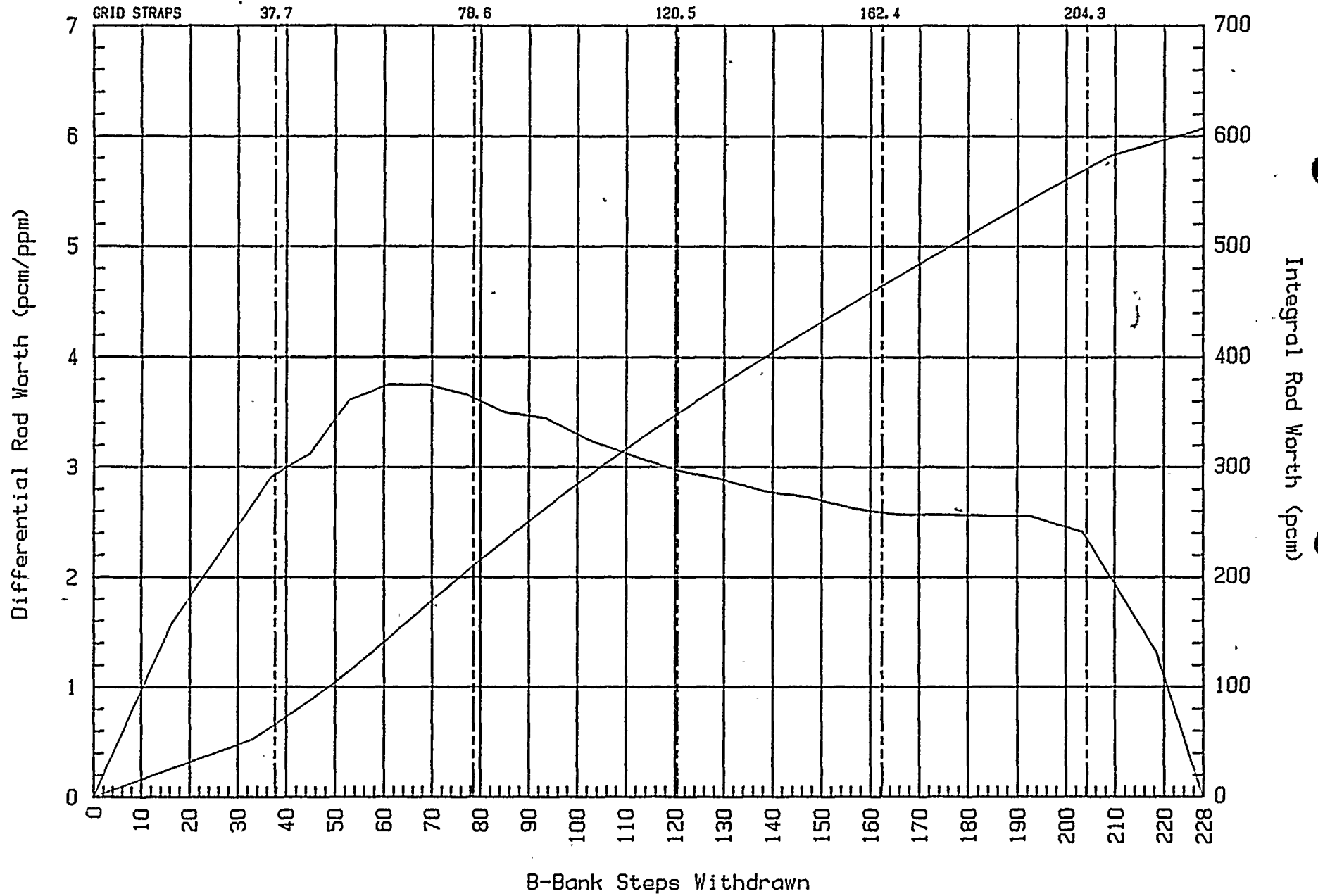
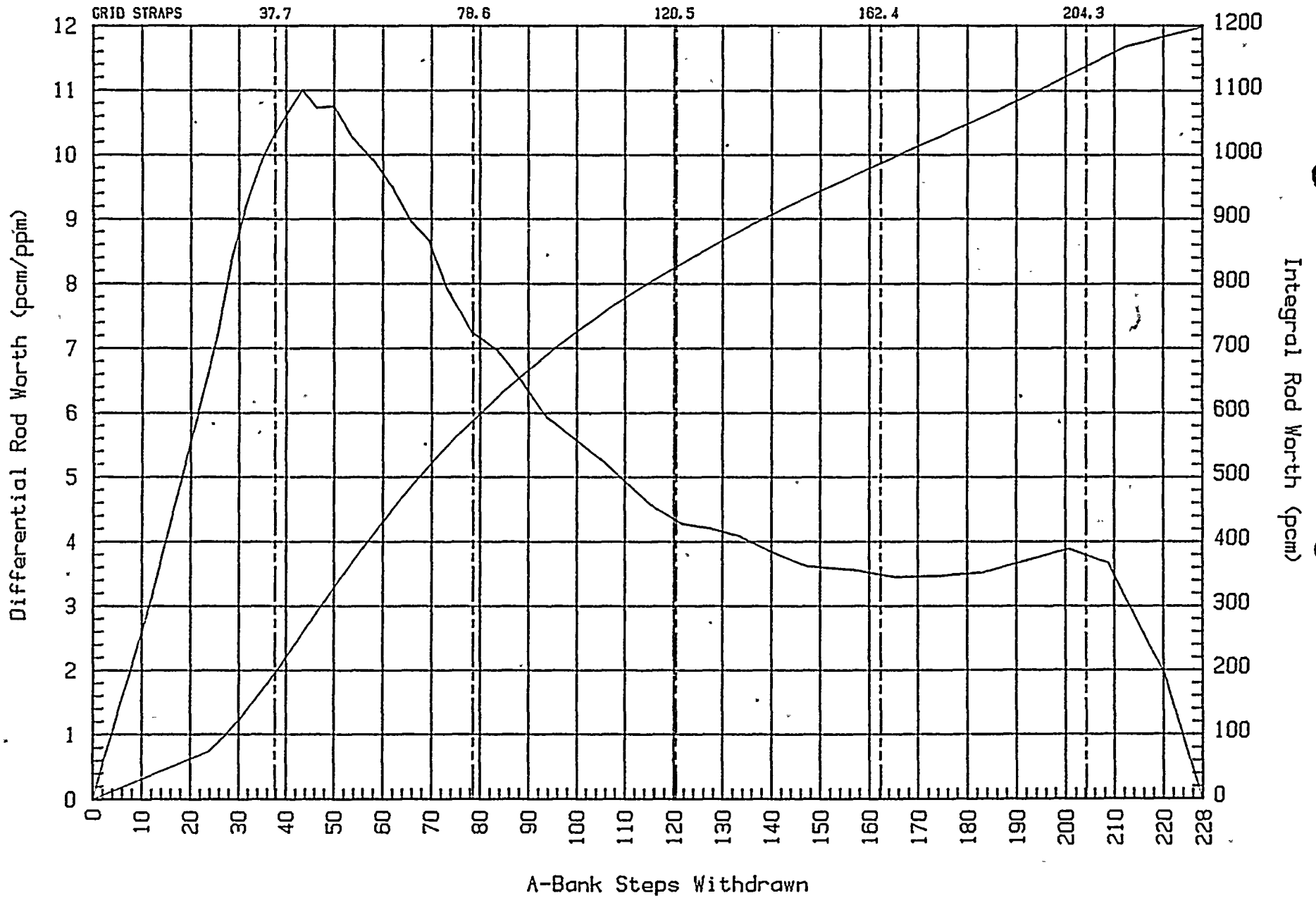
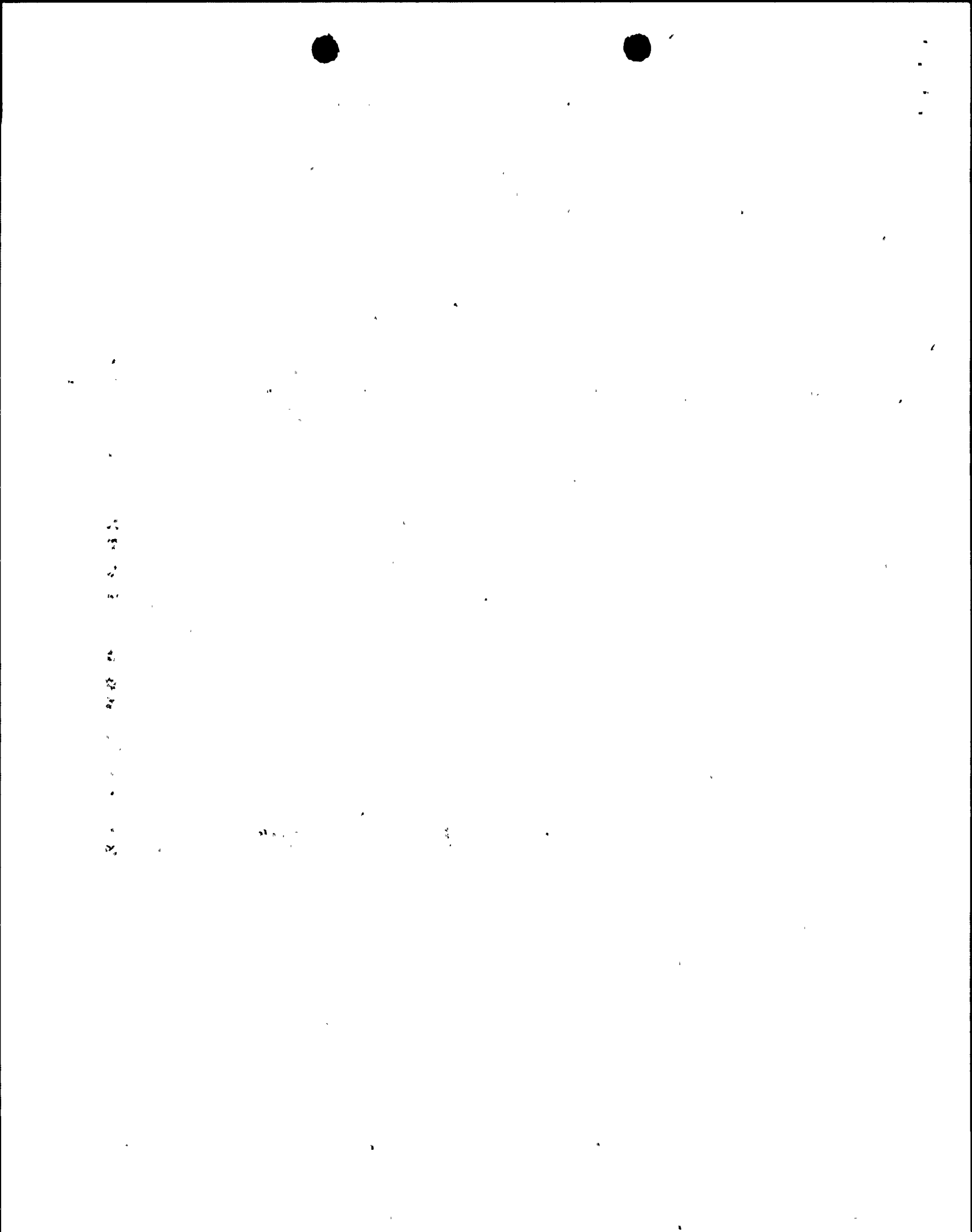


FIGURE IVa:6

D.C. Cook Unit 1 Cycle 8
Differential and Integral Rod Worth of A-Bank, HZP, BOC





IV b Low Leakage Loading Pattern (L³P)

The core design for Unit 1 Cycle 8 is characterized as a low leakage design. By comparing the Unit 1 Cycle 7 and Unit 1 Cycle 8 design manual core loading diagrams, the difference becomes apparent. The core periphery locations in Cycle 7 were composed entirely of fresh assemblies. In contrast, the Cycle 8 core design includes once and twice burned fuel loaded into periphery locations. A comparison of the two (2) loading patterns can be seen in Figures IVb.1a and IVb.1b. The effect of loading lower "worth" fuel into the core periphery is to cause these locations to run at a lower power as compared to the previous cycle. This is illustrated quite well in Figure IVb.2 (see attachments). This figure was obtained directly from power distribution maps from the cycle design manuals. The values listed represent relative assembly powers. A value of 1.00 indicates an assembly producing a power equal to the average assembly power. It follows that a value less than 1.00 is a low power assembly and a value greater than 1.00 a high power assembly. It can be seen from Figure IVb.2 that for the same power level the periphery assemblies for Cycle 8 are producing significantly less power than the same locations in Cycle 7. In Figure IVb.3 a comparison can be seen of actual measured power distributions for 90% RTP conditions with burnups of $152 \frac{\text{MWD}}{\text{MTU}}$ and $168 \frac{\text{MWD}}{\text{MTU}}$ for the U1C7 and U1C8 cores respectively. The figure was obtained from a flux map output map of the nuclear enthalpy rise hot channel factor $F_{\Delta H}^N$. By definition, $F_{\Delta H}^N$ represents essentially the identical quantity as the computer generated relative assembly powers shown in Figure IVb.2. A comparison of Figures IVb.2 and IVb.3 show excellent agreement.

An assembly producing less power is undergoing fewer fissions per second and, therefore, producing fewer neutrons per second. Based on the neutron diffusion length, peripheral assemblies can be shown to be the significant contributors to neutron leakage flux from the core. Based on the core power distribution maps and the two (2) important statements above it becomes apparent that at the same power level the Cycle 7 core had a much greater leakage flux than the Cycle 8 core.

Since all nuclear instrumentation protective functions supplied by the excore instruments rely on the leakage flux, it was important to consider the low leakage core design effects on the excore detectors. Of particular concern was obtaining a method to generate excore detector calibration factors for initial startup. Work on this problem was pursued independently at D. C. Cook, AEPSC and Westinghouse.

All of the approaches were quite similar, using an equation of the general form:

$$I_{c8} = I_{c7} \times \frac{\sum_{i=1}^N k^i P_8^i}{\sum_{i=1}^N k^i P_7^i} = I_{c7} \times R_{8/7}$$

I_{c8} = Calculated Cycle 8 current at 0.0% A.O.

I_{c7} = Cycle 7 current from last In/Ex at 0.0% A.O.

k^i = Assembly i weighting factor

P_8^i = Assembly i Cycle 8 power

P_7^i = Assembly i Cycle 7 power

$R_{8/7}$ = Weighting ratio

This equation essentially represents a ratio of integrated corner power which will consequently represent a ratio of leakage fluxes. The approach actually used for the problem involved using EOC U1C7 excore currents generated by the last Incore/Excore calibration and an applied weighted ratio. Comparing the results of their independent studies, D. C. Cook, AEPSC and Westinghouse agreed to also apply a geometric weighting factor (k^i) based on the number of exposed faces. Assemblies with two (2) exposed faces were assigned a value of 1, one (1) exposed face a value of 1/3, and 0 exposed faces a value of 1/6. These values were then multiplied by the appropriate computer generated relative assembly power for BOC 8 and by measured power distribution for EOC 7. Then taking the ratio of these values ($\frac{BOC8}{EOC7}$) the weighting ratio was found to be 0.5645.

Also of concern for initial startup was the effect of the low leakage core design on trip set points. The initial calibration factor obtained from the analysis previously discussed ensured conservative operation of power range (PR) excore detectors with respect to trip set points. To ensure conservatism of the power range trip set point due to uncertainty of the initial calibration, the PR trip was set at 80% RTP until after the 50%

Incore/Excore calibration. The normal setpoint is 109% RTP. Based on the expected power distribution on the 0° and 180° flats, the Intermediate Range (IR) trip set points were not expected to be affected significantly by the low leakage core design. To monitor the affect on the IR detectors, step 8.20 was added to **12 THP 6040 PER.359, Zero Power and Ascension Testing. This step required IR detector current readings taken at various ΔT power levels. The IR current was plotted versus ΔT power to ensure our IR trip setpoint of 25% RTP (30% maximum allowed) was not violated. Figure IVb.4 is the data that was taken during power ascension.

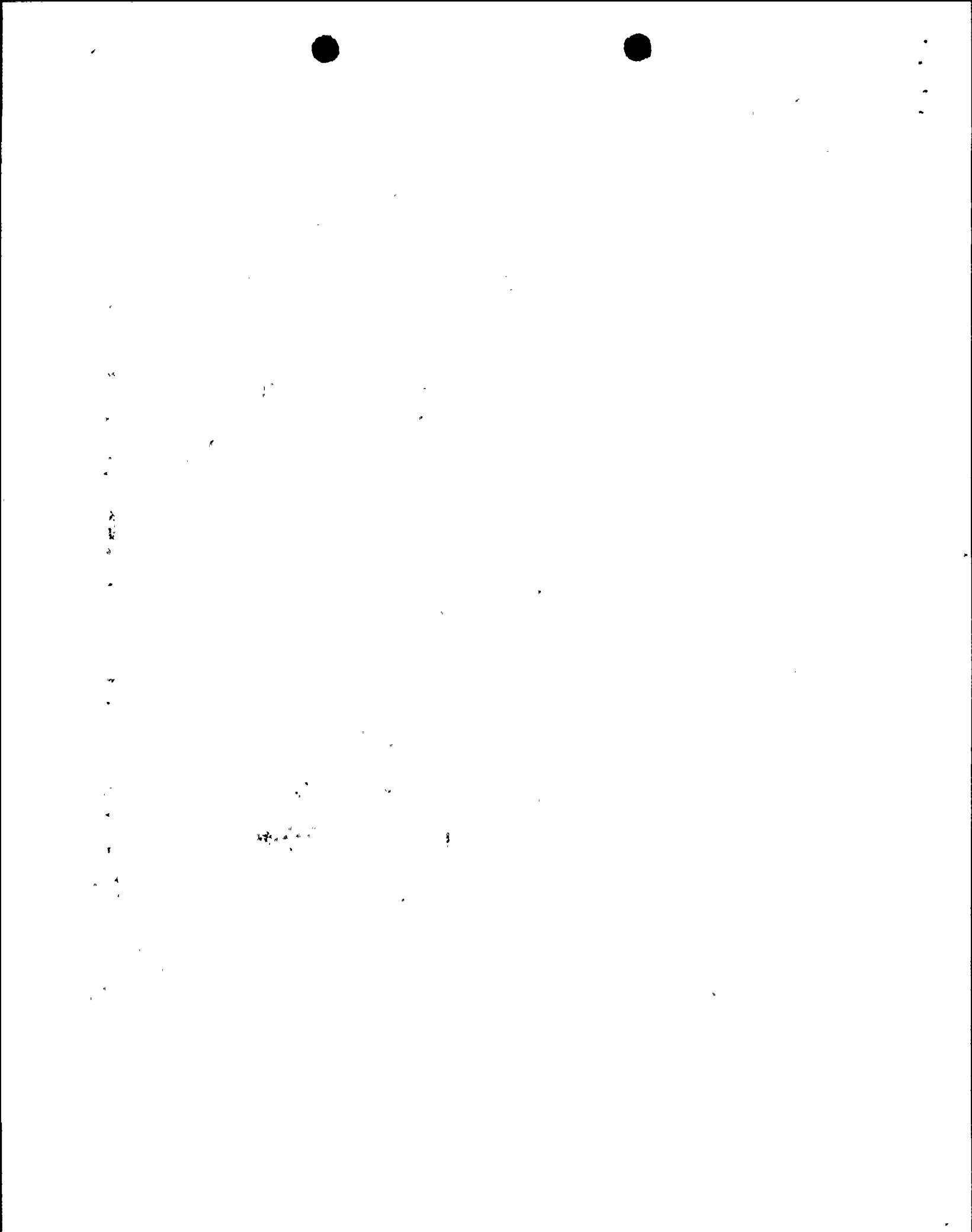


FIGURE IV b.1a

Unit 1 Cycle 7

Core Loading Diagram

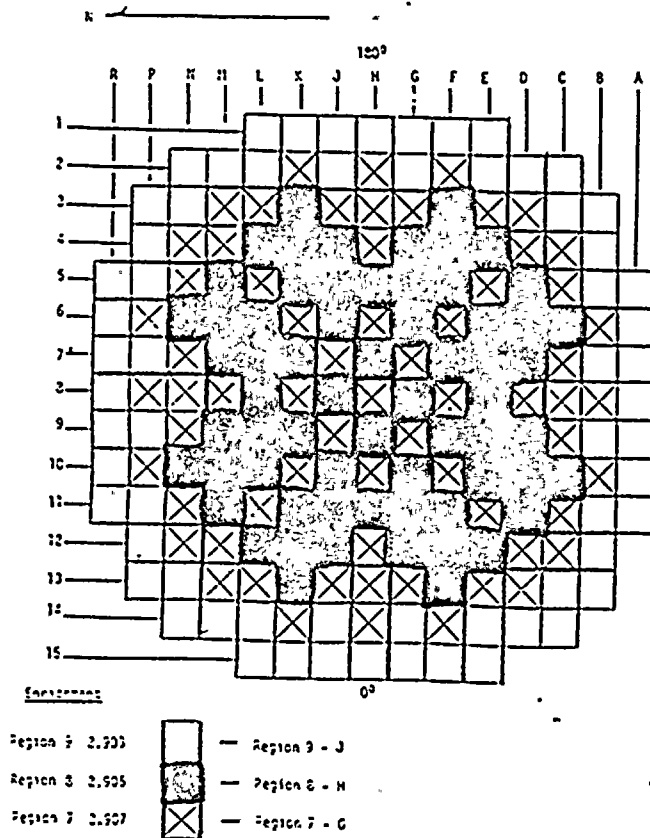


FIGURE IV b.1b

Unit 1 Cycle 8

Core Loading Diagram

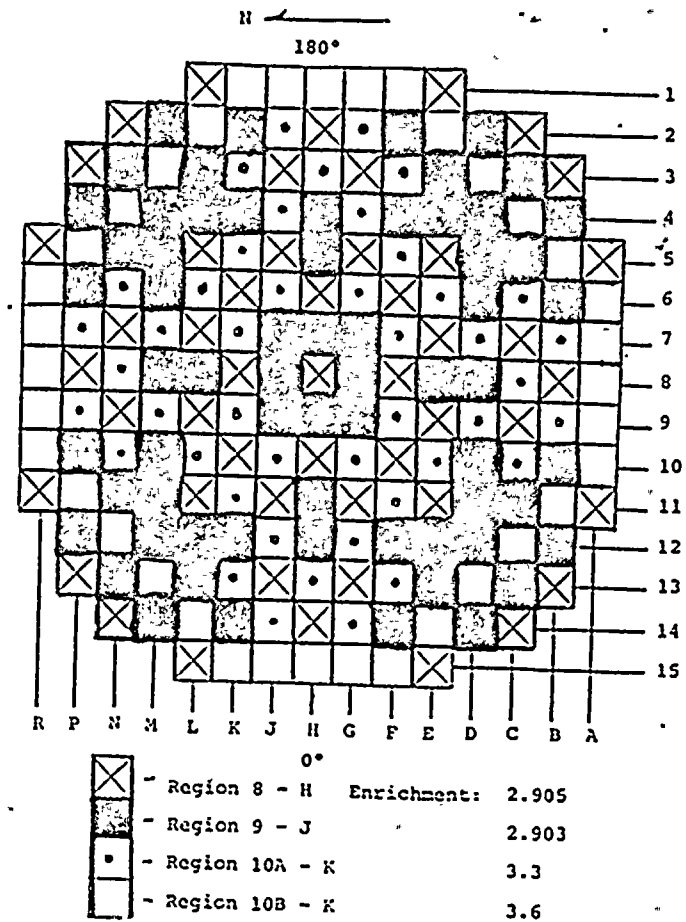


FIGURE IV, b.2

Comparison of Predicted Relative Power Distribution

.916	1.086	.977	1.156	.885	.825	.880	.908
.91	1.11	.94	1.08	1.10	1.12	0.97	1.05
1.085	1.002	1.220	1.162	1.091	.883	1.217	.929
1.11	1.13	1.20	.95	1.14	.94	1.23	1.01
.975	1.216	1.025	1.204	1.224	1.110	.904	.844
.94	1.20	.96	1.13	1.09	1.22	1.16	.95
1.54	1.159	1.204	1.022	1.197	.951	1.132	.646
1.08	0.95	1.13	.97	1.22	1.15	1.05	.40
.884	1.091	1.225	1.200	.949	.888	.911	
1.10	1.14	1.09	1.23	1.16	1.15	.58	*
.825	.883	1.111	.952	.889	1.025	.620	
1.12	0.94	1.22	1.15	1.15	.71	.28	*
.880	1.217	.904	1.133	.911	.620		
0.97	1.23	1.16	1.05	.58	.28		*
.908	.929	.844	.646				
1.05	1.01	.95	.40				*

U1C 7
HFP 150 $\frac{MWD}{MTU}$

U1C 8
HFP 100 $\frac{MWD}{MTU}$

* Assemblies considered to affect excore PR detectors

FIGURE IV.b.3

Comparison of Measured Relative Power Distribution

.840	1.051	.999	1.194	.925	.828	.883	.850
.887	1.073	.916	1.068	1.124	1.170	.999	1.081
1.048	1.033	1.229	1.186	1.160	.901	1.175	.879
1.073	1.084	1.182	.930	1.164	.950	1.261	1.036
.994	1.222	1.022	1.179	1.255	1.125	.899	.796
.920	1.182	.944	1.129	1.079	1.249	1.157	.956
1.193	1.180	1.179	1.045	1.239	.978	1.118	.626
1.068	.934	1.129	.943	1.188	1.152	1.057	.398
.922	1.165	1.259	1.245	.978	.904	.871	
1.127	1.155	1.079	1.188	1.129	1.140	.578	
.824	.901	1.127	.980	.905	1.007	.603	
1.182	.950	1.249	1.152	1.140	.712	.277	
.886	1.175	.901	1.120	.876	.604		
1.006	1.261	1.151	1.057	.577	.277		
.850	.879	.796	.626				
1.081	1.030	.956	.396				

U1C7 Map #11

90% RTP; 152 $\frac{MWD}{MTU}$

$F_{\Delta H}^N$ measured

U1C8 Map #8

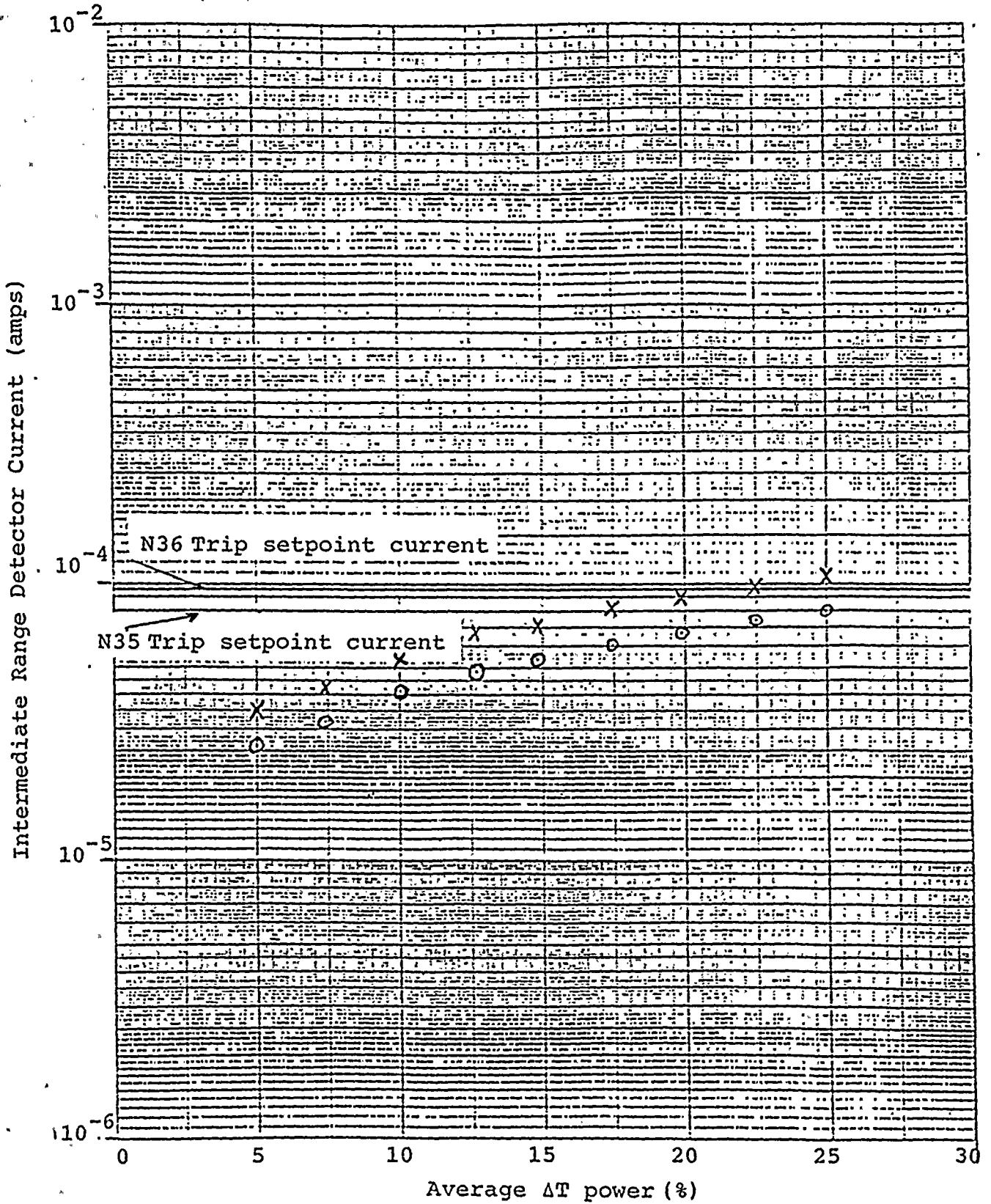
90% RTP; 168 $\frac{MWD}{MTU}$

$F_{\Delta H}^N$ measured

N35 - 0
N36 - X

FIGURE IV. b.4

I.R. DETECTOR CURRENT VS. AVERAGE ΔT POWER



IVc ICRR Plot Shapes for Unit 1 Cycle 8

Due to constraints imposed by RCCA and BPRA locations in the Unit 1 Cycle 8 core design, there were only a few locations in which secondary neutron sources could be placed. It can be seen from the core loading patterns in the fuel shuffle portion of this report that the sources went from a location two assemblies in from the core edge at H3 and H15 to the core periphery locations (F15 and K1) in the Cycle 7 to Cycle 8 transition. This movement put the secondary sources closer to the source range (SR) nuclear instrumentation. The SR detectors are used to monitor subcritical multiplication during plant shutdown and approaches to criticality.

When the sources were moved from their Cycle 7 to Cycle 8 locations an increase in counts of 20 to 30 times was observed on the source range instruments. Based on this information, an investigation by D. C. Cook Nuclear Engineering personnel was initiated to study the effects of this source range placement on ICRR (1/M) plots used during approaches to criticality. An ICRR plot is simply the ICRR ($\frac{\text{initial counts}}{\text{counts}}$) plotted versus any parameter that increases k_{eff} toward criticality. Some examples of ICRR plots are given in Figure IVc.1. The plot is considered conservative if it underpredicts criticality and non-conservative if it overpredicts critical conditions. In a situation where the source range detector is dominated by artificial source neutrons a non-conservative shape can be expected. The secondary neutron source dominates the SR detector and the detector can not detect changes in core neutron population accurately. This is sometimes referred to as source shine. The sources in Unit 1 Cycle 8 are situated in such a fashion.

A simple relationship was established to calculate the ICRR values for different values of baseline counts. The model was based on data from Unit 1 Cycle 7 initial criticality. The following equation was used to generate predicted curve shapes for U1C8 initial approach to criticality:

$$\text{ICRR} = \frac{A C_o}{A C_o + M}$$

A = Constant which the U1C7 baseline is multiplied by (ex. 10 x, 20 x, etc.).

C_o = U1C7 baseline counts

M = U1C7 multiplication at some dilution level.
(counts - baseline)

Based on this analysis, the expected curve shapes were quite non-conservative. To compensate for this expected effect, two (2) cuts in dilution rate were added to **12 THP 6040 PER.357 to give operators a slower approach to criticality. In anticipation

of future startups following plant trip, a new source range detector N-33a was installed 90° from the current detector locations. It is important to note that when criticality is close the counts on N33a will be approximately equal to Channels N31 and N32. Figures IVc.2 and IVc.3 represent actual data taken from (N31 or N32) and N33a respectively.

FIGURE IVc.1.

ICRR Plot Shapes

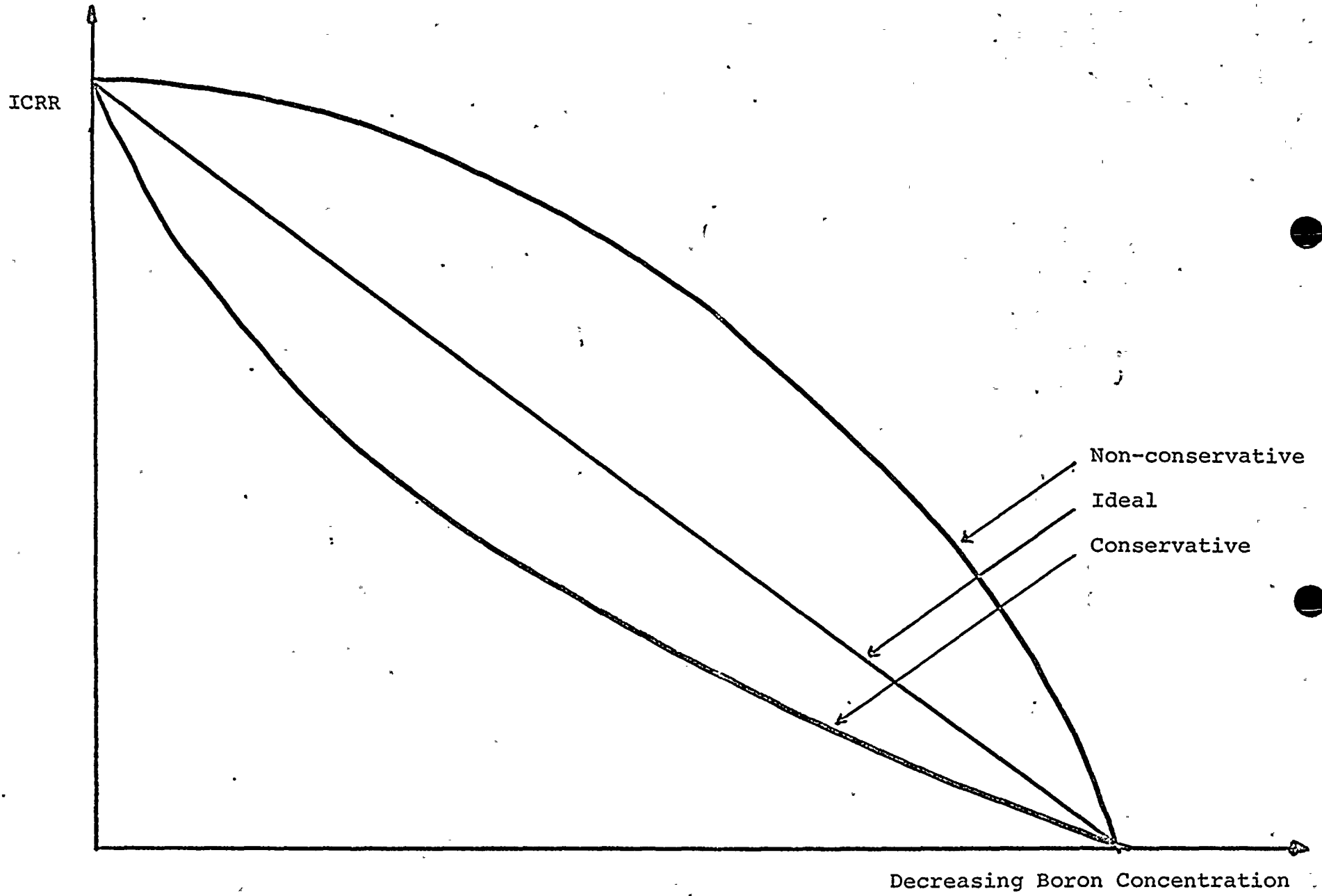
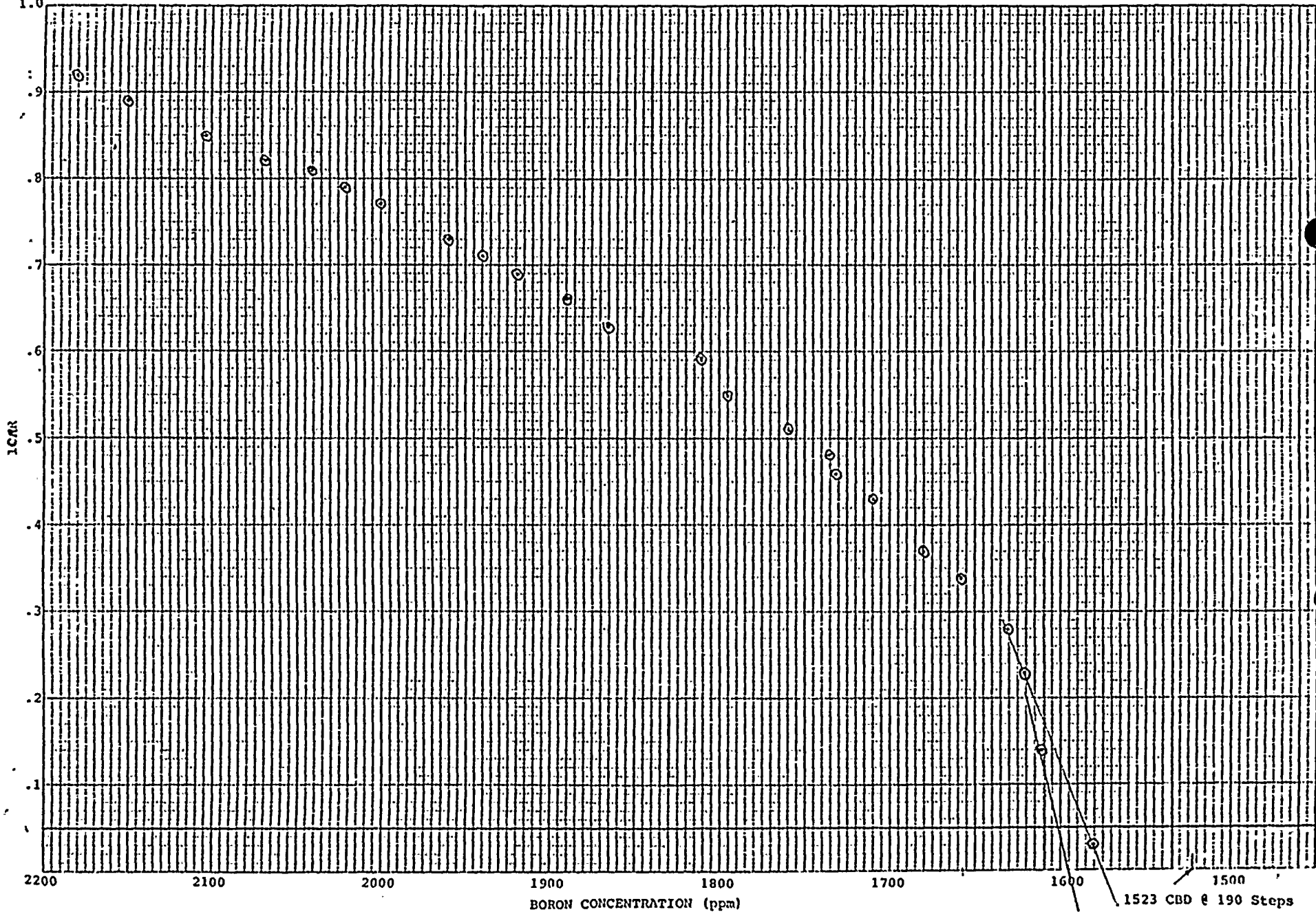


FIGURE IVc.2

UNIT 1 CYCLE 8 ICRR vs. BORON CONCENTRATION



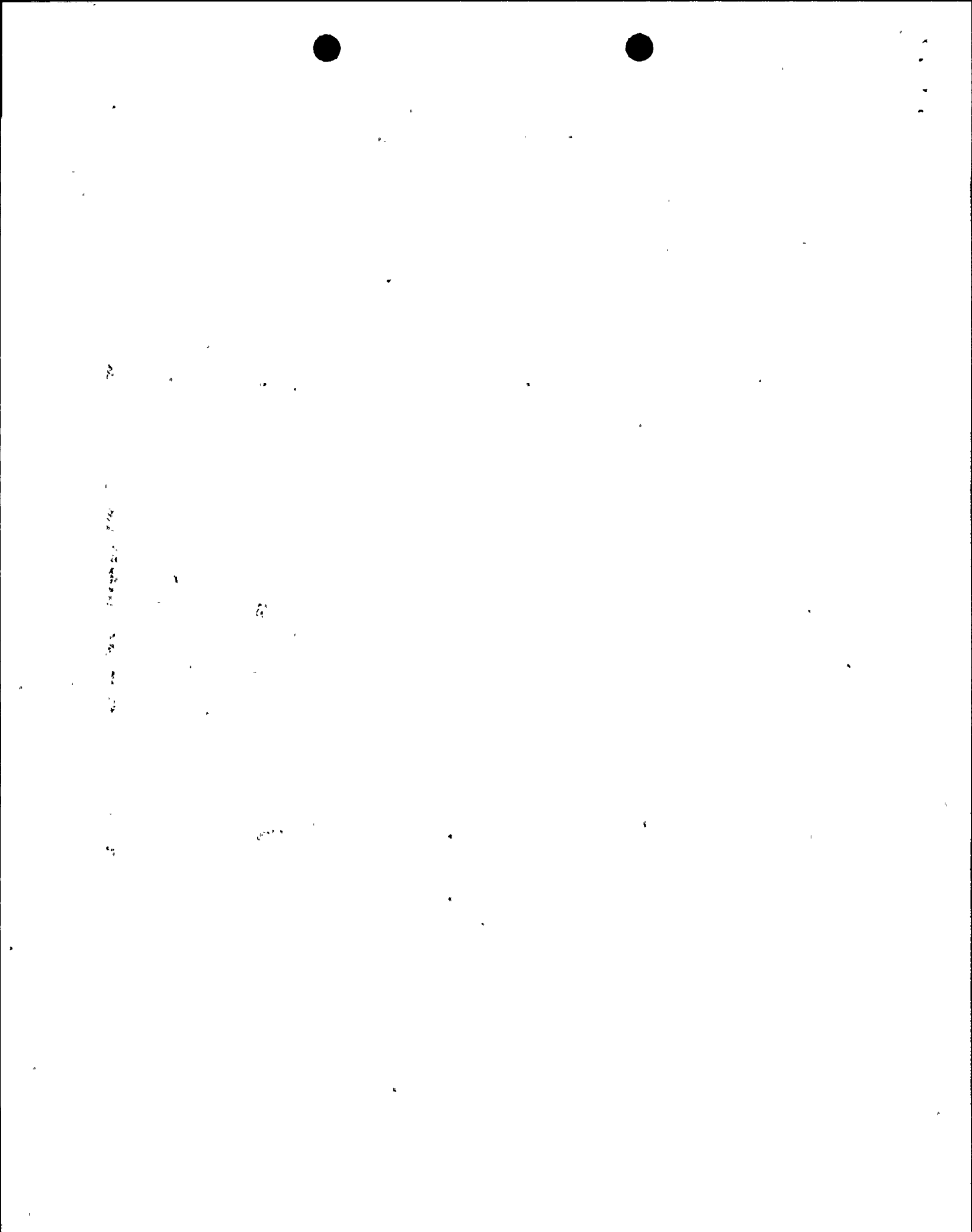
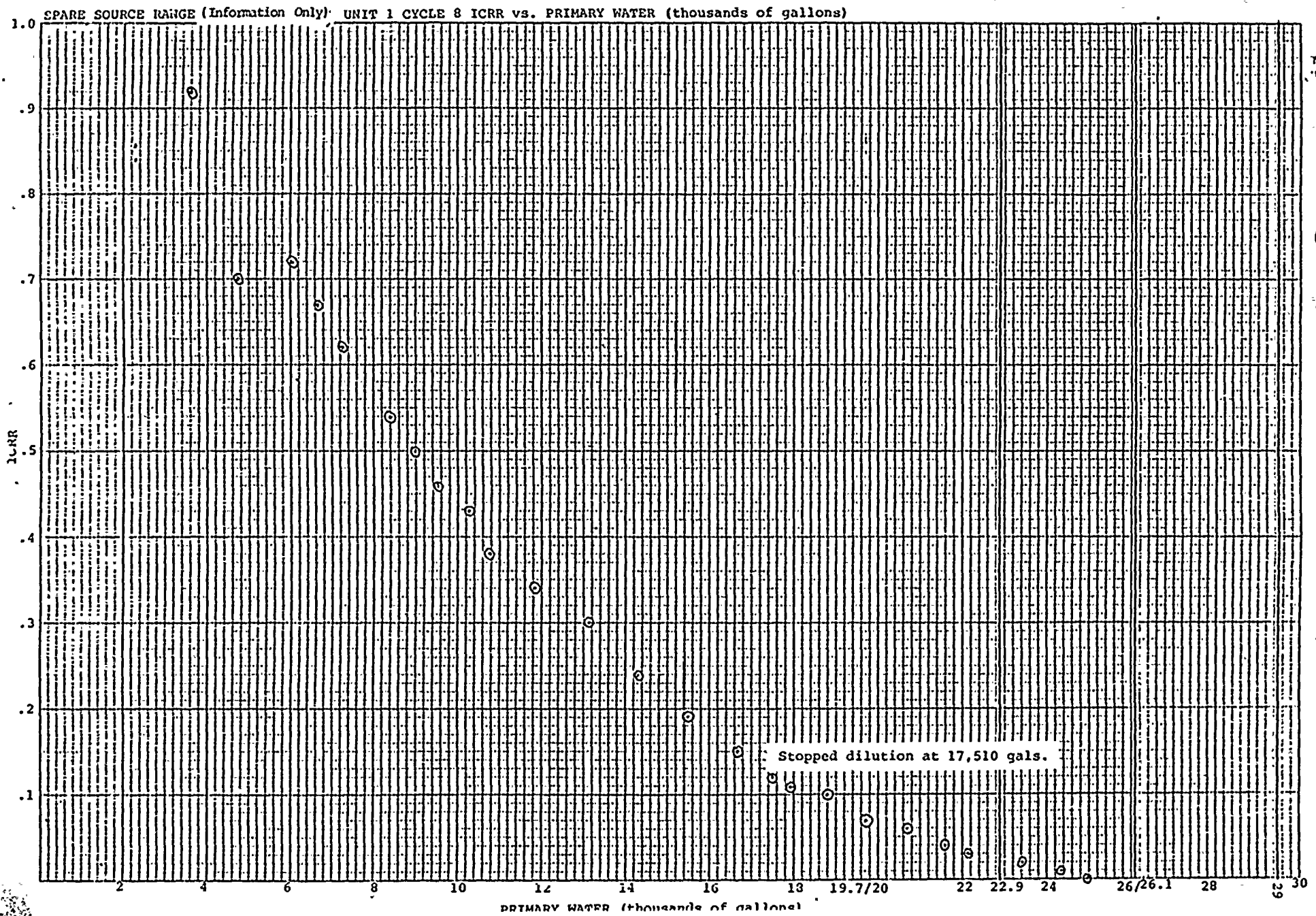


FIGURE IVc.3



IVd Problems Associated with Flux Mapping System

On October 18, 1983, during Zero Power Physics Testing, the flux mapping system leak detection alarm began to alarm intermittently. An Emergency Job Order was written to investigate whether there was a leaking thimble or a malfunction in the alarm system. Upon entering the seal table area, water was observed flowing from detector C's ten-path rotary transfer device (see Figures IVd.1 and IVd.2). The technicians investigating the situation conducted a temperature determination on the guide tubes running from detector C's ten-path rotary transfer device to the isolation valves and found thimble J-1 to be leaking (see Figure IVd.3). The J-1 isolation valve was subsequently closed and the water flow ceased.

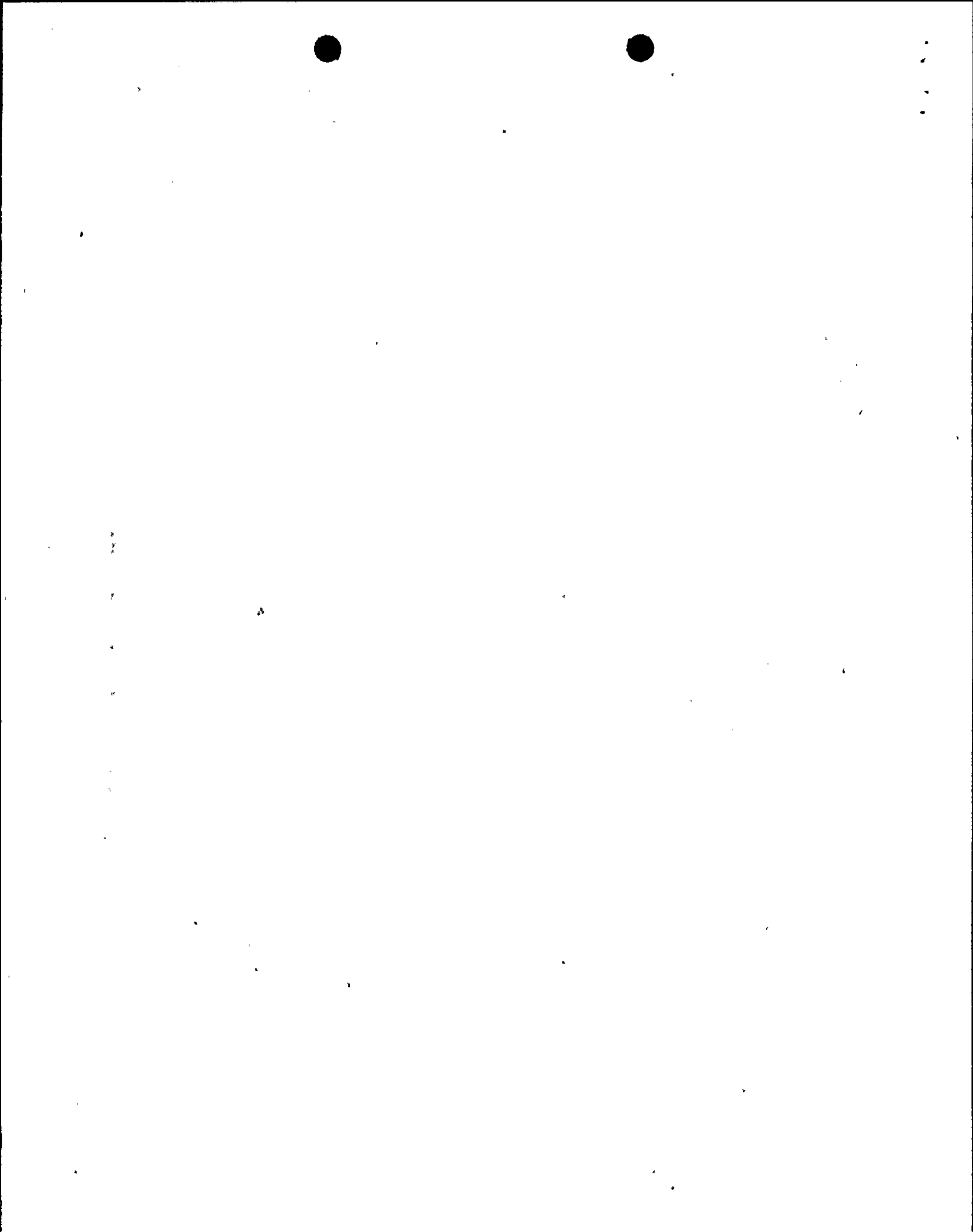
An inspection of the ten-path rotary transfer devices associated with the other five (5) detectors was conducted on October 19, 1983, to determine if borated water had "backed up" those ten-path rotary transfer device drains. All six (6) ten-path rotary transfer device drains are connected to a common line which contains the leak detector. Water was found in three (3) of the five (5) ten-path rotary transfer devices. As the potential existed for water to have gotten into the bore of the thimbles associated with these ten-path rotary transfer devices, and the detector C ten-path rotary transfer device, NUS Corporation was contracted to dewater and air-dry these thimbles as an interim step until they could be properly cleaned.

On October 26 and 27, 1983, between flux maps of the Power Ascension 50% Incore/Excore Calibration, NUS Corporation dewatered and air-dried the thimbles associated with the four (4) ten-path rotary transfer devices which contained water. Only the nine (9) thimbles of C's ten-path rotary transfer device had water within their thimble bore. No water was discharged from the thimbles associated with the three (3) other ten-path rotary transfer devices.

During the dewatering and air-drying, on October 27, 1983, a problem arose with thimble H-3 (see Figure IVd.3). During the dewatering/air-drying process the isolation valves of the suspect thimbles were disconnected from the guide tube frame assembly (see Figure IVd.2). When H-3's isolation valve was disconnected, the reactor coolant system pressure forced the thimble approximately four and one-half (4.5) inches out of the core through the seal table middle high pressure seal (see Figure IVd.4). The isolation valve was secured to the guide tube frame assembly via rope and the dewatering/air-drying of the remaining thimbles was completed.



H-3's isolation valve remained tied to the guide tube frame assembly until November 30, 1983. Prior to the cleaning of the Unit's thimbles by NUS Corporation, plant personnel reseated the H-3 thimble and tightened the middle high pressure seal. Thimble cleaning was completed on December 1, 1983.



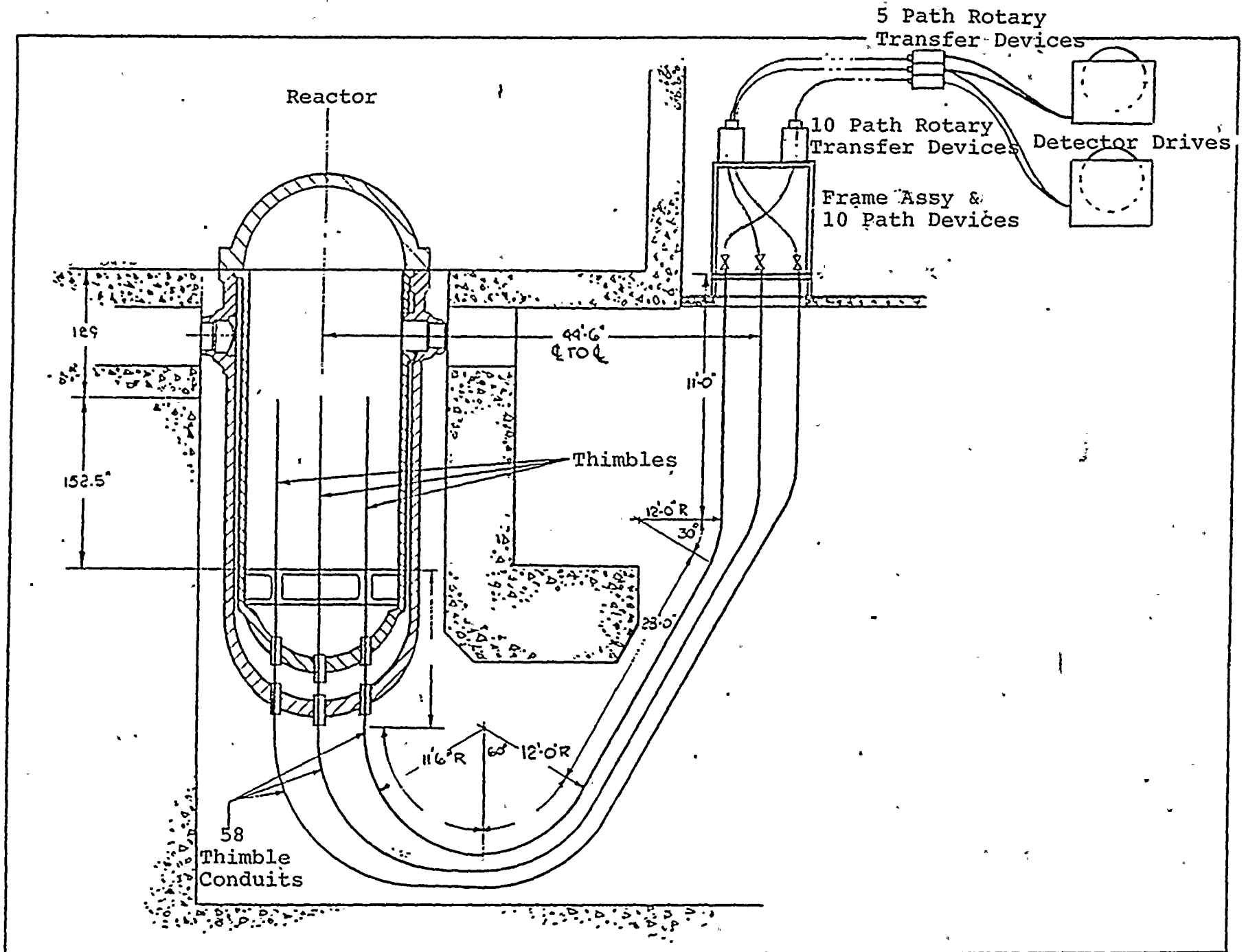


FIGURE IVd.1

GENERAL ARRANGEMENT OF REACTOR, THIMBLES AND SEAL TABLE AREA

IV d.-4

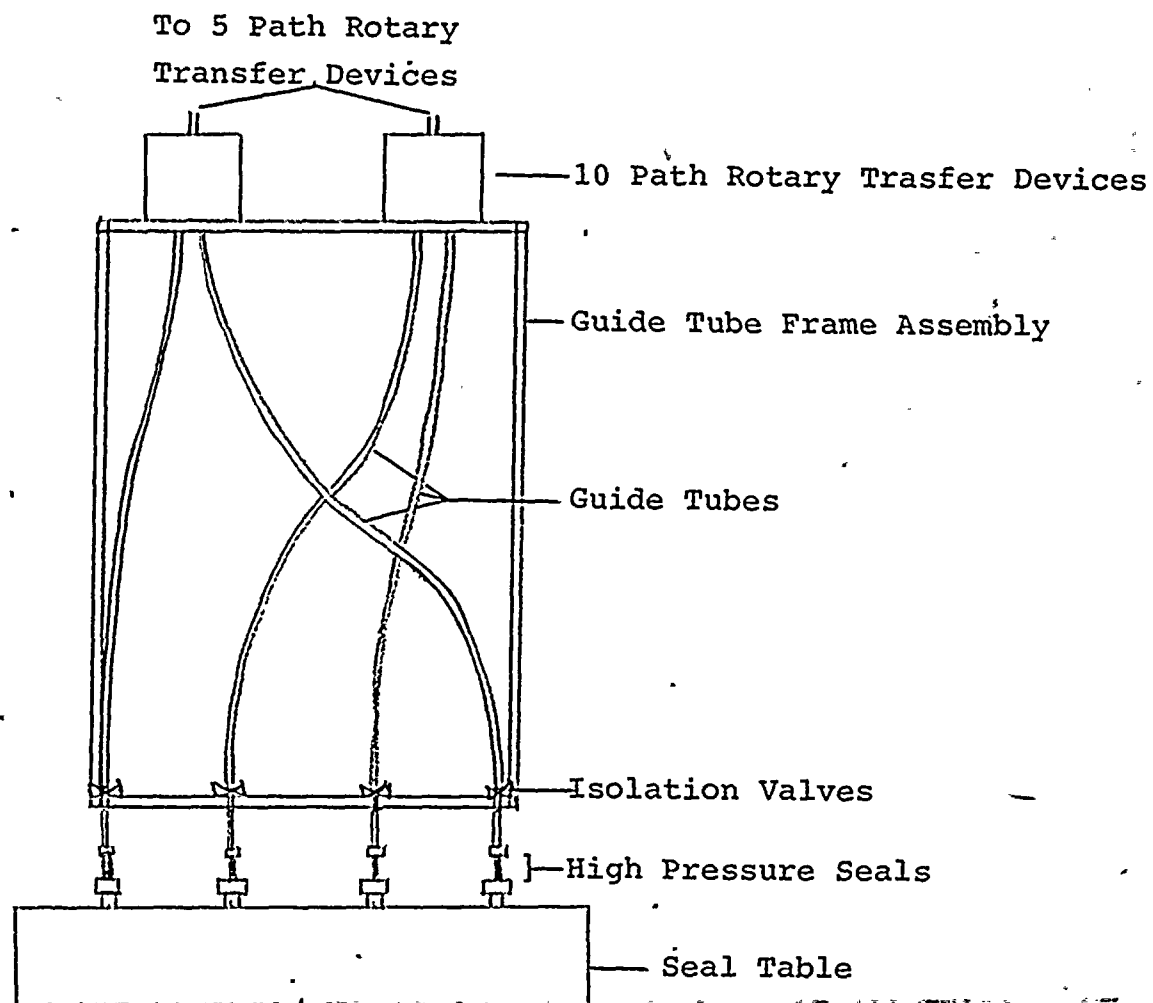
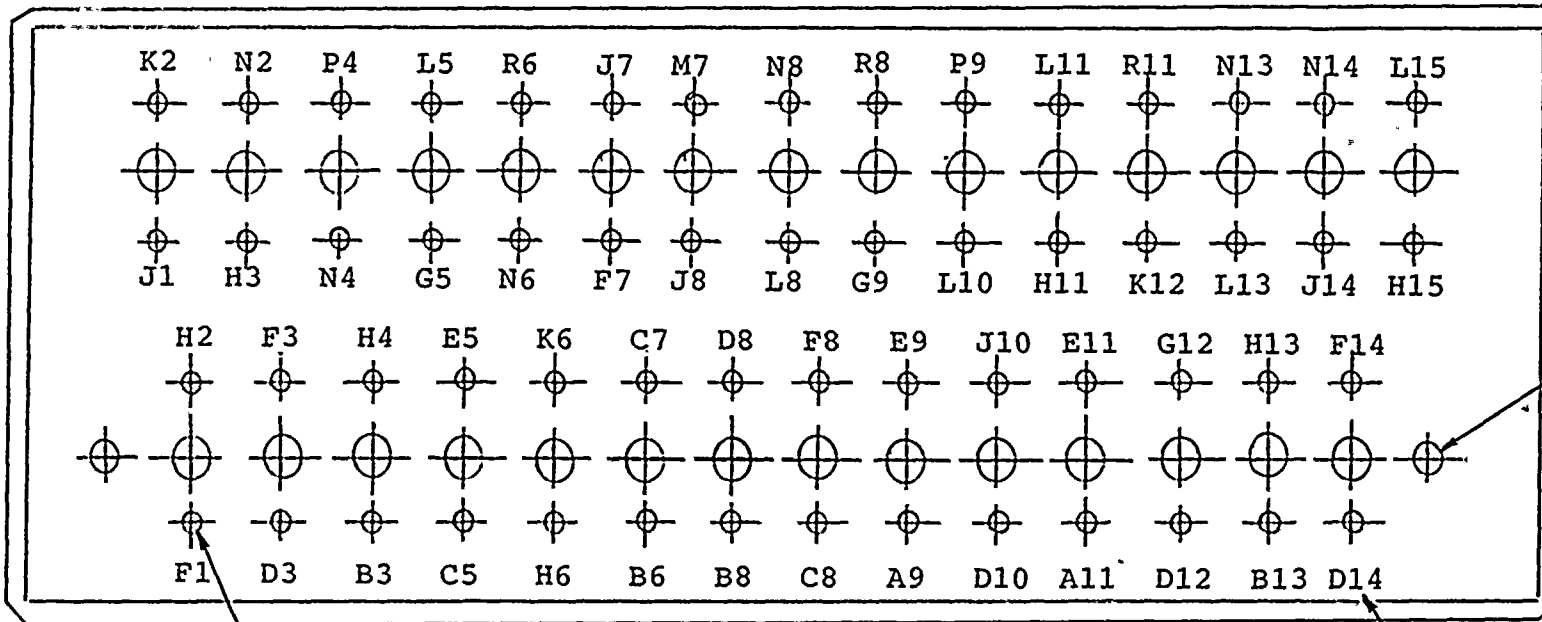


FIGURE IVd.2
SEAL TABLE AREA



1
2
3

TOWARD REACTOR



SEAL TABLE

DRAIN HOLE (2)

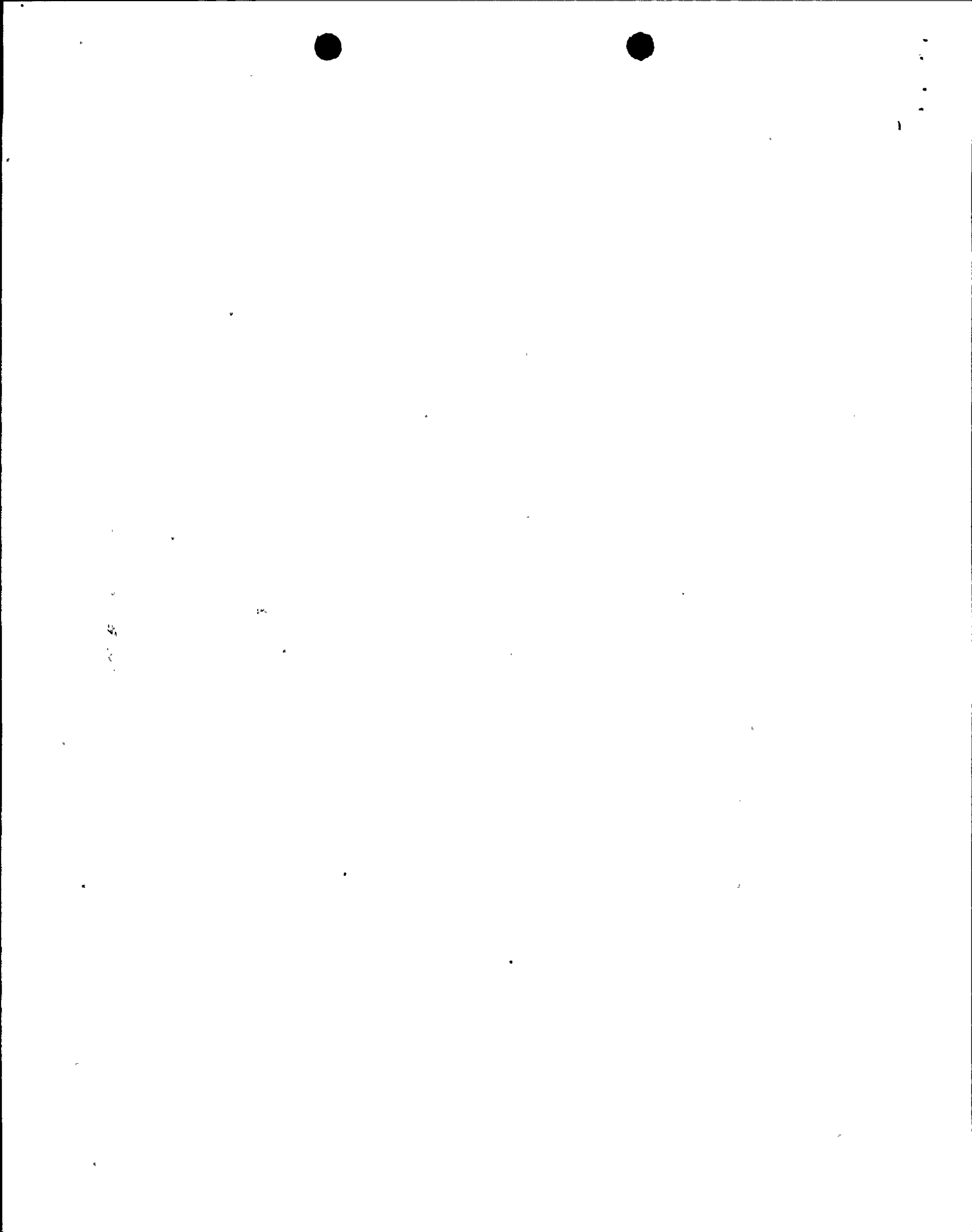
IV P 5

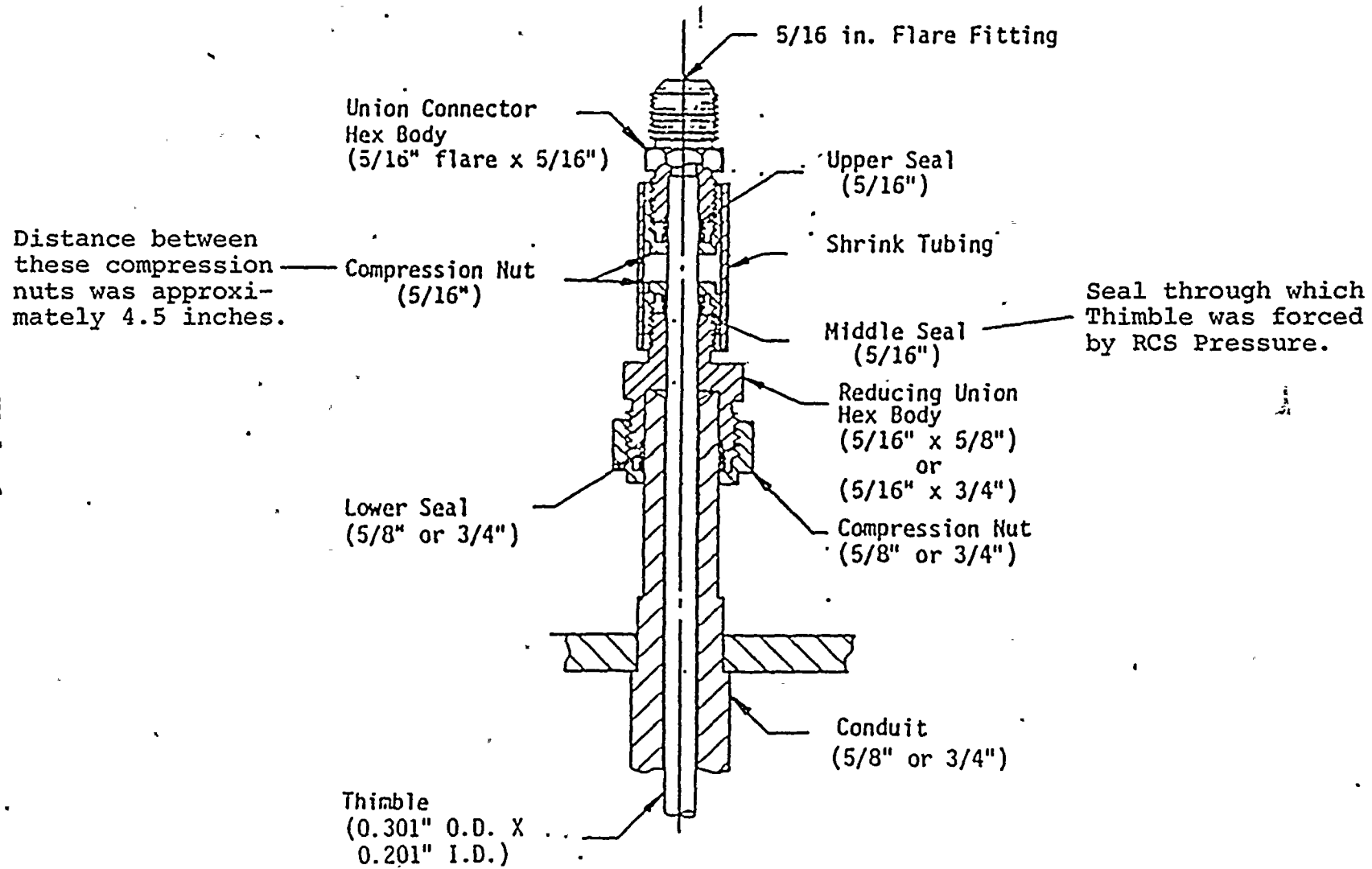
TYPICAL LOCATION OF ISOLATION VALVE, THIMBLE AND CONDUIT AT SEAL TABLE (58 LOCATIONS)

CORE LOCATION NUMBER

FIGURE IVd.3

ISOLATION VALVE AND THIMBLE ORIENTATION A SEAL TABLE





OPERATIONAL POSITION

FIGURE IVd.4

SEAL TABLE HIGH PRESSURE SEAL

Va POWER ASCENSION TESTING

The Unit 1, Cycle 8 power ascension testing commenced at 1221 hours on October 24, 1983, and was completed at 1021 hours on November 8, 1983. Figure Va.1 displays the power ascension testing program as a function of time. The power ascension testing consisted of the following:

- 1) Core power distribution measurements
- 2) Incore/excore detector cross calibration
- 3) MTC, DPC, $\Delta T/\Delta P$ testing

Flux maps were obtained at various power levels in the course of power ascension. Maps were taken at approximately 30%, 48%, 68%, 89%, 95% and 100% RTP. The power distributions were calculated by the DETECTOR code, using data obtained with the incore moveable detector system and analytical factors supplied by Westinghouse. For all of the flux maps, the power distribution measurements were in compliance with Technical Specification limits. A summary of the peaking factors at the mentioned power levels is given in Table Va.1.

At 30% RTP, a flux map was taken with control bank D positioned at the 100% RTP Rod Insertion Limit (182 steps on CBD). The flux map was taken with this configuration to verify that the Rod Insertion Limits need not be revised. Results of this map are given in Table Va.1.

At 48% RTP, four (4) full core flux maps, 108-03, 04, 05, and 06, were obtained with axial offsets ranging from -26.88% to 21.30%. The reduced data of the four (4) flux maps was used for the incore/excore detector cross calibration. Figures Va.2 through Va.5 give the excore current vs. the incore axial offset for channels N-41 through N-44. Figure Va.6 shows the incore axial offset vs. the excore axial offset for channels N-41 through N-44. Table Va.2 gives the calculated detector upper and lower currents, at selected incore axial offsets, using the least square fit program.

After C&I calibrated the NIS, making use of the reduced data, power was raised to approximately 68% RTP. Power was held constant for 24 hours to condition the fuel and to obtain a flux map. After the 24 hour hold, the MTC, DPC, and $\Delta T/\Delta P$ tests were conducted. The MTC and DPC tests were performed by control rod substitution. For the MTC, control bank D, CBD, was inserted or withdrawn while holding power constant which resulted in a temperature change. In the DPC test, the temperature was held constant for CBD insertion or withdrawal which resulted in a power change. The changes in temperature and power along with the reactivity change due to rod insertion or withdrawal were used to calculate the MTC and DPC. The $\Delta T/\Delta P$ test was performed by increasing or decreasing turbine load to acquire a temperature and power change simultaneously. Table Va.3 gives a summary of the MTC, DPC and $\Delta T/\Delta P$ tests results.

The MTC test was performed to assure a negative moderator temperature coefficient exists when power is raised above 70% RTP. The Doppler Power Coefficient test was performed to compare measured data to the design.

The $\frac{\Delta T}{\Delta P}$ test was performed to check data consistency. By comparing the measured $\frac{\Delta T}{\Delta P}$ to the measured $(-\frac{MTC}{DPC})$ and the measured $(\frac{\Delta T}{\Delta P})$ to the measured $(-\frac{DPC}{ITC})$, a check on the reliability of the measurements can be made. The ITC is derived from the measured MTC. See Table Va.3.

Due to the introduction of the WABA's in Cycle 8, the American Electric Power Service Corporation, AEPSC, determined that the use of three-dimensional, 3-D, theoretical factors was necessary for providing a better estimate of the measured local heat flux factors. Prior to power ascension, plant personnel and AEPSC personnel detected errors in the Westinghouse generated 3-D theoretical factors. Consequently, the 89% RTP flux map was analyzed using the conventional Westinghouse generated two-dimensional, 2-D, theoretical factors. As recommended by Westinghouse, the following penalties were applied to the heat flux hot channel factors, F_Q , Technical Specification limits when using the 2-D theoretical factors during power ascension:

- 1) 15% reduction in the F_Q limit for the top and bottom ten, 10, percent of the core,
- 2) 2% reduction for the next 10%, and
- 3) 1% reduction for the center sixty, 60, percent of the core.

The Allowable Power Level, APL, of the 89% RTP flux map was sufficient to allow power ascension to 95% RTP. On November 4, 1983, Westinghouse provided a set of corrected 3-D theoretical factors. After a thorough review of the 3-D theoretical factors, by AEPSC, the 89% RTP and 95% RTP flux maps were reprocessed using the corrected 3-D theoretical factors. The APL of the 89% RTP and 95% RTP flux maps, when using the corrected 3-D theoretical factors, was sufficiently high enough to allow power ascension to 100% RTP.

From an incore power distribution standpoint, power ascension went well, with little time lost due to APL (Allowable Power Level) restrictions.

CORE POWER DISTRIBUTION

<u>Map #</u>	<u>Power (%)</u>	<u>A.O. (%)</u>	<u>F_Q^{Penalized}</u>	<u>F_Q^L</u>	<u>APL (%)⁴</u>	<u>F_{ΔH}</u>	<u>F_{ΔH}^L</u>
108.02	30	-5.983 ⁵	2.1483	3.9400	80.9 ¹	1.5146	1.8033
108-03	48	-3.455	1.9611	3.9301	88.2 ¹	1.4455	1.7236
108-07	68	1.719	1.7950	2.8556	95.5 ¹	1.4196	1.6348
108-08	89	-2.262	1.8006	2.1964	96.3 ²	1.3944	1.5401
108-08	89	-2.292	1.7656	2.2184	99.2 ³	1.3639	1.5401
108-09	95	-1.428	1.7263	2.0838	101.1 ³	1.3687	1.5144
108-10	100	-2.568	1.7238	1.9726	102.3 ³	1.3612	1.4906

Penalized = Measured Value x 1.05 x 1.03

L = Technical Specification Limit

APL = Allowable Power Level

1 = 2D Factors for 50%, BOL

2 = 2D Factors for HFP, penalized K(Z)

3 = 3D Factors

4 = APL calculated for ±5% Target Band

5 = FCFM 108-02 was obtained at the 100%
Rod Insertion Limit

Table Va.2

Unit 1 Cycle 8

INCORE AND EXCORE DET. CAL 10/26/83-10/27/83 BASED ON MAPS 10803, 04, 05 and 06

DETECTOR CURRENTS IN μ AMPS CALCULATED FROM THE LEAST SQUARE FIT

	<u>Incore Axial Offsets</u>						
	-30.0	-20.0	-10.0	0.0	10.0	20.0	30.0
UPPER CURRENTS FOR DETECTOR 41	69.5917	74.8268	80.0619	85.2970	90.5322	95.7673	101.0024
LOWER CURRENTS FOR DETECTOR 41	113.9109	106.6792	99.4474	92.2157	84.9839	77.7522	70.5205
UPPER CURRENTS FOR DETECTOR 42	91.0223	98.3774	105.7325	113.0877	120.4428	127.7979	135.1531
LOWER CURRENTS FOR DETECTOR 42	133.3245	125.3725	117.4205	109.4685	101.5165	93.5645	85.6125
UPPER CURRENTS FOR DETECTOR 43	94.2801	101.7934	109.3067	116.8201	124.3335	131.8468	139.3602
LOWER CURRENTS FOR DETECTOR 43	133.9680	125.8832	117.7983	109.7135	101.6286	93.5438	85.4590
UPPER CURRENTS FOR DETECTOR 44	85.0729	92.0106	98.9483	105.8860	112.8237	119.7613	126.6990
LOWER CURRENTS FOR DETECTOR 44	130.8142	122.9700	115.1258	107.2816	99.4374	91.5931	83.748

Table Va.3

Unit 1 Cycle 8

Summary of MTC, Doppler Coefficient
and $\Delta T/\Delta P$ Test Data at <70% RTP

	<u>1</u>	<u>2</u>	<u>3</u>	<u>4</u>	<u>Avg.</u>	<u>Design</u>	<u>Deviation</u> ³
MTC (pcm/°F)	-1.14	-2.64	-1.67	-2.59	-2.01	-2.96 ¹	-0.95
DPC (pcm/%)	-10.33	-10.88	-	-	-10.61	-11.25 ¹	-0.64
R ⁴ (°F/%)	-8.42	-4.49	-6.24	-	-6.38	-5.28 ²	1.10
R' ⁵ (°F/%)	-4.73	-2.52	-3.50	-	-3.58	-3.00 ²	0.58

NOTES: ¹ Values were calculated from the vendor's design report, ARO condition

² Values were calculated using available measured test results
(i.e., MTC, DPC, etc.)

³ Deviation = Design value - Measured data

$$^4 R = \frac{\Delta T}{\Delta P} = - \frac{DPC}{MTC} \left(\frac{\text{Doppler Power Coefficient}}{\text{Moderator Temp. Coefficient}} \right)$$

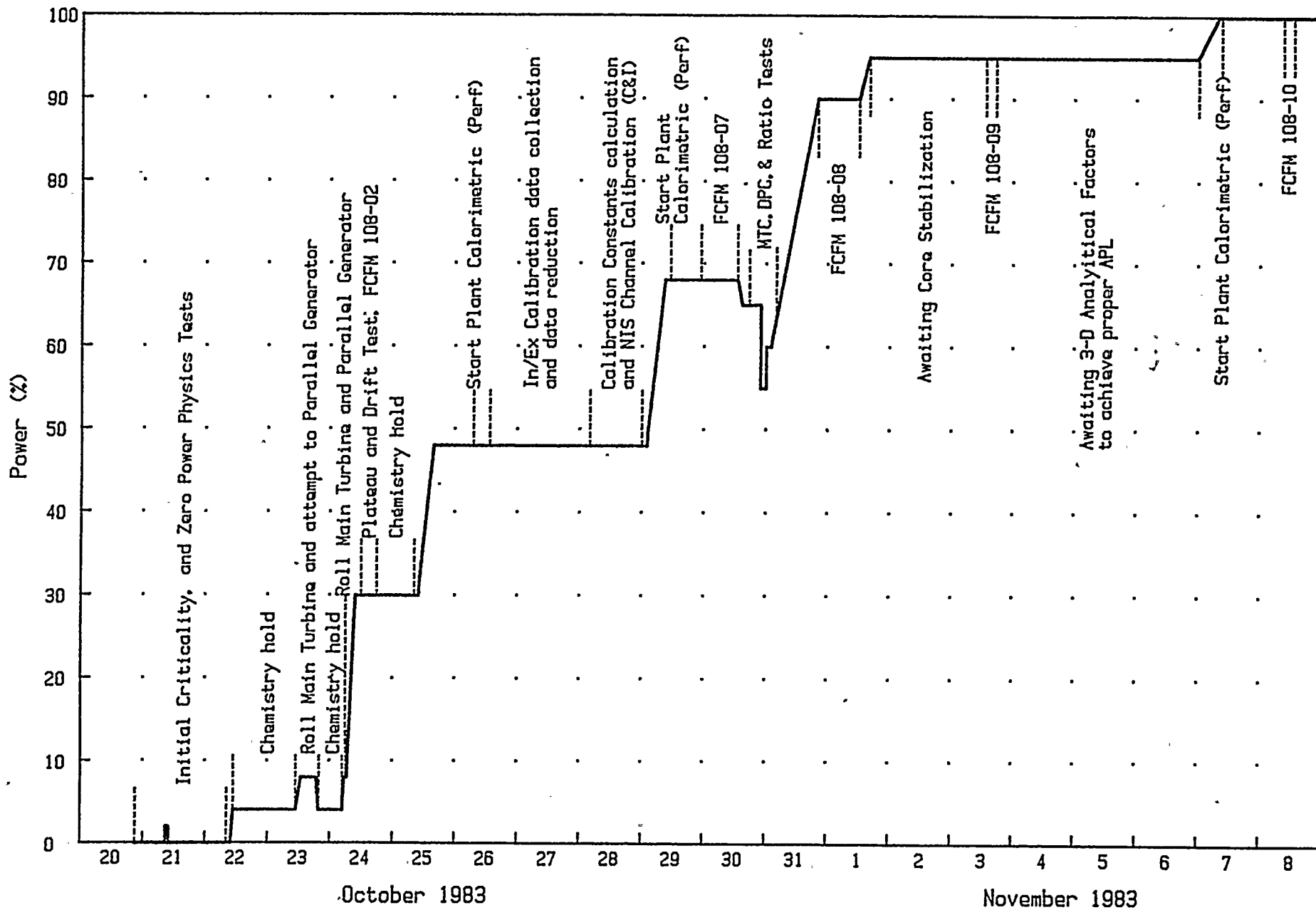
$$^5 R' = \frac{\Delta T'}{\Delta P} = - \frac{DPC}{ITC} \left(\frac{\text{Doppler Power Coefficient}}{\text{Isothermal Temp. Coefficient}} \right)$$

$$ITC = MTC + DPC = -3.54 \text{ pcm/°F}$$

$$DPC = -1.53 \text{ pcm/°F}$$

FIGURE Va.1

Unit 1 Cycle 8 Power Ascension vs. Time





Faint, illegible horizontal text or markings near the top center of the page.

Faint, illegible vertical text or markings on the right side of the page.

Faint, illegible markings or text at the bottom left corner of the page.

FIGURE Va.2

N-41 Excore Current vs Incore A.O. Unit 1 Cycle 8

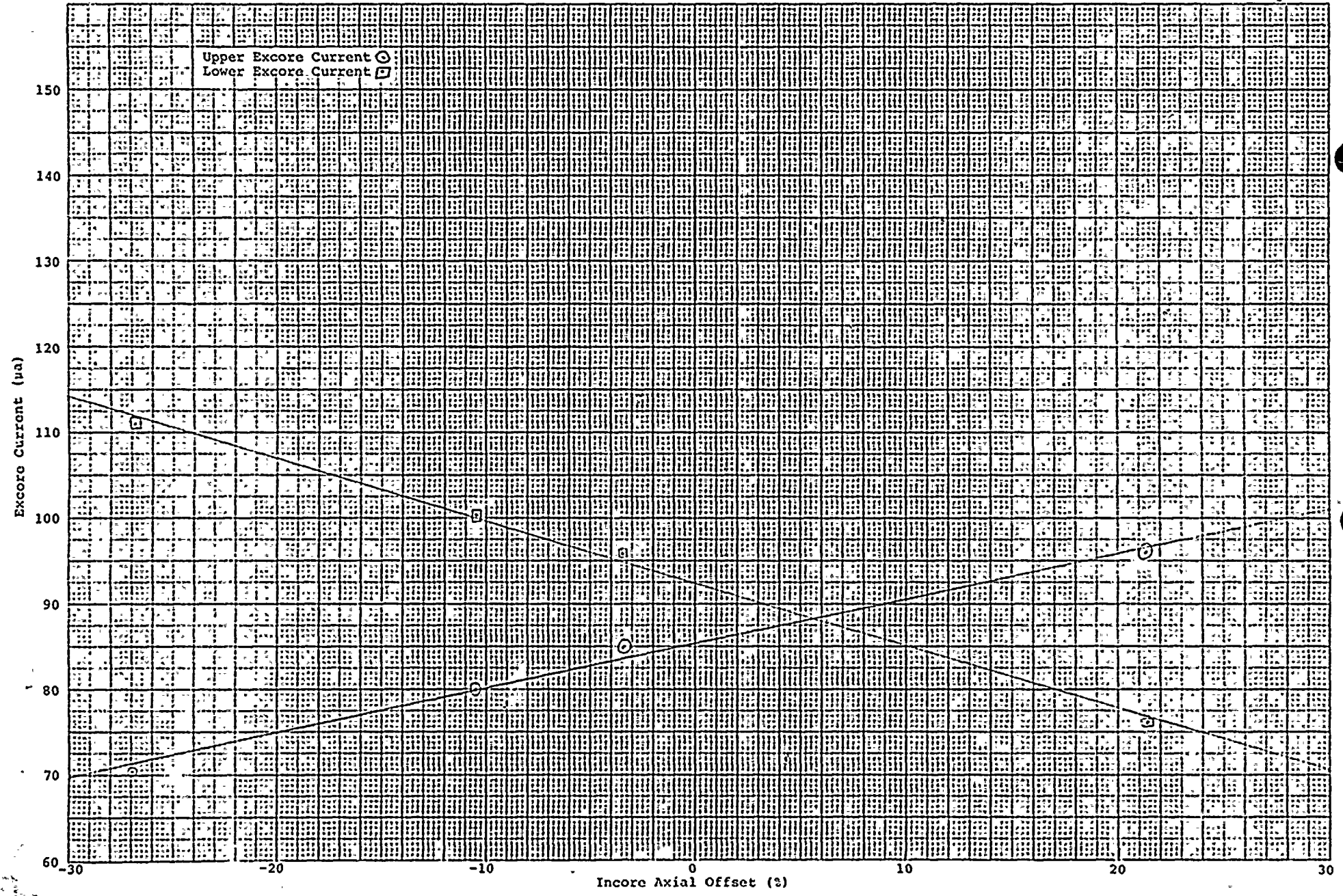
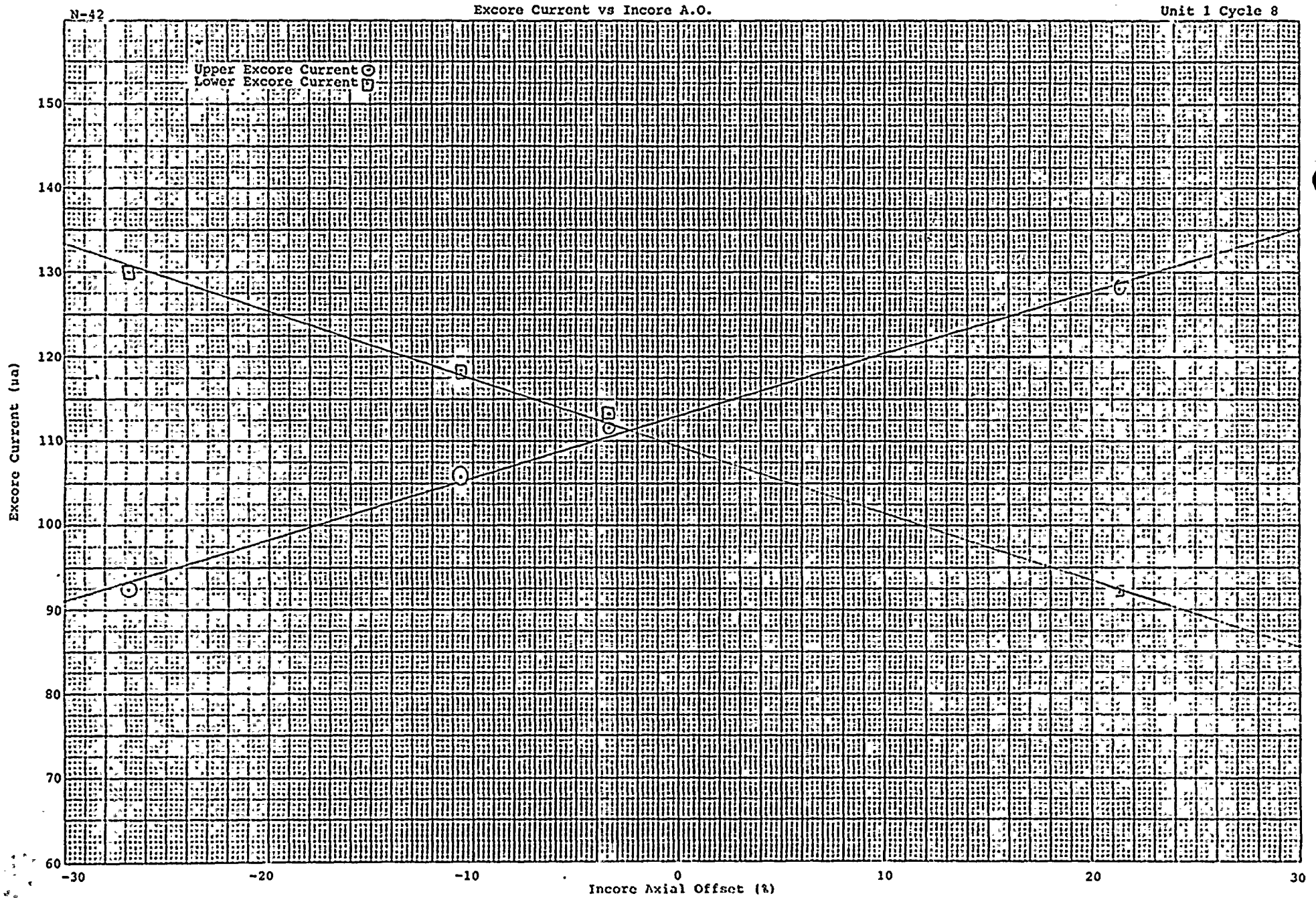


FIGURE Va.3



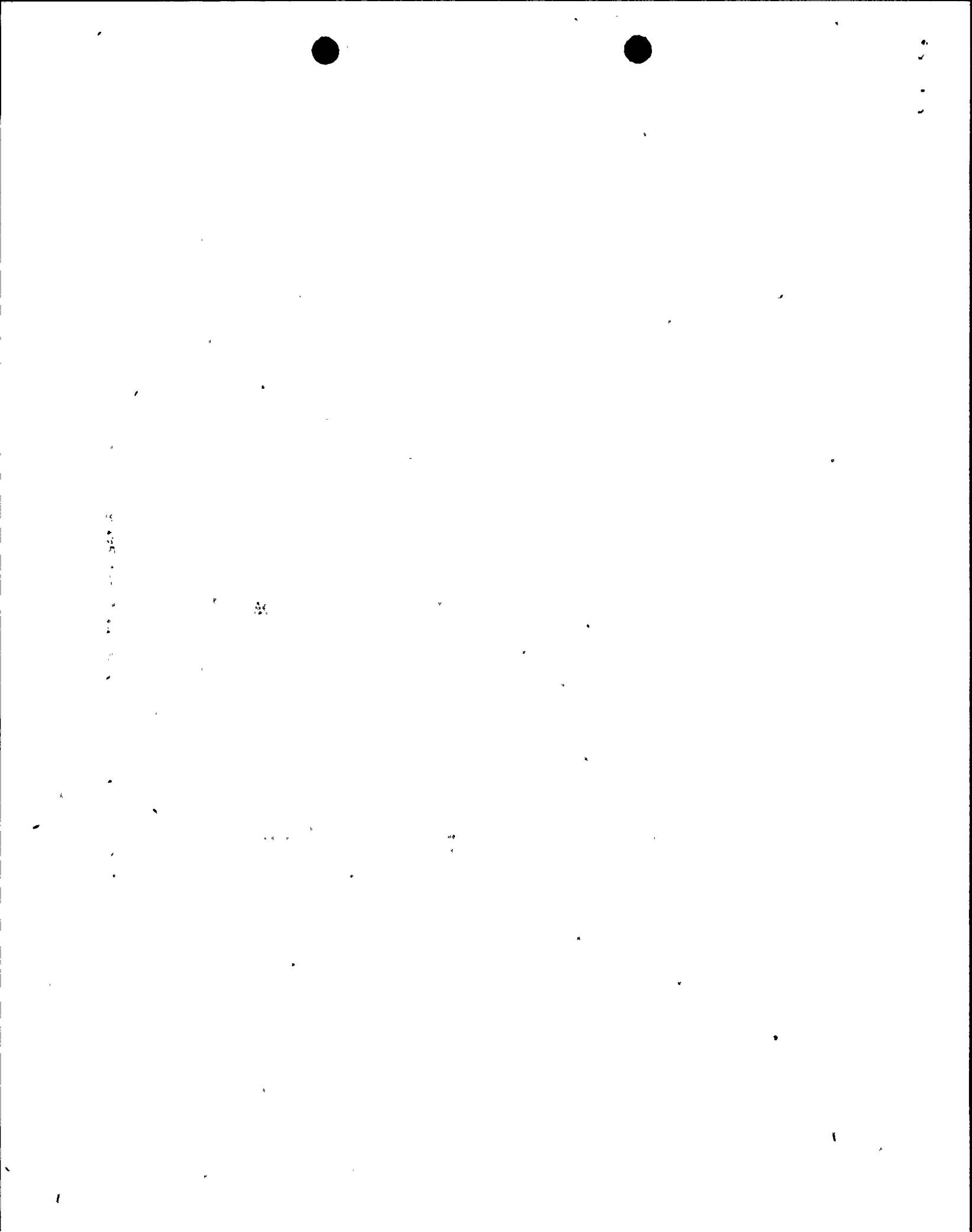
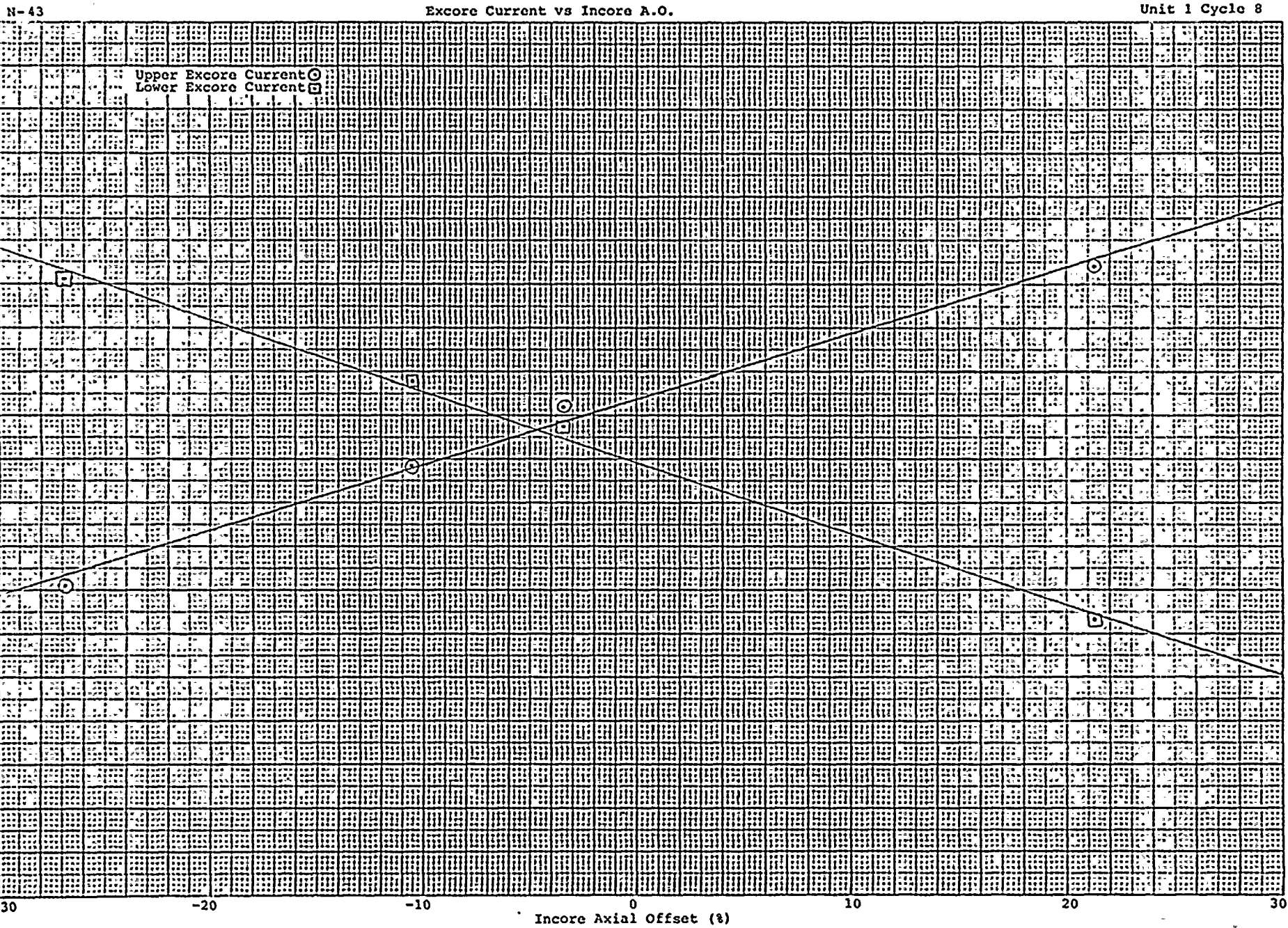


FIGURE Va.4



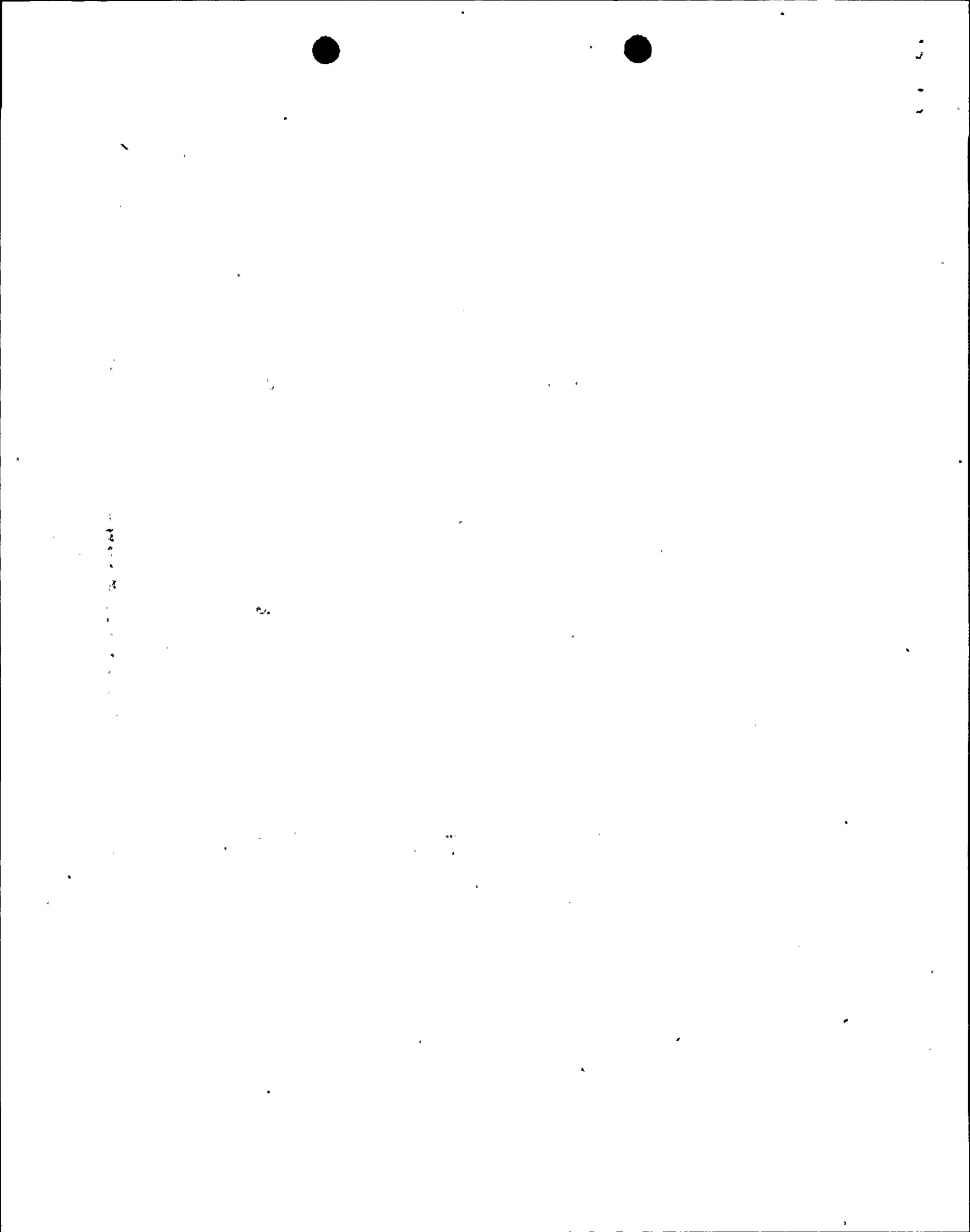
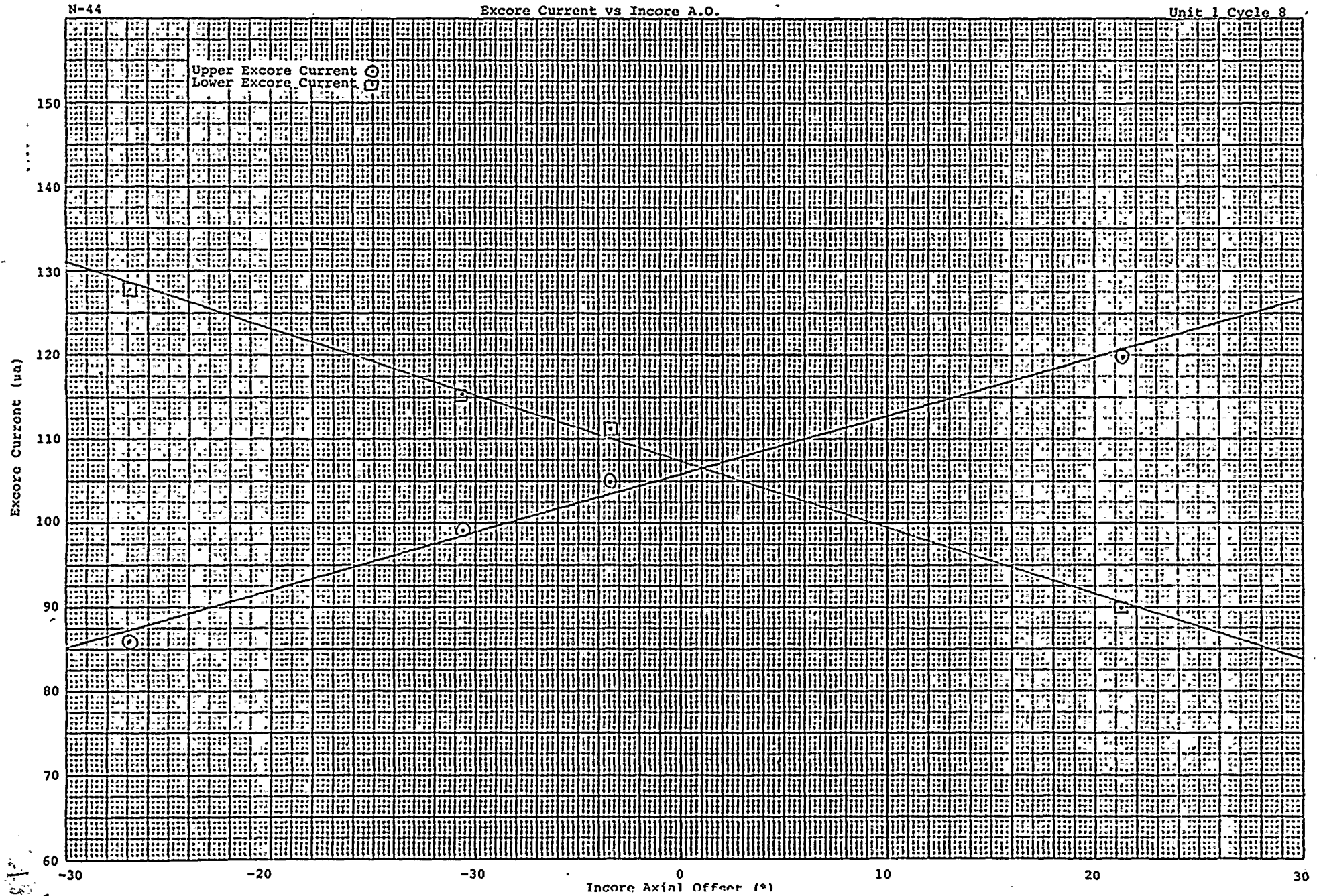


FIGURE Va. 5



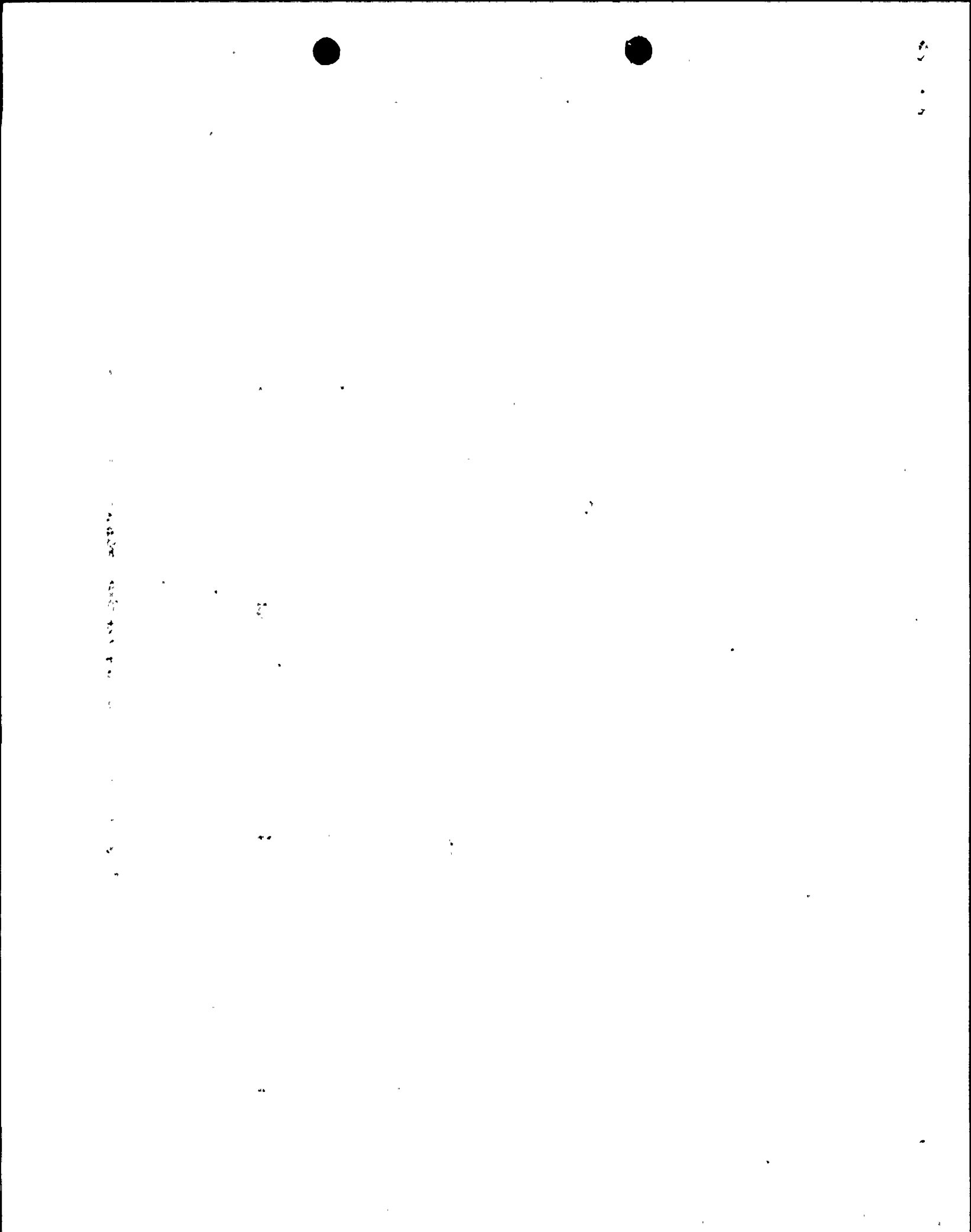
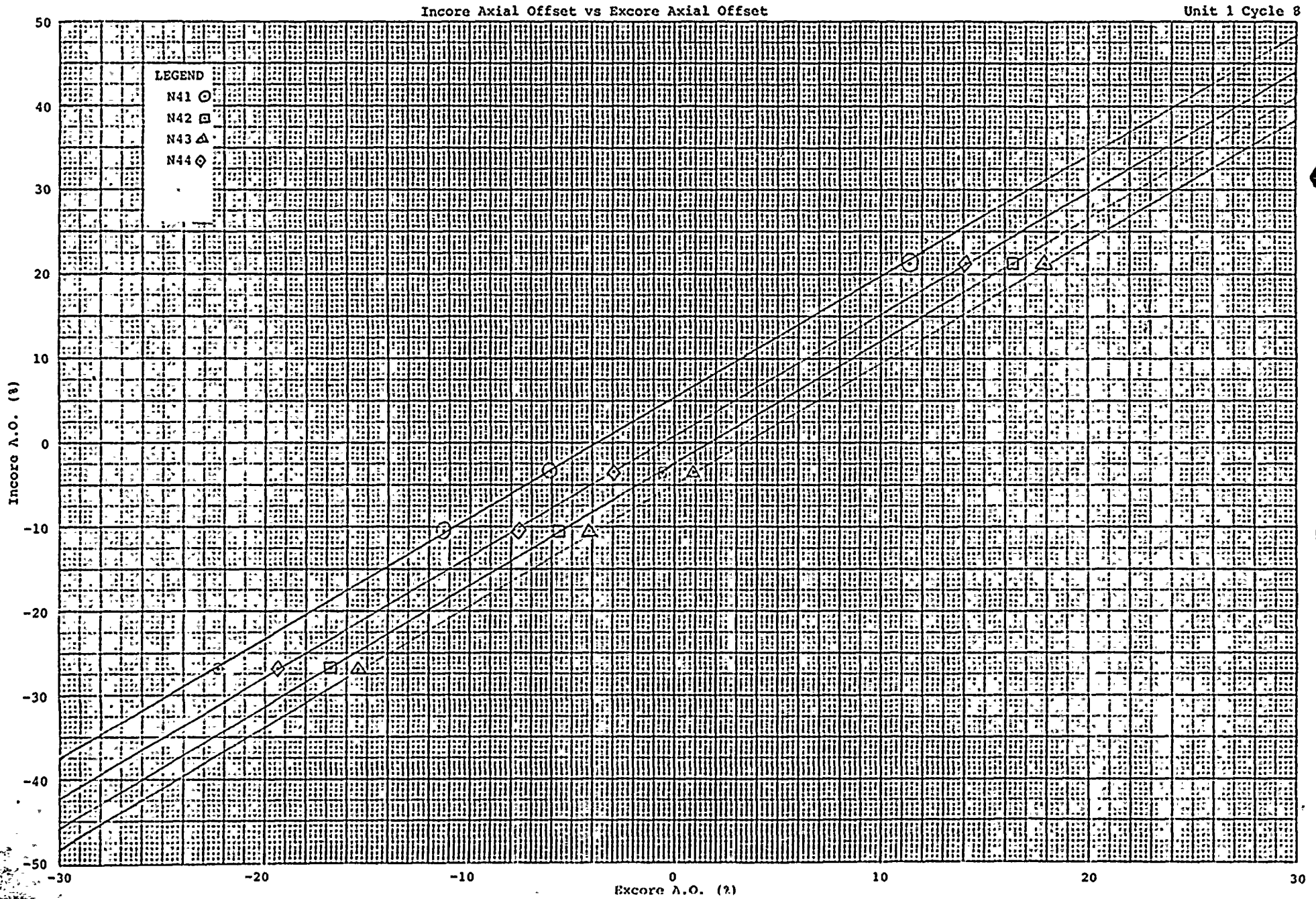


FIGURE Va.6



Vb Plant Chemistry History

The Unit 1 refueling outage began on July 16, 1983. Prior to this refueling outage, the reactor coolant system activities in general, and dose equivalent iodine-131 in particular, were quite low. Dose equivalent iodine-131 was approx. 1.00×10^{-3} $\mu\text{Ci/cc}$. No fuel defects or leaks were suspected. After the shutdown, maximum coolant system dose equivalent iodine-131 was 1.20×10^{-1} $\mu\text{Ci/cc}$. Reactor coolant system degassing was complete in 39 hours in preparation for the refueling and in particular, the addition of hydrogen peroxide for Co-58 solubilization. Once degassed and the reactor coolant system less than 180°F, 30% hydrogen peroxide was added to the primary coolant to "clean up" the core. A total of four (4) gallons of 30% hydrogen peroxide was added with a maximum detected reactor coolant Co-58 activity of 1.14 $\mu\text{Ci/cc}$. Cleanup via maximum CVCS letdown purification flow took approx. 52 hours of critical path time and resulted in the removal of just over 300 curies of Cobalt-58. This standard cleanup operation results in the steam generator area radiation levels remaining at relatively low levels cycle after cycle. Maximum radiation level detected was 8 R/hr. Following this "cleanup", the unit continued into its refueling operation.

Reactor coolant system monitoring during the subsequent startup has detected no new source of activity and the fuel integrity seems as sound as the previous cycle.

The secondary system chemistry prior to shutdown was fairly good. Minimal adverse affect was noted due to condenser inleakage based on specifications in effect during that cycle. Steam generator limits during this cycle were ≤ 2.0 μmho cation conductivity with < 100 ppb sodium contamination. Steam jet air ejector flow was 25-30 scfm actual with no specification in effect. When the new secondary cycle specifications were drafted, they were an initial effort to meet all the Steam Generator Owners Group Guidelines published by EPRI. The new specifications included reduction of the steam generator cation conductivity to 1.5 μmho 's, steam generator sodium to 20 ppb and established a 10 scfm limit on the steam jet air ejector, among other changes. In order to meet the new, more restrictive power operation specifications, limits were written for various steps during the startup. For example, prior to entering mode 2, prior to turbine roll, 30%, 50%, and 75% power. The 75% power specifications were later amended to be in effect at 80% power or greater. Full power operation, as far as secondary chemistry specifications, was defined at greater than 80% power.

As is standard practice during refueling outages, the steam generators were sludge lanced to remove accumulated deposits from the tube sheet. This operation succeeded in removing 445, 140, 445, and 140 lbs. of sludge from steam generators 11 through 14.

As a means of achieving these new specifications, a program of steam generator crevice flushing was initiated in mode 4. This basically involves rapid depressurization of the steam generators while at 280-300°F, causing agitation (boiling) at the tube sheet and hopefully in the crevices. The exact procedural method for performing this activity remains in question; several methods were attempted not only at this site but by other utilities and no "standard" method exists to date. (EPRI is hoping to issue a standard method for testing in March, 1984.) The crevice flushing activities created a 48 hour hold until the flushing was complete.

Startup and power ascension was delayed due to holds caused by the new chemistry specifications. Operational experience gained during this initial application of the new secondary system specifications should be used to minimize holds in future startups.

V c PLANT RADIATION SURVEYS

The adequacy of the shielding design for the reactor and associated primary coolant system was verified during the initial plant start-up. Surveys during subsequent start-ups were performed for the following purposes:

1. Verify the adequacy of any radiation and shielding that has been significantly modified since the last start-up.
2. Verify the adequacy of radiation shielding systems that have been significantly modified such that the source term may have changed, thus changing the shielding adequacy.
3. Verify that general plant radiation levels have not significantly changed due to variations in sources that may have been affected by feed changes.

No significant modifications were made to primary shielding or the primary coolant systems such that the source term for existing shielding would have been changed.

As in past refueling periods, surveys of accessible areas were performed during the transfer of fuel from the refueling cavity, through the transfer tube, and into the spent fuel pool. No significant differences were found from previous similar surveys. However, because of the rate at which fuel moves through the transfer tube, there was some doubt that all areas of radiation leakage had been identified. In an effort to locate any radiation leaks that might only exist for a few seconds during normal transfer tube usage, a spent fuel element was "parked" in various locations of the transfer tube to allow a more thorough search for radiation leakage points.

Increases were seen inside some of the already posted high radiation areas, especially in the annulus near the Reactor Coolant Drain Tank. On the 633' level, at the junction of the Containment dome and the Auxiliary Building, maximum levels went from 0.2 mR/hr to 50 mR/hr with fuel in the transfer tube.

The most significant radiation level increases were noted inside the Containment Building at the 612' area between the ice condenser walls. During the time the fuel bundle was at rest in the transfer tube, the shield walls on either side of the transfer tube read a maximum of 17 R/hr. Although the time-weighted average exposure rate with fuel moving normally through the tube would not require posting the area, rope boundaries were established such that outside the boundaries the instantaneous dose-rate was less than 100 mRem/hr.

The routine surveys and Shield Survey conducted at the start-up following refueling did not show significant differences from previous start-up surveys.

Vd Reactor Coolant Flow Measurement

The primary purpose of this test was to determine the total reactor coolant flowrate independent of the reactor coolant flow transmitters. The reactor coolant flowrate was computed from a steam generator heat balance calculation utilizing steam generator secondary side parameters.

In addition, it was also the purpose of this test to recalibrate the reactor coolant flow elbow tap differential transmitters, as required, based on the computed reactor coolant flow rates and elbow tap differential pressure data.

The total coolant flowrate was determined at both the 48%, 68% and 100% levels of reactor thermal power. The table below indicates that the total reactor coolant flowrate fell within the acceptable region of the Technical Specification Graph 3/4.2-11.

Table Vd.1
Computed Reactor Coolant System Flowrates
at 48%, 68% and 100% Reactor Thermal Output

	<u>Flow @ 48%</u> (#/hr)	<u>Flow @ 68%</u> (#/hr)	<u>Flow @ 100%</u> (#/hr)
Loop #1	3.42×10^8	3.52×10^8	3.43×10^8
Loop #2	3.94×10^8	3.92×10^8	3.82×10^8
Loop #3	3.55×10^8	3.61×10^8	3.78×10^8
Loop #4	3.38×10^8	3.48×10^8	3.61×10^8
Total Flowrate	14.28×10^8	14.53×10^8	14.40×10^8

Table Vd.2

Average Value of Plant Parameters
Used in Flow Determination

<u>Parameter</u>	<u>Value @ 48%</u>	<u>Value @ 68%</u>	<u>Value @ 100%</u>
RCS Pressure	2232	2234	2232
RCS T Hot (F)	570.4	580.4	595.6
RCS T Cold (F)	541.3	539.7	537.4
Main Steam Pressure (psia)	878.3	840.9	789.6
Feedwater Pressure (psia)	898.1	867.5	827.5
Feedwater Temperature (F)	370.9	401.0	433.7
Feedwater Flow (PPH)	1530696.	2292028.	3510713.

The computed reactor coolant flowrates and the elbow tap differential pressure data, obtained as part of the 100% power data set, were used to recalibrate the reactor coolant flow elbow tap differential transmitters.

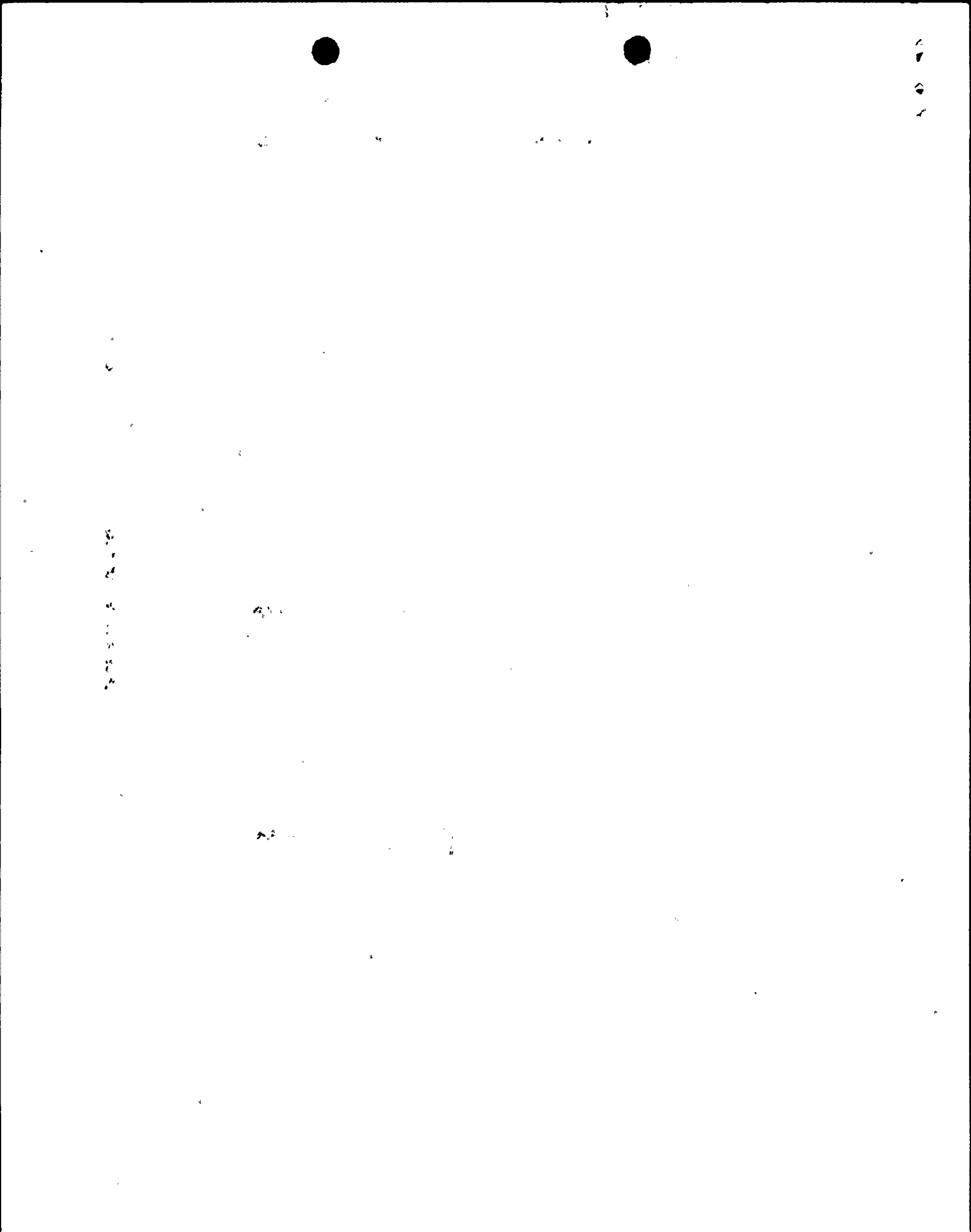
Each reactor coolant loop flowrate was computed by performing heat balance calculations around the shell and tube side of the loop's associated steam generator. As is shown in Figure Ve-1 steam generator primary and secondary side pressure and temperature data was simultaneously trended to provide the required inputs to the heat balance equations. All of the required data was obtained while the unit was in a steady state mode of operation and steam generator blowdown was secured. The feedwater flow, corrected for specific weight of the fluid and associated piping characteristics, was calculated from the venturi differential. The steam generator thermal output was then computed from the feedwater flow and the associated increase in enthalpy. Finally, this thermal output value was transferred to the primary side where it was used in conjunction with the reactor coolant enthalpy drop to calculate reactor coolant flow. The total reactor coolant flow was simply the sum of the individual loop flowrates.

Table Vd.1 summarizes the calculated flowrates. The total RCS flowrate was verified by Nuclear Section to fall within the acceptable region of Technical Specification Graph 3/4.2-11.

Table Vd.2 lists the primary and secondary side plant parameter average values used in the reactor coolant flow determinations.

The reactor coolant flow determination was made at 48%, 68%, and 100% power levels. At each level the flow determination and the reactor coolant flow elbow tap differential pressure data (trended simultaneously with the pressure and temperature data used in the heat balance equations) were used to evaluate the accuracy of the elbow tap differential transmitters.

The current trip point for the indicated RCS flow is 93%. Since the actual RCS flow is greater than the indicated flow the 93% trip point is conservative and a transmitter recalibration was again deemed unnecessary.



Ve Plant Thermal Power Calibration

The purpose of this test was to determine reactor thermal power by measuring secondary system feedwater flow and steam parameters, and to verify the accuracy of the following computer outputs:

1. Reactor thermal power
2. Feedwater flows
3. Feedwater temperatures
4. Nuclear power range instrumentation

By measuring the secondary side parameters the reactor thermal output can be calculated. The parameters that are measured for this power determination are feedwater flow, feedwater temperature, feedwater pressure, and steam pressure. The power determination has been completed at power levels of 48%, 68% and 100%.

<u>% Power</u>	<u>Computer Value (U-1118)</u>	<u>Calculated Value</u>
48%	47.86	47.37
68%	67.90	67.36
100%	99.50	99.09

During the initial power ascension program the reactor thermal output was calculated at various power levels by measuring secondary side parameters. These parameters are summarized in Table Ve.1.

By measuring the feedwater parameters before the steam generators and the steam parameters after, the amount of energy added by the steam generators was determined. The energy gained by the steam side of the steam generator is the equivalent energy given off by the reactor coolant system. By knowing the heat transferred by each of the four steam generators, the total heat added to the secondary side of the reactor coolant system is determined. This total heat added to the secondary side minus the heat added by RCP operation and RCS system losses is the actual reactor power.

All measurements taken for this thermal power measurement were from instruments calibrated specifically for this test independent of computer points. The pressure measurements were read using dead weight testers, feedwater flows were measured at the local transmitter for each loop and temperatures were read using thermocouples installed in test wells for each loop's feedwater piping.

Before the test is begun the steam generator blowdown is isolated and all plant parameters are as stable as possible. These conditions prevailed throughout the test.

The computer thermal power is monitored during the actual thermal power test. After the test is completed, a comparison is made between the computer value and the actual measured value.

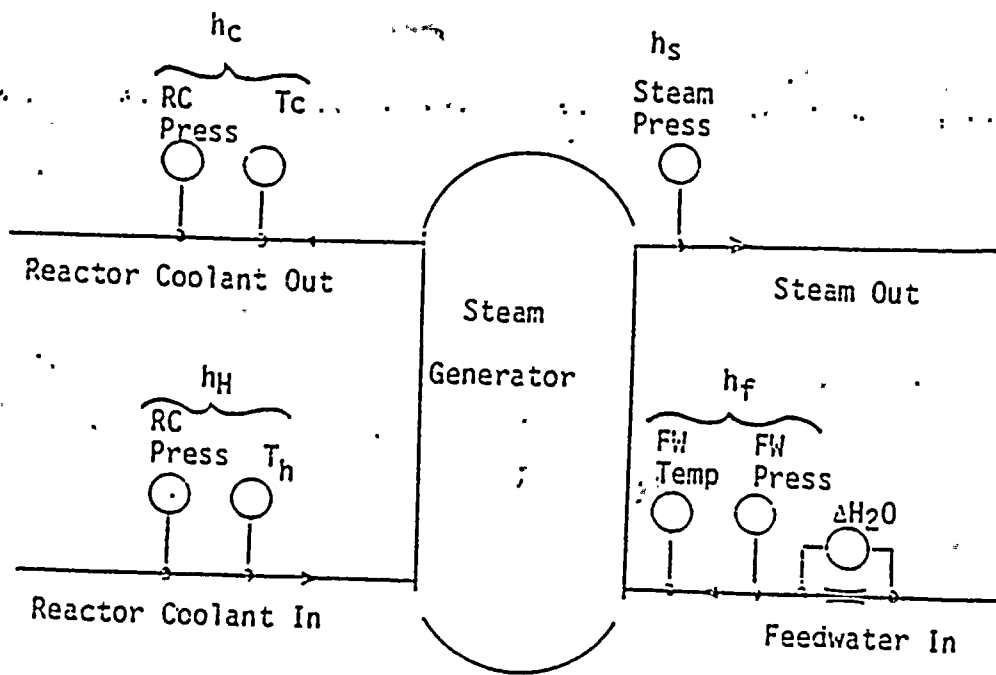
THERMAL POWER CALIBRATION DATA

% POWER		FW PRESSURE (PSIA)				FW TEMPERATURE (°F)				STM. PRESSURE (PSIA)			
CALCULATED	COMPUTER VALUE (U-1118)	1	2	3	4	1	2	3	4	1	2	3	4
47.37	47.86	897.72	897.72	898.22	898.82	369.70	371.20	371.49	370.34	878.7	877.9	878.1	878.3
67.36	67.90	866.42	866.52	866.52	867.52	400.24	401.45	401.79	400.80	841.5	840.4	839.4	842.1
99.09	99.50	827.68	826.48	825.38	830.58	433.31	434.42	434.21	433.00	788.6	785.9	783.2	789.6

TABLE Ve.1

FIGURE Ve.1

Reactor Coolant Flow Determination



1. Feedwater Flowrate = $Wf = (359.1)d^2 C Fa (\sqrt{Y})(\sqrt{\Delta H2O}) \left(\frac{1}{\sqrt{1-(d/U)^2}} \right)$
 Where: d = throat diameter of venturi (inches)
 C = coefficient of discharge
 Fa = venturi thermal expansion factor
 Y = specific weight of feedwater ($\#/ft^3$)
 $\Delta H2O$ = differential pressure across venturi (inches)
 D = pipe diameter at inlet pressure tap (inches)
2. Steam Generator Thermal Output = $Bs = Wf(hs - hf)$
 Where: hs = enthalpy of steam (BTU/ $\#$)
 hf = enthalpy of feedwater (BTU/ $\#$)
3. Reactor Coolant Loop Flow = $Bs / (hh - hc)$
 Where: hh = enthalpy hot leg (BTU/ $\#$)
 hc = enthalpy cold leg (BTU/ $\#$)
4. Total Reactor Coolant Loop Flow = sum of the loop flows

